On pricing and hedging options and related first-passage time problems

Marc Jean-Claude Jeannin

Department of Mathematics, Imperial College London

London SW7 2AZ, United Kingdom

Submitted to Imperial College London
for the degree of
Doctor of Philosophy

25 November 2010

To my parents, Charles and Françoise Jeannin, for their constant encouragement.

Abstract

On pricing and hedging options and related first-passage time problems. In the financial industry, a derivative is a contract whose value is derived from the value of the underlying asset price. The model of reference for the pricing of derivatives is the Black-Scholes model. This thesis examines the limitations of the Black-Scholes model and focuses on plausible alternative models in the equity markets. First, I investigate the effects of hedging strategies on the so-called pinning effect, which is the tendency of stock prices to close near the strike prices of heavily traded options as the expiration date nears. Then I concentrate on alternative stock price models that are more flexible and maintain a degree of analytical tractability for the pricing and hedging of barrier options. I consider the cases for which the logarithm of the stock price gives rise to (i) a Lévy process and (ii) an additive process. Based on the Wiener-Hopf factorisation, I develop some transform algorithms to derive semi-analytical expressions, in the case of barrier options, for first-passage-time probabilities, prices, and Greeks. The outcomes are compared to Monte-Carlo simulations, and I find that the proposed algorithms lead to faster, more accurate results.

Acknowledgements

This thesis would not have been possible without the help of many people. First, I would like to express my deepest gratitude to my supervisor, Dr Martijn Pistorius, for his advice and support over the last six years. This thesis is the fruit of a challenging part-time collaboration. I am deeply indebted to Professor Lane Hughston for sharing his knowledge and experience of life: he truly made a difference in my own life. Special thanks are due to Professor Giulia Iori who put me on the right track for postgraduate research and has all along been supportive. I am grateful to colleagues at Nomura, particularly Patrick Howard, Dr Slava Obraztsov, and Denis Wallez. Their support and encouragement has been extremely valuable. I owe special thanks to Jurgen Tistaert at ING, who gave me the first opportunity to work on Lévy processes: the summer of 2003 was a great experience. I am grateful to my fellow PhD students at King's and Imperial for their support and companionship. Last but not least I thank all my friends that have been there over these six years, Fabien Darche, Benjamin Delaunay, Maud Gallet, Thomas Moquet, Darren and Grainne O'Driscoll, Anton Talpa, and especially Jeffrey Goodman.

The work presented in this thesis is my own.

Contents

1 Introduction and overview **9**

2 Beyond Brownian motion **12**

2.1 The Black-Scholes model and its limitations 12

2.2 Lévy processes 15

2.3 Additive processes 19

2.4 Pricing of barrier-options 19

3 Modelling stock pinning **21**

3.1 Introduction 21

3.2 Stock pinning and option pricing 22

3.3 Extensions of the Frey-Stremme model 24

3.4 A microstructure model for stock pinning 32

3.5 Concluding remarks 37

4 A transform approach to compute the prices and Greeks of barrier options driven by a class of Lévy processes **38**

4.1 Introduction 38

4.2 Log-Lévy models 41

4.3 First-passage theory 45

4.4 Laplace transforms of barrier-option prices 49

4.5 Calculating sensitivities 53

4.6 Numerical results 57

4.7 Convergence of prices and sensitivities 63

4.8 Concluding remarks 65

4.9 Appendix Chapter 4 67

5 Pricing and hedging barrier options in a hyper-exponential additive model **71**
5.1 Introduction 71
5.2 Log-additive models 74
5.3 First-passage probabilities 77
5.4 Prices and Greeks of digital and barrier options 84
5.5 Numerical results 85
5.6 Appendix Chapter 5 93

Bibliography **100**

List of Figures

2.1 Historical analysis of FTSE daily returns 14

3.1 Avellaneda-Lipkin model - Time decay 24
3.2 Frey-Stremme model - Drift and volatility 26
3.3 Frey-Stremme model - Drift and volatility 26
3.4 Avellaneda-Lipkin and Frey-Stremme models - Pinning probabilities 27
3.5 Modified Frey-Stremme model - Drift and volatility 29
3.6 Modified Frey-Stremme model - Variance of jump prices 30
3.7 Modified Frey-Stremme model - Pinning probabilities 30
3.8 Modified Frey-Stremme model - Volatility effect 32
3.9 Microstructure model - Schematic order book mechanism 33
3.10 Microstructure model - Pinning probabilities 34
3.11 Microstructure model - Drift and volatility 35
3.12 Microstructure model - Volatility 36
3.13 Microstructure model - Pinning probabilities 36
3.14 Microstructure model - Non constant impact model 37

4.1 NIG - Down-and-out put options 60
4.2 VG - Down-and-in digital options 63

5.1 Hyper-exponential additive model - Schematic representation . . 81
5.2 Hyper-exponential additive model - Calibration 87
5.3 Hyper-exponential additive model - Down-and-in digital options . 90
5.4 Hyper-exponential additive model - Down-and-in digital options . 90
5.5 Hyper-exponential additive model - Down-and-in call options . . . 91
5.6 Hyper-exponential additive model - Down-and-in call options . . . 91

List of Tables

4.1 VG and NIG calibrations 58
4.2 NIG - Down-and-out put options 59
4.3 VG - Down-and-in digital options 62

5.1 Hyper-exponential additive model - Parameters 87
5.2 Hyper-exponential additive model - Down-and-in digital options . 92
5.3 Hyper-exponential additive model - Down-and-in call options . . . 92

Chapter 1

Introduction and overview

> The ideas of economists and political philosophers, both when they are right and when they are wrong, are more powerful than is commonly understood. Indeed, the world is ruled by little else. Practical men, who believe themselves to be quite exempt from any intellectual influences, are usually the slaves of some defunct economist. Madmen in authority, who hear voices in the air, are distilling their frenzy from some academic scribbler of a few years back ... soon or late, it is ideas, not vested interests, which are dangerous for good or evil.
>
> — J. M. Keynes (1883-1946)

The Black-Scholes model is the model of reference for the pricing of derivatives. It has been of great interest to academics and practitioners over the last three decades, who have relaxed some of the main limiting assumptions; there include Gaussian log-price returns, constant risk-free rates, constant volatility, no transaction costs, no short-selling restrictions, and liquid markets. In this thesis, we examine the limitations of the Black-Scholes model in equity markets, and focus on plausible alternative models for the pricing and hedging of options, and for related first-passage time problems. The contents of the thesis are adapted in part from the following papers: Iori & Jeannin [49], "Modelling stock pinning"; Jeannin & Pistorius [53], "A transform approach to compute prices and Greeks of barrier options driven by a class of Lévy processes"; and Jeannin & Pistorius [52], "Pricing and hedging barrier options in a hyper-exponential additive model".

In Chapter 2, I examine some of the limitations of the Black-Scholes model. The assumptions of frictionless and perfectly liquid markets imply that market participants can rebalance delta-hedges without affecting the underlying stock, even though they may trade in large volumes of stock. These assumptions have been questioned in the literature, and a number of investigations have concentrated on the feedback effects of dynamic hedging strategies. The Black-Scholes model also assumes that log-stock-price returns are Gaussian, but empirical analysis shows that the distribution is highly peaked, with fat tails. The volatility parameter is not constant, and we see fluctuations with periods of high and low volatility, and jumps. Researchers have attempted to address these limitations with more advanced models: These include Lévy models, additive models, and stochastic volatility models. Such models can be especially important when one considers the pricing of path-dependent products such as barrier options.

In Chapter 3, I investigate the effects of hedging strategies on the so-called pinning effect, i.e., the tendency of stock prices to close near the strike prices of heavily traded options as the expiration date nears. In this chapter we propose an explanation of stock pinning in terms of delta-hedging strategies for long option positions. We adopt a model introduced by Frey & Stremme [43, 44] and show that under the original assumptions of the model the pinning effect is driven by two factors: a hedging-dependent drift term that pushes the stock prices toward the strike price, and a hedging-dependent volatility term that constrains the stock price near the strike as it approaches it. Finally, we show that pinning can be generated by simulating trading in a double-auction market.

In Chapter 4, I propose an efficient and accurate method to calculate the prices and Greeks of barrier options when the underlying stocks are driven by Lévy processes. Barrier options are contracts that are activated or de-activated when the underlying process crosses a specific level; they are among the most widely traded of exotic contracts. The pay-offs of barrier options are path-dependent, and their valuation requires the specification of the first-passage distribution. We derive analytical expressions for the Laplace transforms of the prices and sensitivities (Greeks) of barrier options in an exponential Lévy stock price model with

hyper-exponential jumps. These results are subsequently employed to construct an approximation for barrier option prices and the corresponding sensitivities in an exponential generalised hyper-exponential model. This class of models includes many of the Lévy models employed in financial applications, such as variance gamma (VG), CGMY, generalised hyperbolic, and normal inverse Gaussian (NIG) processes. Theoretical convergence results for the constructed approximations are provided. As a numerical illustration, we compare the results obtained by this approximation to those obtained by Monte-Carlo simulations. We look, in particular, at the cases for which the driving process is a VG or an NIG Lévy process, with parameters calibrated to Stoxx50E call-option prices.

In Chapter 5, I develop an algorithm to calculate the prices and Greeks of barrier options driven by a class of additive processes. Additive processes are time-inhomogeneous Lévy processes, or equivalently, processes with independent but inhomogeneous increments. We derive a semi-analytical expression for the first-passage probability of an additive process with hyper-exponential jumps. This solution of the first-passage problem rests on an explicit matrix Wiener-Hopf factorisation. Employing these results we obtain explicitly the Laplace-Fourier transforms of the prices and Greeks of digital and barrier options. As a numerical illustration, we simultaneously calibrate the model to Stoxx50E call options at four different maturities, and then calculate the prices and Greeks of down-and-in digital options and down-and-in call options. Comparison of the outcomes to the results of Monte-Carlo simulation shows that the approach is fast, accurate, and stable.

Chapter 2

Beyond Brownian motion

In this chapter we examine the limits of the applicability of the Black-Scholes model in equity markets and review alternative models. On some appropriate probability space $(\Omega, \mathcal{F}, \mathbb{P})$, we assume that the stock price process $S = \{S_t, t \geq 0\}$ is modelled by setting

$$S_t = S_0 \mathrm{e}^{X_t}.$$

For simplicity, S is taken to be non-dividend-paying. To guarantee the absence of arbitrage, S must satisfy $E[\mathrm{e}^{-rt} S_t] = S_0$ under the risk-neutral measure $\mathbb{P}$ where r is the risk-free rate of return which for simplicity we take to be constant. As a consequence, the discounted stock price $\mathrm{e}^{-rt} S_t$ is a martingale under $\mathbb{P}$.

2.1 The Black-Scholes model and its limitations

In the Black-Scholes model, the stochastic process $X = \{X_t, t \geq 0\}$ is defined by

$$X_t = (r - \frac{1}{2}\sigma^2)t + \sigma W_t,$$

where r is the risk-free rate, σ is the volatility parameter. Here W is a standard Brownian motion defined on $(\Omega, \mathcal{F}, \mathbb{P})$. We note that the stochastic process X has independent, homogeneous, and Gaussian increments.

We consider the class of derivatives for which the payoff H_T at time T is given by a functional

$$H_T = H(\{S_t\}_{0 \leq t \leq T}).$$

We observe that H_T depends on the trajectory of the stock price process S from time 0 up to time T. European-style options, American-style options, and barrier options all fall into this class. The value H_0 of a derivative with such a payoff function H_T at time T is given by

$$H_0 = E[\mathrm{e}^{-rT} H_T].$$

2.1.1 Feedback effect and discrete hedging

In the Black-Scholes model, a derivative with present value H can be perfectly replicated by holding a portfolio of a certain amount of cash and a certain amount of the underlying stock. The quantity of shares to hold at time t is given by

$$\Delta = \frac{\partial H}{\partial S}\bigg|_{S=S_t}.$$

The Black-Scholes model assumes that markets are frictionless and perfectly liquid, implying that investors can rebalance the deltas of their portfolios without affecting the underlying stock prices. This assumption is not always justified in the presence of large trades.

In a number of papers Frey & Stremme [43, 44], Platen & Schweizer [73], and Schönbucher & Wilmott [79] have concentrated on the feedback effects of dynamic hedging strategies, and propose incorporating a reaction to delta-trading strategies on the price process S. They focus on the impact of option hedging strategies on the volatility of the underlying stock and relate the smile pattern of the implied volatility to the lack of liquidity. Hence the drift of the underlying stock is involved. Avellaneda & Lipkin [9] shows that close to expiry of an option, when gamma is large, dynamic hedging is also responsible for the pinning effect, i.e. the tendency of stock's price to close near the strike price of heavily traded options (in the same stock) as the expiration date nears.

In addition, the Black-Scholes model assumes that investors continuously rebalance their portfolios to remain delta-neutral. However in practice investors trade at discrete times. Mercurio & Vorst [68] discuss the implications of discrete hedging strategies and Whalley & Wilmott [85] measure the adjustment required for

pricing derivatives in minimising the variance of the hedged portfolio.

In Chapter 3 we show that dynamic continuous and discrete hedging can be responsible for the pinning effect. We analyse the impact of the hedging strategies on both the drift and the volatility of the underlying stock price.

2.1.2 Empirical analysis

In the Black-Scholes model, the log-stock-price returns are assumed to be Gaussian with a fixed volatility parameter. In Figure 2.1 on the left, the distribution of the FTSE100 log-returns over the last 25 years is highly peaked with fat tails. By measuring the skewness (-0.401) and the kurtosis (9.085), we see that FTSE100 log-returns are not Gaussian. In Figure 2.1 on the right, we estimate FTSE100 daily historical volatilities with a 90-day window and observe clustering with periods of high and low volatility. In addition option pricing models should not only capture empirical historical properties, but also accurately reproduce the options' quoted prices, which are the best estimators of future behaviour.

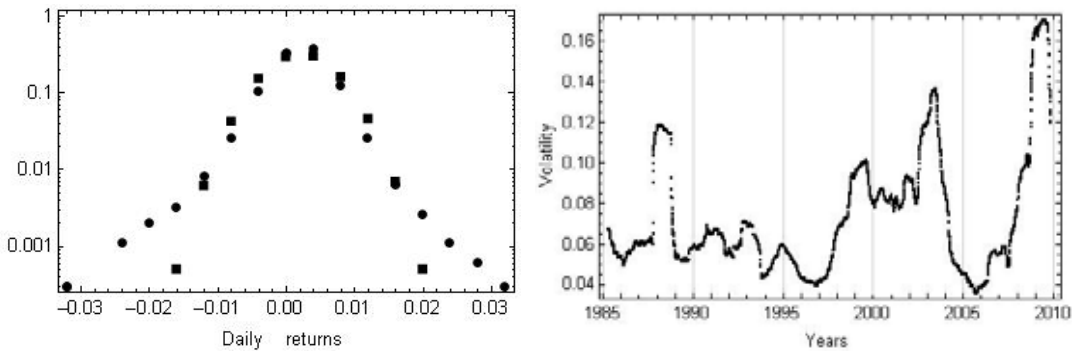

Figure 2.1: Left - Distribution of FTSE100 daily log-returns from 1984 to 2009 (circle dots) and Gaussian log-returns (square dots) with mean and volatility set to 0.01% and 7.83%. Right - Historical volatility of FTSE100 daily log-returns from 1984 to 2009 with a 90-day window.

To address these limitations, academics and practitioners have proposed more advanced models. The local-volatility models introduced by Dupire [36] and Derman & Kani [34] assume that the volatility parameter σ of the log-stock-price

process is a function of price and time. These models have the advantage of calibrating quoted option prices by construction, but as shown by Dumas *et al.* [35] the local-volatility function is not confirmed by the market. For long maturities, the local-volatility function is almost constant and counter-intuitive to market prices of call and put options. The Lévy models with jumps form an alternative. They generate a good fit for call and put option prices, and for long maturities the distribution of the increments remains skewed. We refer to Boyarchenko & Levendorskiĭ [21], Cont & Tankov [30], and Schoutens [80] for background and further references. The additive models with jumps constitute a natural extension of the Lévy models and have the advantage of being more flexible in making parameters time-dependent.

In Sections 2.2 and 2.3 we define Lévy processes and additive processes. In Section 2.4 we define barrier options and briefly review the different pricing tools to value these derivatives.

2.2 Lévy processes

The study of Lévy processes goes back to the 1930s with the work of Kolmogorov [56], Lévy [62], and Khintchine [55]. In this section, we briefly review the main results defining Lévy processes. For further background we refer, e.g., to Bertoin [14] and Sato [78].

Definition 2.2.1 *A stochastic process $X = \{X_t, t \geq 0\}$ is called a Lévy process on $\mathbb{R}$ if the following conditions are satisfied:*

(i) $X_0 = 0$ *almost surely,*

(ii) *For any finite partition $0 \leq t_0 < t_1 \cdots < t_k \leq T$, the random variables $X_{t_k} - X_{t_{k-1}}, \cdots, X_{t_0}$ are independent,*

(iii) *X has stationary increments, for any $s, t \geq 0$ the distribution of $X_{t+s} - X_s$ does not depend on s,*

(iv) *For every $\omega \in \Omega, X_t(\omega)$ is right continuous and has left limits for $t > 0$.*

By sampling the process at regular time intervals, X_t can be rewritten as follows $X_t = \sum_{i=1}^{n} X_{t/n}^i$, where $X_{t/n}^i$ are stationary and i.i.d. random variables. It follows that this process is infinitely divisible.

Definition 2.2.2 *A random variable X_t with characteristic function $\Phi_t(u)$ has an infinitely divisible distribution if and only if $\forall\ n \in \mathbb{N}\ \exists\ \Phi^{(t/n)}(u)$, the characteristic function of some distribution, such that $\Phi_t(u) = \left(\Phi^{(t/n)}(u)\right)^n$.*

We denote by $\Psi(u)$ the characteristic exponent of a Lévy process at time $t = 1$.

Theorem 2.2.1 (Lévy-Khintchine representation) *$\Psi : \mathbb{R} \to \mathbb{C}$ is the characteristic exponent of an infinitely divisible distribution on $\mathbb{R}$ if and only if there exist unique $M, \Sigma \in \mathbb{R}$ and a unique measure Λ on $\mathbb{R}\backslash\{0\}$ with $\int \min\{1, x^2\}\Lambda(\mathrm{d}x) < \infty$ such that $\Phi_1(u) = \mathrm{e}^{\Psi(u)}$ and*

$$\Psi(u) = \mathrm{i}Mu - \frac{1}{2}\Sigma^2 u^2 + \int_{-\infty}^{+\infty} \left(-1 + \mathrm{e}^{\mathrm{i}ux} - \mathrm{i}ux1_{\{|x|<1\}}\right)\Lambda(\mathrm{d}x).$$

The triplet (M, Σ^2, Λ) is called the generating triplet of the distribution. Λ is known as the *Lévy measure*. The Lévy measure determines the frequency and the distribution of the jumps. If we set $\Lambda = 0$ and $\Sigma \neq 0$, the characteristic function is that of a normal random variable with the Gaussian coefficients (M, Σ^2). This theorem was proved in the 1930s by Kolmogorov [56] and Lévy [62]. The probabilistic meaning of the Lévy-Khintchine representation is explained by the Lévy-Itô decomposition, which describes the structure of the paths in terms of three auxiliary Lévy processes.

Theorem 2.2.2 (Lévy-Itô decomposition) *Let X be a Lévy process with a Lévy triplet (M, Σ^2, Λ) and Λ on $\mathbb{R}\backslash\{0\}$ satisfying $\int \min\{1, x^2\}\Lambda(\mathrm{d}x) < \infty$. There exist three independent Lévy processes X^1, X^2, X^3 on a probability space such that*

$$X_t = X_t^1 + X_t^2 + X_t^3,$$

where X^1 is a Brownian motion with drift M and volatility Σ, X^2 is a compound Poisson process, and X^3 is a square integrable martingale with an or most countable number of jumps on each finite interval which are of magnitude less than unity.

The proof is attributed to Itô [50] and Lévy [63]. □

In the following, we give some explicit examples of Lévy processes.

Example 2.2.1 (Poisson process) *The Poisson process* $\{N_t, t \geq 0\}$ *is a jump process with jumps of size one. The probability of* n *jumps in the interval* $[t_1, t_2]$ *is given by the Poisson density with parameter* $\lambda(t_2 - t_1)$,

$$P\left[N_{t_2} - N_{t_1} = n\right] = \frac{\mathrm{e}^{-\lambda(t_2-t_1)}\left(\lambda(t_2-t_1)\right)^n}{n!}.$$

The characteristic exponent of the Poisson process is given by

$$\Psi(u) = \mathrm{i}\lambda\left(\mathrm{e}^u - 1\right).$$

The Lévy triplet is $(0, 0, \lambda\delta_1)$ *where* δ_1 *is a Dirac measure.*

Example 2.2.2 (Compound Poisson process) *The compound Poisson process* $\{X_t, t \geq 0\}$ *is defined as follows*

$$X_t = \sum_{i=1}^{N_t} \xi_i,$$

where N *is a Poisson process with intensity* λ. ξ_i, $i \in \boldsymbol{N}$ *are i.i.d. random variables with density function* f *and characteristic function* $\phi(u)$. *Then the characteristic exponent of the compound Poisson process is given by*

$$\Psi(u) = \mathrm{i}\lambda\left(\phi(u) - 1\right).$$

The Lévy triplet is

$$\left(\lambda \int_{|x|\leq 1} x f(\mathrm{d}x), 0, \lambda f(\mathrm{d}x)\right).$$

Example 2.2.3 (Generalised hyper-exponential process) *The generalised hyper-exponential process* $\{X_t, t \geq 0\}$ *is defined as follows*

$$X_t = \mu t + \sigma W_t + \sum_{i=1}^{M_t} J_i^+ + \sum_{j=1}^{N_t} J_j^-,$$

with drift μ and volatility σ. M and N are two Poisson processes with intensity $\lambda^{\pm}$. $J^{\pm}$ are hyper-exponentially distributed with cumulative distributions

$$\begin{aligned} P[J^+ < x] &= \sum_{z=1}^{n^+} p_z^+ (1 - \mathrm{e}^{-\alpha_z^+ x}), \quad \text{for } x \in [0, \infty), \\ P[J^- < x] &= \sum_{z=1}^{n^-} p_z^- (1 - \mathrm{e}^{\alpha_z^- x}), \quad \text{for } x \in (-\infty, 0]. \end{aligned}$$

The characteristic exponent is given by

$$\Psi(u) = \mathrm{i}\mu u - \frac{\sigma^2}{2} u^2 + \lambda^+ \sum_{z=1}^{n^+} p_z^+ \frac{u\mathrm{i}}{\alpha_z^+ - u\mathrm{i}} - \lambda^- \sum_{z=1}^{n^-} p_z^- \frac{u\mathrm{i}}{\alpha_z^- + u\mathrm{i}}.$$

Example 2.2.4 (Variance gamma process) *The variance gamma process is a standard Brownian motion process with drift θ and volatility σ subject to a time-changed driven by a gamma process with mean 1 and variance ν. Based on the gamma and Brownian motion characteristic functions, the characteristic exponent is defined by*

$$\Psi(u) = \log \left[(1 - \mathrm{i}\theta u + \frac{1}{2}\sigma^2 u^2))^{-1} \right]^{-\nu^{-1}}.$$

Example 2.2.5 (Normal inverse Gaussian process) *The normal inverse Gaussian process is a standard Brownian motion process with a time change driven by an inverse Gaussian process. Based on the Brownian and inverse Gaussian characteristic functions, we derive the characteristic exponent*

$$\Psi(u) = -\delta(\sqrt{\alpha^2 - (\beta + \mathrm{i}u)^2} - \sqrt{\alpha^2 - \beta^2}.$$

2.3 Additive processes

Additive processes are described as Lévy processes with time-dependent characteristics or, equivalently, as processes with independent but non-stationary increments. For further reading, refer to Skorohod [82]

Definition 2.3.1 *For a given $T > 0$, a stochastic process $X = \{X_t, t \in [0, T]\}$ is called an additive process on $\mathbb{R}$ if the following conditions are satisfied:*

(i) $X_0 = 0$,

(ii) *For any finite partition $0 \leq t_0 < t_1 \cdots < t_k \leq T$, the random variables $X_{t_k} - X_{t_{k-1}}, \cdots, X_{t_0}$ are independent,*

(iii) *The sample paths $t \mapsto X_t$ have càdlàg modifications almost surely.*

If X is an additive process, then, for every $t \in [0, T]$, the random variable X_t has an infinitely divisible distribution with Lévy triplet $(M_t, \Sigma_t^2, \Lambda_t)$; that is, the characteristic function of X_t is given by $\Phi_t(u) = \exp[\Psi_t(u)]$. The law of the additive process X is determined by the collection of Lévy triplets $\{(M_t, \Sigma_t^2, \Lambda_t)$ for $t \in [0, T]\}$.

2.4 Pricing of barrier-options

Barrier and barrier-type options are derivatives with pay-offs that depend on whether a reference asset price has crossed a certain boundary. These options belong to the most widely-traded exotic options in the financial markets. In the equity markets, common examples are the knock-in and knock-out digital, call, and put options that are activated or de-activated when the underlying stock price process crosses a specified barrier level. Whereas knowledge of the marginal risk-neutral distribution of the underlying at maturity suffices to work out the prices of European call and put options, the valuation of barrier-options requires specification of the risk-neutral law of the underlying price process, since it depends on the first-passage distribution of this process.

To value barrier-options, a model needs to be sufficiently flexible to calibrate

call option prices at different strikes and maturities. Also, it is desirable to maintain a degree of analytical tractability to facilitate calculations, especially for the Greeks, or equivalently, the sensitivities. It is well known that accurate evaluation of the Greeks is a challenging numerical problem, since standard PDE or Monte-Carlo methods generally tend to be slow and unstable. For further reaing, we refer to Malliavin and Thalmaier [67]

In Chapters 4 and 5 we assume that the log-stock-price process is a Lévy process and an additive process, respectively. Based on the Wiener-Hopf factorisation we have developed transform algorithms to derive semi-analytical expressions for the first-passage time probabilities, for the prices, and for the Greeks of barrier-options. As numerical illustrations, we compare our results to Monte-Carlo simulations.

Chapter 3

Modelling stock pinning

3.1 Introduction

In this chapter we analyse the impact of option hedging strategies on both the drift and the volatility of the underlying stock price and show that dynamic hedging can be responsible for the pinning effect, i.e., the tendency of stock prices to close near the strike prices of heavily traded options as the expiration date nears. A thorough analysis of the pinning effect has been provided by Ni *et al.* [70], who analyse data from the Ivy DB dataset and from a second dataset obtained from the CBOE, from 1996 to 2002. The authors show that over this period, optionable stocks (i.e. stocks with listed options) close near the strike prices on expiration dates, both when the likely delta-hedgers have net purchased option positions and net written option positions. There is no corresponding effect for non-optionable stocks.[1]

Avellaneda & Lipkin [9] introduced the first pinning model by suggesting that stock pinning can be induced by delta-hedging long option positions. We extend their analysis following the approach of Frey & Stremme [43, 44]. Frey & Stremme considered the case of investors who hedge a short option position, which results in positive feedback and hence a destabilising effect around the option strike. In

[1] The CBOE database used by Ni *et al.* provides information, for each transaction, on whether the two parties trading are market makers, public customers, or firm proprietary traders. By assuming that the public customers do not hedge their option portfolio, Ni *et al.* infer from this database if the overall net position of the hedgers is long or short.

contrast, Platen & Schweizer [73] obtained a feedback model that is consistent with pinning, but their resulting equilibrium is highly unstable due to the assumption that the demand of non-hedgers is increasing in price. Here, we adapt the Frey & Stremme formulation of the problem to the case where investors hedge a long option position.

Both the Avellaneda-Lipkin and Frey-Stremme models make a number of assumptions on the dynamics of prices, on the continuous hedging, and on the price impact shape. We relax some of the assumptions of the original Frey-Stremme model and study pinning also when the hedging is discrete and the liquidity is stochastic. We show that while pinning may still arise, these two effects have a strong impact on the volatility of log-stock-price returns and on the pinning intensity. In order to investigate pinning under more realistic market conditions we study the impact of hedging strategies in a microstructure model, by adapting a zero-intelligence model introduced by Daniels *et al.* [32] and Smith *et al.* [83]. We show that the microstructure model generates pinning consistently with the theoretical models and the experimental findings.

In Sections 3.2 and 3.3 we revise the Avellaneda-Lipkin and Frey-Stremme models [9, 43] and highlight the mechanisms in the models that can induce pinning. We study a generalisation when the hedging is discrete and the liquidity is stochastic and compare our analysis to the one performed by Frey & Stremme. In Section 3.4 we describe the microstructure model and the results of numerical simulations.

3.2 Stock pinning and option pricing

We assume that the stock price process $S = \{S_t, t \geq 0\}$ is modelled by a stochastic differential equation of the form,

$$\mathrm{d}S_t = \mu S_t \mathrm{d}t + \sigma S_t \mathrm{d}W_t, \tag{3.1}$$

where μ is a constant drift, σ is a constant volatility, and W is a standard Brownian motion.

Black-Scholes formula (Call options) *The value of a European vanilla call option is given by*

$$C(S_t, T, K, \sigma, r) = S_t N(d_1) - Ke^{-r(T-t)} N(d_2),$$

with

$$d_{1,2} = \frac{\log(\frac{S_t}{K}) + (r \pm 1/2\sigma)^2(T-t)}{\sigma\sqrt{T-t}},$$

where r is the risk-free rate, K the option strike price and T the option maturity. $N(\cdot)$ is the normal distribution function. The number of shares to hold in order to hedge a position is given by the option delta, which is defined by $\Delta = \partial C/\partial S$. After the passage of a small interval of time, the amount of stock to buy or sell to maintain a delta-neutral position is given by $\mathrm{d}\Delta$.

Delta-hedging strategies create a feedback effect on the stock price by inducing an additional drift term in the diffusion equation given by (3.1), which becomes

$$\mathrm{d}S_t = \mu S_t \mathrm{d}t + n\hat{L} S_t \mathrm{d}\Delta(S,t) + \sigma S_t \mathrm{d}W_t. \tag{3.2}$$

In (3.2), $\hat{L}$ is a constant price elasticity and n is the open interest in the call option. Hence, $\hat{L}$ represents a linear impact of the hedgers on the stock price process. The model further assumes that traders do not take into account feedback effects when rebalancing their portfolios. The hedging strategy is based on the assumption that the stock price evolves according to a geometric Brownian motion model. In this case the delta for a long call position is $\Delta = -N(d_1)$.

The dynamics of $\Delta(S,t)$ can be derived by using Itô's Lemma, which gives

$$\mathrm{d}\Delta(S,t) = \frac{\partial \Delta(S,t)}{\partial t}\mathrm{d}t + \frac{\partial \Delta(S,t)}{\partial S}\mathrm{d}S_t + \frac{1}{2}\frac{\partial^2 \Delta(S,t)}{\partial S^2}\langle \mathrm{d}S_t \rangle, \tag{3.3}$$

where $\langle \mathrm{d}S_t \rangle$ denotes the quadratic variation of S_t.

Avellaneda & Lipkin [9] assume that the form of the price dynamics is given by

$$\mathrm{d}S_t = n\hat{L}\,\frac{\partial \Delta}{\partial t} S_t \mathrm{d}t + \sigma S_t \mathrm{d}W_t. \tag{3.4}$$

This can be interpreted as taking only the delta time-decay term in (3.3) above. The model generates pinning when traders hedge a long call position. The term $\partial\Delta/\partial t$ in (3.4) is given by

$$\frac{\partial\Delta}{\partial t} = -\frac{n(h_1)}{\sigma\sqrt{\tau}}\frac{\log y - a\tau}{2\tau}, \tag{3.5}$$

where $\tau = T - t$, $a = r + \sigma^2/2$, $y = S_t/K$, and

$$h_1 = \frac{\log y + a\tau}{\sigma\sqrt{\tau}}.$$

The right handside of equation (3.5) is positive for $y < \mathrm{e}^{-a\tau}$ and negative otherwise, as shown in Figure 3.1. This suggests that when the price is above the strike, $\mathrm{d}\Delta$ is negative, inducing the hedger to sell; and in doing so, the trader pushes the price towards the strike. Similarly when the price is below the strike, $\mathrm{d}\Delta$ is positive, inducing the hedger to buy; and in doing so, the trader again pushes the price towards the strike. This argument then suggests that pinning is possible when the trader hedges a long position. Hedging a short position would have the opposite effect, thus pushing the stock price away from the strike.

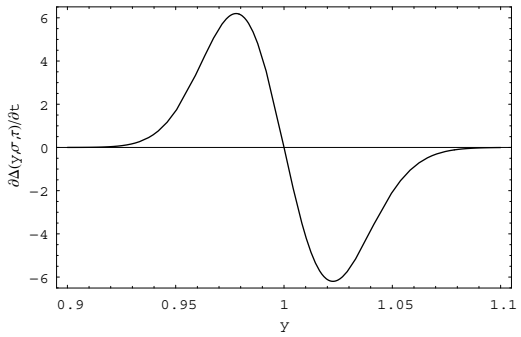

Figure 3.1: In Avellaneda-Lipkin model, the time-decay ($\partial\Delta/\partial t$) as a function of $y = S/K$ for $\tau = 5$ days, $\sigma = 0.16$ and $a = 0$.

3.3 Extensions of the Frey-Stremme model

Frey & Stremme [43, 44] instead consider all the terms in the delta expansion in (3.3), and obtain

$$\mathrm{d}S_t = n\hat{L}S_t\frac{\partial\Delta}{\partial S}\mathrm{d}S_t + n\hat{L}S_t\left(\frac{\partial\Delta}{\partial t}\mathrm{d}t + \frac{1}{2}\frac{\partial^2\Delta}{\partial S^2}\mathrm{d}\langle S_t\rangle\right) + \sigma S_t\mathrm{d}W_t,$$

or equivalently

$$\mathrm{d}S_t = \frac{n\hat{L}S_t}{\left(1 - n\hat{L}S_t\frac{\partial\Delta}{\partial S}\right)}\left(\frac{\partial\Delta}{\partial t}\mathrm{d}t + \frac{1}{2}\frac{\partial^2\Delta}{\partial S^2}\mathrm{d}\langle S_t\rangle\right) + \frac{\sigma S_t \mathrm{d}W_t}{1 - n\hat{L}S_t\frac{\partial\Delta}{\partial S}}.$$

Thus the stock price still follows a diffusion process,

$$\mathrm{d}S_t = b(t, S_t)S_t\mathrm{d}t + v(t, S_t)S_t\mathrm{d}W_t, \tag{3.6}$$

but with a new drift and volatility given by

$$b(t, S_t) = \frac{n\hat{L}}{1 - n\hat{L}S_t\frac{\partial\Delta}{\partial S}}\left\{\frac{\partial\Delta}{\partial t} + \frac{1}{2}\frac{\partial^2\Delta}{\partial S^2}\frac{\sigma^2 S_t^2}{[1 - n\hat{L}S_t\frac{\partial\Delta}{\partial S}]^2}\right\},$$

and

$$v(t, S_t) = \frac{\sigma}{1 - n\hat{L}S_t\frac{\partial\Delta}{\partial S}}.$$

Hence, the dynamic hedging strategy generates not only a change in the drift term, as suggested by Avellaneda & Lipkin [9], but also a change in the volatility term which is constant in the Avellaneda-Lipkin model [1]. The drift term $b(t, S_t)$ incorporates both the delta time-decay and the delta convexity. This drift term is plotted in Figure 3.2 on the right as a function of y for different values of $\hat{L}$. The denominator in the right hand side of the equation for $b(t, S)$ is always positive since we assume that traders hedge a long option position. For $\hat{L}$ sufficiently large, or sufficiently close to maturity, the drift term changes sign around $y = 1$, and generates pinning. When $\hat{L} \to 0$, $v(t, S_t) \to \sigma$, $b(t, S_t) \to 0$, and pinning does not arise. The volatility term reaches its minimum value for $y = 1$, i.e., when S is close to the strike, as shown in Figure 3.2 on the left. As $\hat{L}$ increases, the volatility term v decreases further, reducing random deviation from the strike. Furthermore as we approach the maturity date the drift term becomes stronger close to strike, while the volatility in Figure 3.3 on the left becomes smaller. The combined effect of these terms is not only driving the price towards the strike but also keeping it closer to the strike as it approaches it.

[1] In the Avellaneda-Lipkin model, nonetheless, the pinning strength has the effect of reducing the implied volatilities of options on the same months, with adjacent strikes, and of those of adjacent months.

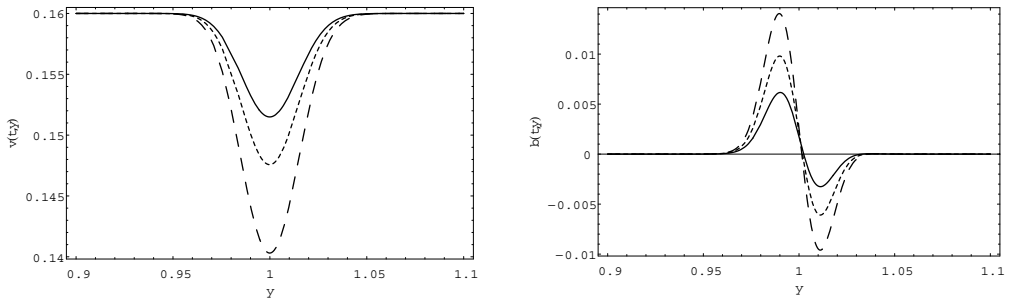

Figure 3.2: In the Frey-Stremme model, the volatility terms $v(t, y)$ on the left and the drift terms $b(t, y)$ on the right as a function of $y = S/K$. The time to maturity is three days. The three lines correspond to three price elasticities: $n\hat{L} = 0.002$ (solid), $n\hat{L} = 0.003$ (dash), $n\hat{L} = 0.005$ (dot).

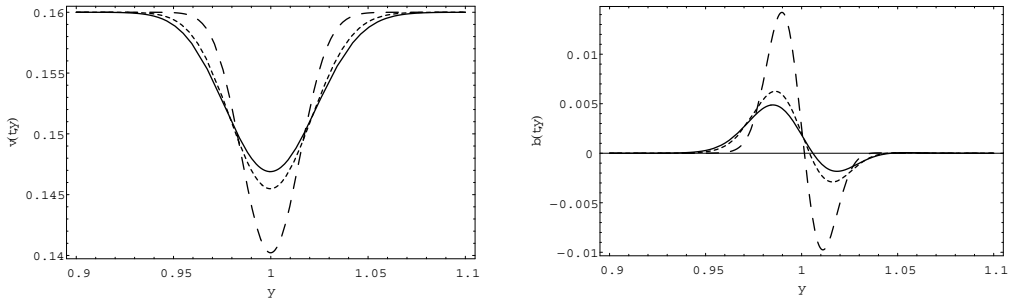

Figure 3.3: In the Frey-Stremme model, the volatility terms $v(t, y)$ on the left and the drift terms $b(t, y)$ on the right as a function of $y = S/K$. The price elasticity is $n\hat{L} = 0.005$. The three lines correspond to three different times to maturity: two days before maturity (dash), four days before maturity (dot), five days before maturity (solid).

To calculate the pinning probability we solve the Frey-Stremme model numerically. Given (3.6), the probability density function $p(t, y)$ of being at y at time t satisfies the forward Kolmogorov equation, so

$$\frac{\partial p(t,y)}{\partial t} = \frac{1}{2}\frac{\partial^2 p(t,y)}{\partial y^2} v(t,y)^2 - \frac{\partial p(t,y)}{\partial y} b(t,y) \tag{3.7}$$

with initial condition the delta function $\delta(\tau_0, y_0) = 1$. Equation (3.7) can be solved using an implicit scheme with an adjusted mesh as we approach maturity due to the singularity at $y = 1$ and $\tau = 0$.

Figure 3.4 shows the solution of the Kolmogorov equation with initial conditions $\tau_0 = 5$ days before maturity and $y_0 = 1.04$. On the left we plot the solution for the Frey-Stremme model and on the right the solution for the Avellaneda-Lipkin model. We see that in both cases the solution becomes bi-modal as nL increases with a pronounced pick at $y = 1$. Hence both models can explain pinning as driven by hedging long call positions but the effect is stronger in the Avellaneda-Lipkin model (3.5%) than in Frey-Sremme model (1.8%). Ni *et al.* estimate that pinning affects 2% of optionable stocks. Our choices of parameters give in both cases comparable values with the empirical result.

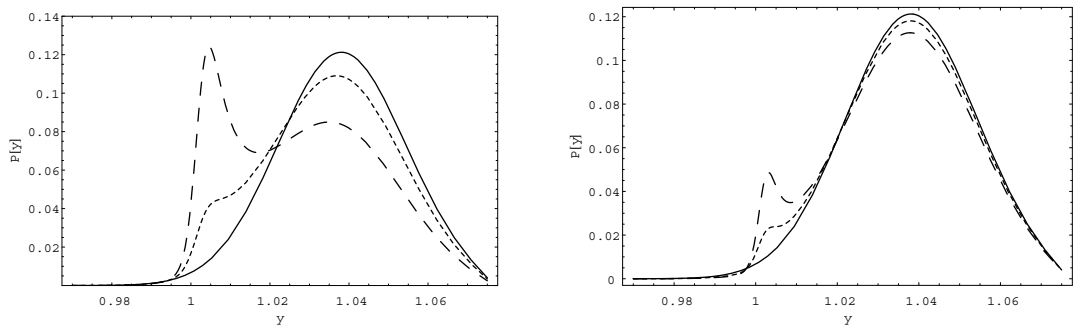

Figure 3.4: Solution of the Kolmogorov forward equation close to maturity, with initial condition, five days before maturity, $y_0 = 1.04$, and for three different hedging positions. On the left, Avellaneda model with $nL = 0$ (solid), $nL = 0.0005$ (small dash), $nL = 0.002$ (large dash). On the right, Frey-Stremme model with $nL = 0$ (solid), $nL = 0.002$ (small dash), $nL = 0.003$ (large dash).

A strong assumption behind the Frey-Stremme model and the Avellaneda-Lipkin model is that hedgers rebalance their positions continuously. If the hedging is discrete, the changes in Δ at the rebalancing dates would normally be larger than when the rebalancing is continuous. The price process in this case would be better modelled as a jump-diffusion process, that we write as

$$dS_t = \mu S_t dt + n\hat{L} S_t J(S_t, t) + \sigma S_t \mathrm{d}W_t \tag{3.8}$$

where

$$J(S_t, t) = \mathbf{1}_A(t)(\Delta(S_{t_k}, t_k) - \Delta(S_{t_{k-1}}, t_{k-1})) \quad \text{if} \quad t_k \in A, \tag{3.9}$$

and A is the set of hedging time. The jumps in (3.8) arrive at deterministic times but have a random size. In the Merton model jumps arrive through a Poisson process and the jump-size is normally distributed, with variance ξ. The conditional volatility of returns is given by $\sigma^2\tau + m\xi^2$ where m is the number of jumps in a period τ. In our case the jump distribution is not known, and it is price and time-dependent, so we cannot extend Merton arguments to derive an expression for the return volatility. Thus, to illustrate the effect of discrete hedging on pinning and on prices, we simulate (3.8) over a period

$$\Delta t = t_1 - t_0.$$

Then we measure the instantaneous drift and volatility (averaged over a period Δt and a number M of trajectories) all starting from the same initial condition S_0, that we write as

$$\mu_{\delta t}(S_0) = \frac{1}{M}\sum_{j=1}^{M} \mu_j, \tag{3.10}$$

$$\sigma_{\delta t}(S_0) = \frac{1}{M}\sum_{j=1}^{M} \sqrt{\frac{1}{m-1}\sum_{i=1}^{m}(r(t_i) - \mu_j)^2}, \tag{3.11}$$

where

$$\mu_j = \frac{1}{m}\log\frac{S^j_{t_0+\Delta t}}{S^j_{t_0}} \quad \text{and} \quad r(t_i) = \log(S_{t_i+\delta t}/S_{t_i}).$$

$\delta t = \Delta t/m$ and m is the number of steps between t_0 and t_1. For the curves plotted in Figure 3.5, we have chosen $M = 10,000$, $t_0 = 3$ days before maturity, and $\Delta t = 2$ days. The value $\Delta t = 2$ was chosen to allow the effect of hedging

to be sufficiently incorporated in the stock price, while being at the same time sufficiently short for the instantaneous volatility in (3.6) not to change too much. As shown in Figure 3.5, when we are hedging at all time-steps (log-dashed line), the model generates similar drift and volatility profiles as the ones generated by the continuous Frey-Stremme model. Nonetheless, when hedging is less frequent we observe a decrease in the drift term and, more surprisingly, a change of shape the volatility term. This change suggests that the volatility of returns increases, as in the Merton model, with the variance of the jumps, the last being plotted in Figure 3.6 (again averaged over the same period Δt). The high variance at $y = 1$ is a consequence of the steepness of the Δ around this point.

A recent paper by Pearson *et al.* [72] provides some empirical evidence for the CBOE where rebalancing of delta-hedges of purchased option positions has the effect of reducing stock return volatility. This suggests that at least in situations where markets are sufficiently liquid and delta-hedging sufficiently frequent the Frey-Stremme model is in agreement with the empirical findings and provides a good framework understanding stock pinning under more general situations.

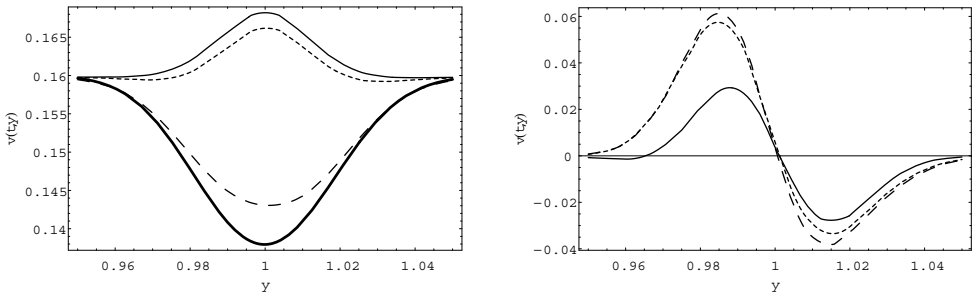

Figure 3.5: In the discrete hedging Frey-Stremme model, the volatility terms $v(t, y)$ on the left and the drift terms $b(t, y)$ on the right as a function of $y = S/K$. The time to maturity is $\tau = 3$ days and $n\hat{L} = 0.01$. The three lines correspond to three hedging frequencies: every tick (dash), eight times a day (dot), twice a day (continuous). Thick line on the left corresponds to the volatility in the Frey-Stremme model.

When the Frey-Stremme model is extended to account for discrete hedging, pinning still arises. However the pinning intensity decreases when the rebalance

frequency decreases as shown in Figure 3.7 on the right. In fact, when hedging less than four times a day, we find that the probability of ending close to the strike is lower than when no hedger is present (given by the straight line).

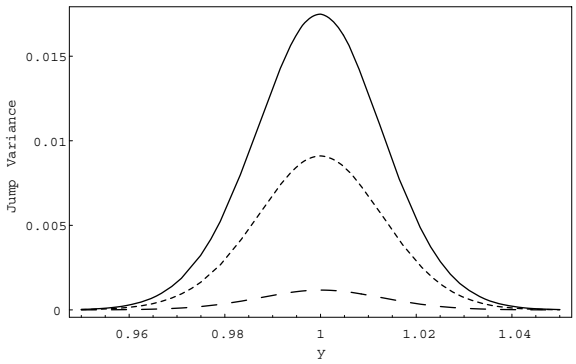

Figure 3.6: In the modified Frey-Stremme model, variance of the jump-size as a function of $y = S/K$. The time to maturity is $\tau = 3$ days and $n\hat{L} = 0.01$. The three lines correspond to three hedging frequencies: every tick (large dashed), eight times a day (small dash),four times a day (continuous).

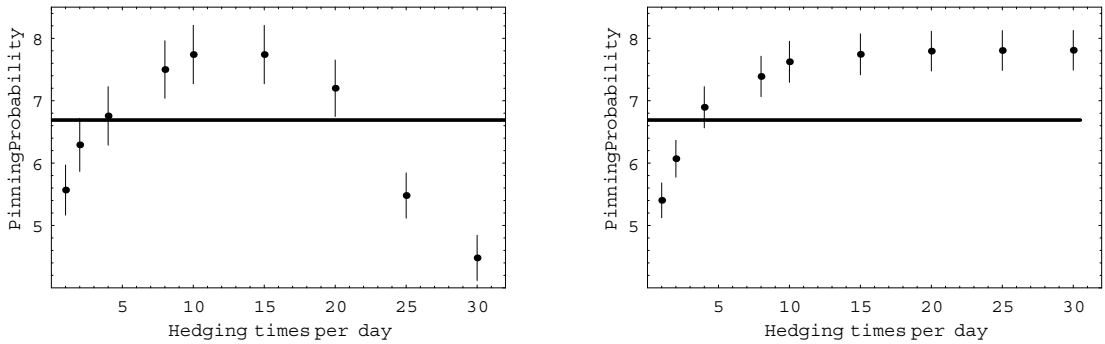

Figure 3.7: Pinning probabilities for $n\hat{L} = 0.01$ as a function of the number of times the traders hedge per day for stochastic liquidity ($z = 60\%$) on the left and deterministic liquidity on the right.

Another strong assumption in the Frey-Stremme model is that the price impact is linear and constant. Empirical studies on the NYSE done by Mantegna *et al.* [40] have shown nonetheless that the price impact function is always concave, typically well approximated by a function

$$dp(\omega) \sim \omega^{\alpha},$$

where dp is the price change caused by an order of volume ω. The exponent α varies from $\alpha \sim 0.5$ to $\alpha \sim 0.2$ depending on stock capitalisation. Furthermore this shape is found only on average. The impact from orders of the same size but submitted under different market conditions, i.e. for different configurations of the order book, can vary considerably. The Frey-Stremme model instead assumes that hedging orders of the same size have the same impact on the stock price.

To incorporate these effects into the Frey-Stremme model we have first studied the model with a price impact of the form $(n\hat{L}S_tJ(S_t,t))^{\alpha}$ for different values of α. A constant, but not linear, liquidity did not substantially change our results. A more interesting outcome is obtained when assuming a stochastic price impact as suggested for example by Esser & Mönch [39]. In particular we assume that the price impact follows a Cox-Ingersoll-Ross (CIR) process

$$\mathrm{d}\hat{L}_t = k(\hat{L}_t - \mu)\mathrm{d}t + z\sqrt{\hat{L}_t}\mathrm{d}W_t,$$

with mean reverting speed $k = 0.5$, mean reverting level $\mu = 1$. This assumption is justified later by the analysis of the microstructure model. In fact, to obtain the distribution of the log-stock-price returns for hedging orders equivalent to the microstructure model in Figure 3.14, we choose a volatility $z = 60\%$. Note that a smaller or higher volatility will give qualitatively the same results. The results of our simulations, plotted in Figure 3.7 on the left, suggest that in this case pinning may only arise for intermediate values of the hedging frequency. Furthermore, if z is sufficiently large, we find that the volatility of the log-stock-price returns increases around the strike also when hedging at every tick (Figure 3.8).

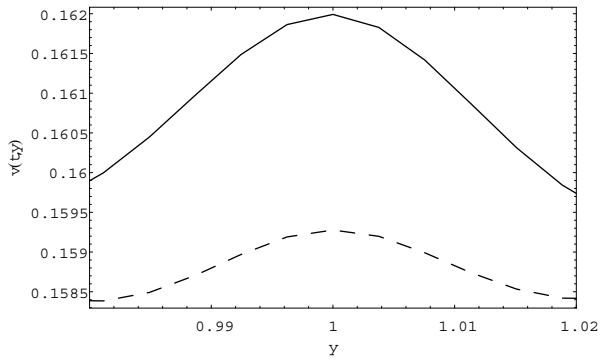

Figure 3.8: Stochastic liquidity effect on the volatility. The two lines correspond to different hedging frequencies: every tick (dash) and four times a day (continuous).

3.4 A microstructure model for stock pinning

The aim of this section is to introduce a microstructure limit-order model where a hedger rebalances his position at discrete times. Trading automatically generates an impact on the order book and on the stock price, and thus provides a more realistic way of determining the probability of pinning.

The model implemented here has been previously introduced in Daniels *et al.* [32]. Alternative microstructure models have been proposed for example by Chiarella & Iori [27], Challet & Stinchcombe [26], and Bouchaud *et al.* [17]. In the market, there exists a mismatch between buy (bid) orders and sell (offer) orders. The order book gives the list, at any given time, of all unmatched buy and sell orders with their relative price and volume. In Daniels *et al.*, the traders can submit only two types of orders on the market: limit orders and market orders. Limit orders are submitted at a specified price and stored in the book in waiting to be executed. Market orders are executed at the current best bid or ask price. If the supply at the best available price is not enough to fulfill the order, the remaining order is executed at the next available prices until the order is complete. A schematic representation of the trading mechanism is plotted in Figure 3.9.

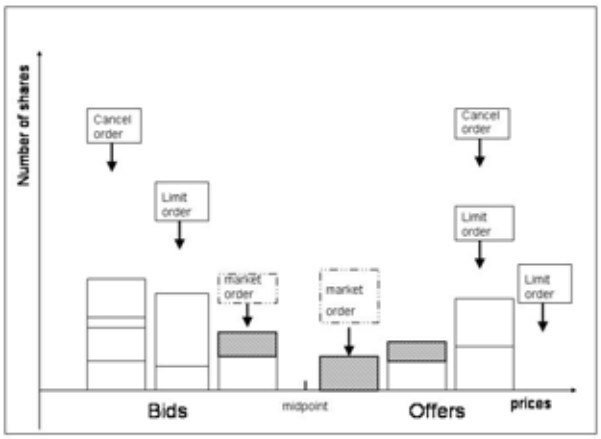

Figure 3.9: Schematic order book mechanism. Limit orders, market orders, and cancellation orders are coming to fulfill the order book (bids and offers).

Limit orders, market orders, and cancellation orders follow Poisson processes. It is assumed that limit orders arrive at a rate of α shares per unit price and per unit time. Similarly market orders arrive at a rate of ν shares per unit time, and with an equal probability for buy and sell market orders. Limit orders can also be removed spontaneously by being cancelled. In the model, this happens at a constant rate of δ per unit time. The size of the limit and market orders are sampled from a log-normal distribution with mean and variance one. The stock price at anytime t is defined as the mid-point $m(t) = (a(t) + b(t))/2$, where $a(t)$ and $b(t)$ are respectively the best ask and the best bid at time t. Prices change discretely at ticks of $\Delta p = 0.02$ cents. Thus bids and offers are placed at integer multiples of the tick size Δp on a window sufficiently large around the mid-point (in the simulations below this was chosen as 200 ticks on each side of the book).

Daniels *et al.* [32] shows that two parameters characterise the average shape of the book: the asymptotic depth α/δ and $\epsilon = 2\delta/\nu$. The asymptotic depth gives the number of shares per price interval far from the mid-point; ϵ determines the depth at the bid and at the ask. ϵ also determines the average price impact function, which is linear for $\epsilon > 0.1$ and concave for smaller values of ϵ. We have chosen the parameters of the model in order to reproduce the average order book shape and the statistical properties of prices for a traded stock (in this case

L'OREAL on August 2004). For the calibration we have used DataReuters. This software provides the flow of market orders, allowing us to estimate the market order arrival rate μ. Furthermore DataReuters gives the limit orders at the first five ticks on each side of the bid and ask. From this we can calculate the average book shape, and choose the parameters α and δ in order to recover approximately the slope of the book around the mid-point and the stock volatility. The calibrated rates are $\nu = 0.16$ (which implies in our case that market orders arrive with a frequency of about two a minute), $\alpha = 0.31$ per unit price and per unit time, and $\delta = 0.08$ per unit time. With these values we obtain a return volatility of about 15% per annum. For the calibrated values of the parameters the average impact function is linear ($\epsilon = 1$), in line with the assumptions of Frey & Stremme [43, 44]. We will later compare this case with a concave impact ($\epsilon = 0.025$).

To study pinning we initially focus on the impact of a trader who rehedges a long call position four times a day. The option expires in five days. In the model, hedging is achieved by submitting market orders and not limit orders because immediacy in execution is important for the hedger. When the stock price increases, the hedger places a market order to sell the variation of $\Delta(S,t)$, and when the stock price decreases, the trader places a market order to buy the variation of $\Delta(S,t)$. In Figure 3.10 we show that pinning still arises in the microstructure

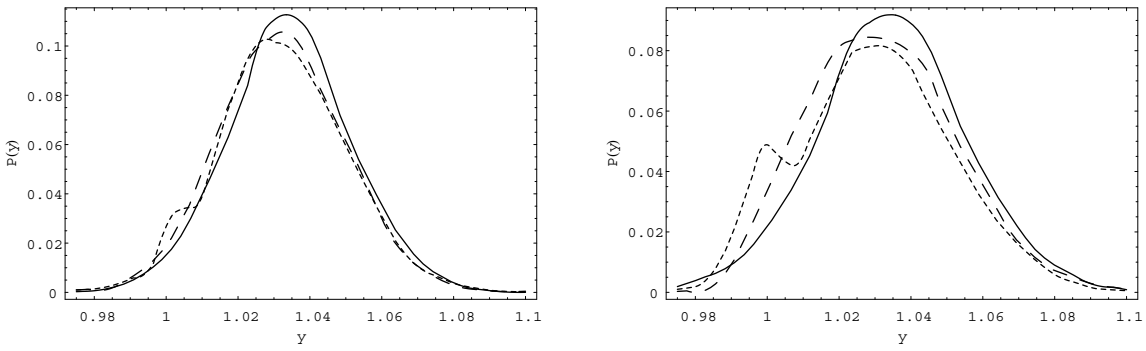

Figure 3.10: In the microstructure model, stock price distribution at maturity without the hedger (solid) and with the hedger $n = 600$ (dash) and $n = 1000$ (dot) for two different ϵ: $\epsilon = 0.025$ on the left, $\epsilon = 1$ on the right. The trader rebalances their position four times a day.

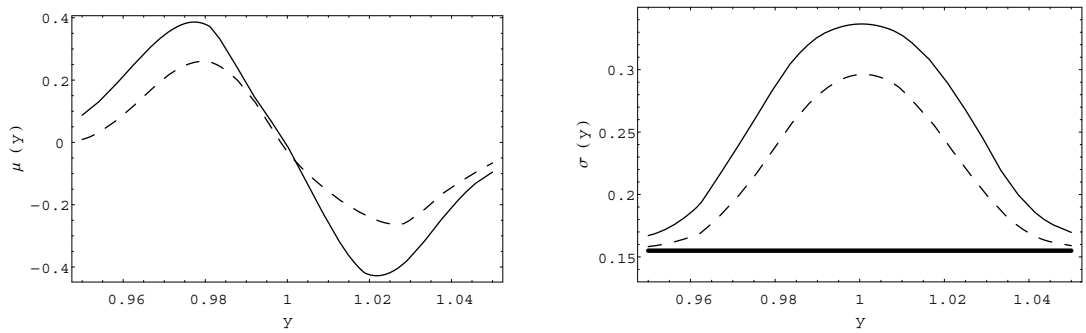

Figure 3.11: In the microstructure model, the drift terms on the left and the volatility terms on the right for two differents ϵ: $\epsilon = 0.025$ (dash), $\epsilon = 1$ (solid) for $n = 1000$ when the trader rebalances their position four times a day. The thick line on the right corresponds to the volatility without hedgers.

model as revealed by the increased probability to be at $y = 1$ when the hedger position increases. In the model the maximum amount of orders that the hedger can submit is limited by the overall trading activity in the market. In fact if the amount of orders submitted by the hedger is higher than the amount of orders submitted by the rest of the market, the book becomes empty. Hence there is a maximum option position that can be simulated, and a limit to the pinning generated by the microstructure model. Nonetheless the pinning probabilities we obtain in Figure 3.10 are comparable with the empirical findings. Figure 3.10 also shows that pinning is more likely to arise when ϵ is large (right), i.e., when the price impact is linear.

We then test if the mechanisms that generate pinning are consistent with the theoretical models. To this extent we study the behaviour of the instantaneous drift and volatility in the microstructure model, as defined in (3.10), (3.11), for the same choice of parameters as in the previous section ($M = 10,000$, $\Delta t = 2$ days, $t_0 = 3$ days before maturity). Figure 3.11 shows that without the hedger the volatility profile (thick solid line) is constant, as expected. When introducing discrete hedging we observe that the microstructure model generates a drift profile similar to the one in the Frey-Stremme model in Figures 3.2, 3.5. The volatility profile shows a maximum around the point $y = 1$ for both values of ϵ (Figure 3.11 on the right) and both when hedging four times a day or at each

time-step (Figure 3.12), in a similar way as in Figure 3.8.

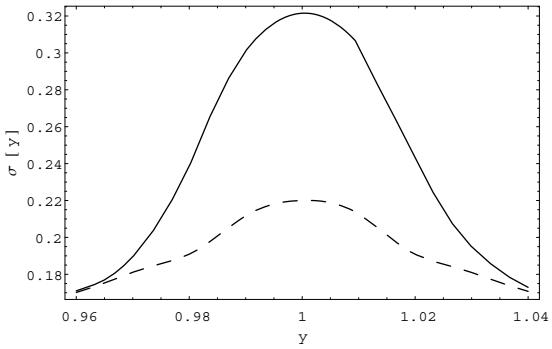

Figure 3.12: Hedging effect on volatility for $n = 1000$ with $\epsilon = 1$. The two lines correspond to hedging frequencies: each tick (dash), four times a day (continuous).

In Figure 3.13 we also show that the pinning intensity as a function of the hedging frequency has a similar profile as the one in Figure 3.7 on the left. Thus pinning in the microstructure model seems to be consistent with the Frey-Stremme model when both discrete hedging and stochastic liquidity effects are taken into account.

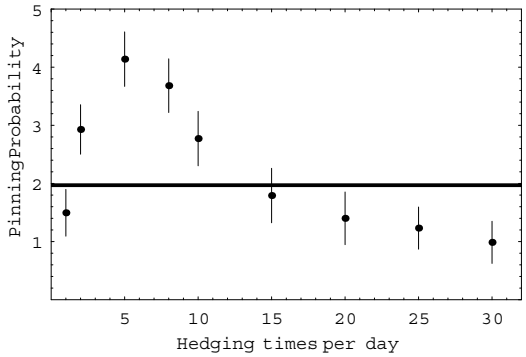

Figure 3.13: Pinning probabilities for $n = 1000$ with $\epsilon = 1$ as a function of the number of times the traders hedge per day.

The model is in fact characterized by a non-constant impact, as shown in Figure 3.14, where we plot as an example the price changes corresponding to hedging orders of the same size. The distribution is quite spread out with a variance that is consistent with the parameter z used in Figure 3.7.

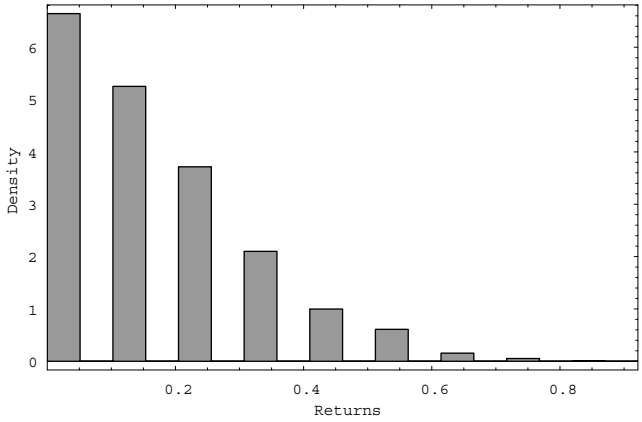

Figure 3.14: Distribution of log-stock-price returns for hedging orders of the same size at different times.

3.5 Concluding remarks

We conclude with the following remarks. In this chapter, we have compared different models that are all capable of generating pinning under different market conditions. The models share a common pinning mechanism, i.e. an excess drift generated by delta-hedging that pushes the stock price towards the strike.

We have shown that a simple microstructure model generates results that are consistent with the Frey-Stremme model when discrete hedging and stochastic volatility are taken into account. In particular we have shown that pinning can arise for a wide range of hedging frequencies even if the impact of hedging on the volatility of the underlying stock may differ.

It is reasonable to point out nonetheless that the results of the proposed models depend on the specific way in which hedge rebalancing is implemented. The assumption that hedgers do not take into account their own trading is an approximation in the Frey-Stremme model. If traders were capable of correcting their orders by taking into account the feedback effect of their own trades on prices, as they probably do in real markets, the impact of hedging on the volatility of the underlying stock and on the pinning probability may differ.

Chapter 4

A transform approach to compute the prices and Greeks of barrier options driven by a class of Lévy processes

4.1 Introduction

Barrier options are derivatives with pay-offs that depend on whether a reference price has crossed a certain boundary. The valuation of barrier options requires the specification of the risk-neutral law of the underlying price process. At least as important as the calculation of prices is the evaluation of the sensitivities of the prices to various model parameters (the Greeks) for which the law of the process is also required.

A class of models that has been shown to be capable of generating a good fit of observed call and put option price data is formed by the infinite-activity Lévy models. These include, for example, the extended Koponen or KoBoL [19], variance gamma [66], normal inverse Gaussian [12], and generalised hyperbolic processes [37]. In this chapter we consider barrier options driven by Lévy processes with a completely monotone Lévy densities on each half-axis which we call generalised hyper-exponential. This class contains many of the Lévy models used in financial modelling, such as the previously mentioned ones and also jump-diffusions with double-exponential jumps, as shown in Section 4.2.

The calculation of first-passage distributions and barrier option prices in specific Lévy models has been investigated in a number of papers. Geman & Yor [47] calculated prices and deltas of double-barrier options in the Black-Scholes model. For spectrally one-sided Lévy processes with a Gaussian component, Rogers [76] derived a method to evaluate first-passage distributions. Kou & Wang [59], Lipton [64], and Sepp [81] followed a transform approach to obtain barrier prices for a jump-diffusion with exponential jumps. In the setting of infinite-activity Lévy processes with jumps in two directions, Cont & Voltchkova [31] investigated the discretisation of the associated integro-differential equations; Boyarchenko & Levendorskiĭ [20] employed Fourier methods to investigate barrier option prices for Lévy processes of regular exponential type; Asmussen *et al.* [8] priced an equity default swap in a CGMY model, by fitting a hyper-exponential density to the CGMY Lévy density.

In this chapter we adopt the latter approach. As a first step we obtain, in a Lévy model with hyper-exponential jumps, analytical formulae for the Laplace transform in time of knock-in and knock-out barrier option prices by exploiting the availability of an explicit Wiener-Hopf factorisation. Using these results we also establish analytical formulae for the corresponding sensitivities with respect to the initial price (delta and gamma) and the time of maturity (theta) up to one Laplace transform in time. The actual barrier option prices and sensitivities are then obtained by numerically inverting these single Laplace transforms, using Abate & Whitt's algorithm [2], yielding fast and accurate results. Since hyper-exponential Lévy processes are dense in the class of generalised hyper-exponential Lévy processes, the idea is to approximate barrier option prices and sensitivities in a generalised hyper-exponential model by those in an appropriately chosen hyper-exponential Lévy model. At this point it is worth remarking that for a general Lévy process the Wiener-Hopf factors are not available in analytically tractable form (as they are expressed in terms of the one-dimensional distributions that are generally not available); and, furthermore, even if the Wiener-Hopf factors have been obtained a three-dimensional Laplace/Fourier inversion would be needed to obtain the knock-in and out call option prices (see e.g. [30, p. 372]).

Following the approach described in the previous paragraph barrier option prices and sensitivities under a generalised hyper-exponential Lévy model can, at least in principle, be approximated arbitrarily closely. Indeed, we shall prove that, when a sequence of hyper-exponential Lévy processes converges weakly to a given generalised hyper-exponential Lévy process of infinite-activity, the corresponding first-passage times converge in distribution, and the barrier-option prices and smoothed sensitivities converge pointwise to those of the limiting model.

We illustrate this approximation procedure by implementing it for the exponential variance gamma (VG) and normal inverse Gaussian (NIG) models, with parameters calibrated to Stoxx50E options. We determine the parameters of the approximating hyper-exponential Lévy densities by using a least-squares algorithm to minimise the root-mean-square error of the approximating density with respect to the target density over a grid, with seven upward and downward phases. The resulting hyper-exponential Lévy processes are employed as approximations to the VG and NIG processes.

We calculate the prices and sensitivities of European and American digital options and down-and-out put options following this approach, and also by Monte-Carlo simulations. We find a general agreement between the results, with relative errors in the range of 0.5-2.5% for prices and deltas, some distance away from the barrier. Numerical experiments show that closer to the barrier errors may be larger, especially for the delta, suggesting that a more accurate approximation of the target density by a hyper-exponential density is needed to reduce the size of the error, which can be achieved by increasing the number of phases or by employing one of the methods from the approximation theory of real-valued functions. The phenomenon of larger errors in the vicinity of the barrier is also observed by Kudryatsev & Levendorskiĭ [61] when approximating first-touch digital option prices under a NIG Lévy model using the Kou model. It would be desirable to analyse the dependence of the error on the different parameters and the distance to the barrier, and how the presented approach compares to alternative approaches such as finite difference schemes, but, in the interest of brevity, these questions are left for future research.

In Section 4.2 the generalised hyper-exponential Lévy model is defined and it is shown that many of the existing Lévy models used in quantitative finance are contained in this class. Results on the Wiener-Hopf factorisation and first-passage times for processes from this class can be found in Section 4.3. Analytical results for Laplace transforms in time of barrier-option prices are obtained in Section 4.4. Using these results explicit expressions are derived in Section 4.5 for the Laplace transforms of the theta, delta and gamma of the barrier and digital options. In Section 4.6 numerical results are presented for prices and sensitivities of barrier-options in a VG and a NIG model respectively, with convergence results presented in Section 4.7. Some proofs are relegated to the Appendix.

4.2 Log-Lévy models

We consider the model for the risk-neutral evolution of the stock price S given by $S_t = S_0 \exp(X_t)$ for $t \geq 0$. X is a Lévy process and can be described as a stochastic process with independent and homogeneous increments, normalised such that $X_0 = 0$. For background on the fluctuation theory of Lévy processes and the application of Lévy processes in quantitative finance we refer the reader to Bingham [15], Bertoin [14], and Cont & Tankov [30], respectively. We shall restrict ourselves to the following class of Lévy processes.

Definition 4.2.1 *A Lévy process is said to be generalised hyper-exponential (we denote this class of process by GHE) if its Lévy measure admits a density k of the form*

$$k(x) = k_+(x)\mathbf{1}_{\{x>0\}} + k_-(-x)\mathbf{1}_{\{x<0\}},$$

where k_+, k_- are completely monotone functions on $(0,\infty)$ and $\mathbf{1}_A$ denotes the indicator of a set A.

In view of Bernstein's theorem a Lévy process is a member of the class GHE if and only if its Lévy density k is of the form

$$k(x) = \mathbf{1}_{\{x>0\}} \int_0^\infty \mathrm{e}^{-ux}\mu_+(\mathrm{d}u) + \mathbf{1}_{\{x<0\}} \int_{-\infty}^0 \mathrm{e}^{-|ux|}\mu_-(\mathrm{d}u) \tag{4.1}$$

for some measures μ_+, μ_- on $(0,\infty)$ and $(-\infty,0)$ respectively. The mass of the interval $[a,b]$, under the measure μ_+, corresponds to the frequency of positive

exponential jumps of mean sizes between $1/a$ and $1/b$. A similar statement holds true for the negative jumps and μ_-. In the case that the measure μ_+ is a convex combination of point-masses, the locations $u_i > 0$ and sizes $p_i > 0$ of the point-masses respectively correspond to average size $1/u_i$ and frequency p_i of the exponential jumps. Below we show that many of the Lévy processes employed in financial modelling are generalised hyper-exponential by explicitly calculating the corresponding measures $\mu_\pm$. In particular, the class GHE contains the time-changes of Brownian motion by a generalised hyper-exponential subordinator.

Proposition 4.2.1 *Let W be a Brownian motion and Y an independent generalised hyper-exponential subordinator. Then, for $\mu \in \mathbb{R}$,*

$$X_t = W(Y_t) + \mu Y_t$$

is a Lévy process in the class GHE.

Proof of Proposition 4.2.1 Denoting by ρ the Lévy density of Y and μ_Y the measure in the representation (4.1), Theorem 30.1 in Sato [78] implies that the Lévy density k of X is given by

$$k(x) = \int_0^\infty \frac{1}{\sqrt{2\pi s}} \mathrm{e}^{-(x-\mu s)^2/(2s)} \rho(s) \mathrm{d}s.$$

An interchange of the order of integration yields

$$\begin{aligned} k(x) &= \int_0^\infty \frac{1}{\sqrt{2\pi s}} \mathrm{e}^{-(x-\mu s)^2/(2s)} \int_0^\infty \mathrm{e}^{-su} \mu_Y(\mathrm{d}u)\mathrm{d}s \\ &= \int_0^\infty \int_0^\infty \frac{1}{\sqrt{2\pi s}} \mathrm{e}^{-(x-\mu s)^2/(2s)} \mathrm{e}^{-su} \mathrm{d}s \mu_Y(\mathrm{d}u) \\ &= \int_0^\infty \frac{1}{\sqrt{\mu^2+2u}} \mathrm{e}^{-|x|\sqrt{\mu^2+2u}+\mu x} \mu_Y(\mathrm{d}u), \end{aligned}$$

and the claim follows. □

The following result gives necessary and sufficient conditions on the measures μ_+, μ_- such that k in (4.1) is a Lévy density.

Proposition 4.2.2 *Let μ be a measure on $\mathbb{R}\backslash\{0\}$ and set*

$$\mu_\pm(\mathrm{d}x) = \mathbf{1}_{\{\pm x>0\}} \mu(\mathrm{d}x).$$

Then k defined in (4.1) is a Lévy density if and only if

$$\int \frac{1}{|u|} \wedge \frac{1}{|u|^3}\, \mu(\mathrm{d}u) < \infty. \tag{4.2}$$

Proof of Proposition 4.2.2 By interchanging the order of integration it can be verified that

$$\begin{aligned} \int_1^\infty \int_0^\infty \mathrm{e}^{-ux} \mu(\mathrm{d}u)\mathrm{d}x &= \int_0^\infty \frac{\mathrm{e}^{-u}}{u} \mu(\mathrm{d}u), \\ \int_0^1 x^2 \int_1^\infty \mathrm{e}^{-ux} \mu(\mathrm{d}u)\mathrm{d}x &= \int_1^\infty \frac{2}{u^3} - \frac{\mathrm{e}^{-u}}{u}\left(1 + \frac{2}{u} + \frac{2}{u^2}\right) \mu(\mathrm{d}u). \end{aligned}$$

Further we note that

$$\int_0^1 x^2 \int_0^1 \mathrm{e}^{-ux} \mu(\mathrm{d}u)\mathrm{d}x$$

is bounded below and above by $\mu(0,1)/3\mathrm{e}$ and $\mu(0,1)/3$, respectively. In view of these calculations we read off that k in (4.1) satisfies the integrability condition

$$\int [1 \wedge x^2] k(x)\mathrm{d}x < \infty,$$

which is the requirement for k to be a Lévy density if and only if (4.2) holds. □

In the following examples, we explicitly determine the measures $\mu_\pm$. We shall write k_+ for the density k restricted to the positive half-axis.

Example 4.2.1 (Double-exponential model) *See [57]. For a jump-diffusion model where the jumps follow a double-exponential distribution, μ_+ is a point-mass located at the reciprocal of the mean jump-sizes*

$$k_+(x) = \lambda^+ \alpha^+ \mathrm{e}^{-\alpha^+ x}, \qquad \mu_+(\mathrm{d}u) = \lambda^+ \alpha^+ \delta_{\alpha^+}(\mathrm{d}u),$$

where $\alpha^+, \lambda^+ > 0$.

Example 4.2.2 (Hyper-exponential model) *See [7]. This model is an extension of Kou's model by allowing for exponential jumps with a finite number of different means. For p_i^+, α_i^+, and $\lambda^+ > 0$ with $\sum_{i=1}^n p_i^+ = 1$ we thus get*

$$k_+(x) = \lambda^+ \sum_{i=1}^n p_i^+ \alpha_i^+ \mathrm{e}^{-\alpha_i^+ x}, \qquad \mu_+(\mathrm{d}u) = \lambda_+ \sum_{i=1}^n p_i^+ \alpha_i^+ \delta_{\alpha_i^+}(\mathrm{d}u).$$

Example 4.2.3 (KoBoL/CGMY model) *See* [19, 22]. *In the* KoBoL *model (also called* CGMY *model), the measure μ has a continuous density k, and it holds that*

$$k_+(x) = \frac{C}{|x|^{Y+1}} \mathrm{e}^{-M|x|}, \qquad \mu_+(\mathrm{d}u) = C\frac{(u-M)^Y}{\Gamma(1+Y)} \mathbf{1}_{\{u \geq M\}} \mathrm{d}u,$$

where $C, M, Y > 0$. The form of μ_+ invokes the definition of the gamma function

$$\frac{1}{x^{Y+1}} = \int_0^\infty \mathrm{e}^{-ux} \frac{u^Y}{\Gamma(1+Y)} \mathrm{d}u.$$

In particular, for the variance gamma model, we set $Y = 0$ and get

$$k_+(x) = Cx^{-1}\mathrm{e}^{-Mx} \quad \textit{and} \quad \mu_+(\mathrm{d}u) = C\mathbf{1}_{\{u \geq M\}} \mathrm{d}u.$$

Example 4.2.4 (Meixner model) *See* [80]. *The Lévy density of a Meixner Lévy process is given by*

$$k_+(x) = \frac{\delta \mathrm{e}^{\beta x/\alpha}}{x \sinh(\pi x/\alpha)} = 2\mathrm{e}^{\beta x a - \pi|x|/\alpha} \sum_{n=0}^\infty \frac{\mathrm{e}^{-2\pi n|x|/\alpha}}{|x|}, \quad x \neq 0,$$

where $\delta, \alpha > 0$, $-\pi < \beta < \pi$, so we find that

$$\mu_+(\mathrm{d}u) = 2\delta \sum_{n=0}^\infty \mathbf{1}_{\{u \geq (2\pi n + \pi - \beta)/\alpha\}} \mathrm{d}u.$$

Example 4.2.5 (Normal inverse Gaussian (NIG)) *See* [12]. *In the* NIG *model, the measure μ has a density which reads*

$$k_+(x) = \frac{C\delta\alpha}{\pi} \mathrm{e}^{\beta x} \frac{K_1(\alpha x)}{x}, \qquad \mu_+(\mathrm{d}u) = \frac{C\delta\alpha}{\pi} ([u+\beta]/\alpha)^2 - 1)^{1/2} \mathbf{1}_{\{u \geq \alpha - \beta\}} \mathrm{d}u,$$

where $\alpha > \beta > 0$, $\delta, C > 0$ and K_1 is the Mcdonald function. The form of μ_+ is based on the following representation (see [4]*) of K_1*

$$K_1(x) = x \int_1^\infty \mathrm{e}^{-xv} (v^2 - 1)^{1/2} \mathrm{d}v.$$

Example 4.2.6 (Generalised hyperbolic (GH)) *See* [37]. *The* GH *process can be represented as a time-change of Brownian motion by a generalised inverse Gaussian* (GIG) *subordinator. The Lévy density of* GIG *is a generalised gamma convolution which means in particular that it is of the form* (4.1).

4.3 First-passage theory

First-passage distributions are an essential element in the valuation of barrier-options. In this section we briefly review elements of the first-passage theory for Lévy processes that will be needed in what follows.

4.3.1 Wiener-Hopf factorisation

The distributions of the running supremum and the running infimum of X are linked to the distribution of X_t via the famed Wiener-Hopf factorisation of the Lévy exponent of X, denote by

$$\Psi(u) = \log E[\mathrm{e}^{\mathrm{i}uX_1}].$$

For $v \in \mathbb{C}$, let $\Im(v)$ denote the imaginary part of u.

Definition 4.3.1 *A Wiener-Hopf factorisation of Ψ is a pair of characteristic functions F_q^+, F_q^- of infinitely divisible distributions on the positive and negative half-line, that satisfy, for $u \in \mathbb{R}$ and $q > 0$, the relation*

$$q(q - \Psi(u))^{-1} = F_q^+(u)F_q^-(u), \tag{4.3}$$

where, for fixed $q > 0$, $u \mapsto F_q^{\pm}(u)$ are continuous and non-vanishing on $\pm\Im(u) \geq 0$ and analytic on $\pm\Im(u) > 0$ with $F_q^{\pm}(0) = 1$, and

$$\lim_{\substack{|u|\to\infty \\ \Im(u)=0}} u^{-1} \log F_q^{\pm}(u) = 0. \tag{4.4}$$

Denote by $\overline{X}_t$ and $\underline{X}_t$ the running supremum and infimum of X up to time t,

$$\overline{X}_t = \sup_{s\leq t} X_s, \qquad \underline{X}_t = \inf_{s\leq t} X_s,$$

and let $q^{-1}\Phi_q^+$, $q^{-1}\Phi_q^-$ be the respective Fourier-Laplace transforms

$$\Phi_q^+(u) = \int_0^\infty q\mathrm{e}^{-qt}E[\mathrm{e}^{\mathrm{i}u\overline{X}_t}]\mathrm{d}t, \qquad \Phi_q^-(u) = \int_0^\infty q\mathrm{e}^{-qt}E[\mathrm{e}^{\mathrm{i}u\underline{X}_t}]\mathrm{d}t.$$

It is not hard to verify that $\Phi_q^{\pm}$ satisfy the condition (4.4). Rogozin [77] established the following result.

Theorem 4.3.1 (Rogozin) $\Phi_q^+(u), \Phi_q^-(u)$ *is the unique Wiener-Hopf factorisation of* Ψ.

If the Lévy measure has support in both half-axes the factorisation is generally not explicitly known, except if the Lévy measure of X is of a particular form. The observation that the Wiener-Hopf factorisation and related first-passage distributions are tractable for a random walk in the case that the jump distribution on the positive half-axis follows an exponential distribution can already be found in Feller [42].

See also the books by Borovkov [16] and Asmussen [6] for background on the Wiener-Hopf factorisation for random walks. Mordecki [69] and Lipton [64] calculated the Laplace transforms of first-passage time distributions for a Lévy process with hyper-exponential jumps. Asmussen *et al.* [7] derived explicitly the Wiener-Hopf factorisation if the jump distributions of the Lévy process are of phase-type.

In the sequel we will employ the known factorisation results for a jump-diffusion with Lévy density also to be called a hyper-exponential jump-diffusion (HEJD) given by

$$k(x) = \lambda^+ \sum_{i=1}^{n^+} p_i^+ \alpha_i^+ \mathrm{e}^{-\alpha_i^+ x} \mathbf{1}_{\{x>0\}} + \lambda^- \sum_{j=1}^{n^-} p_j^- \alpha_j^- \mathrm{e}^{-\alpha_i^- x} \mathbf{1}_{\{x<0\}}, \tag{4.5}$$

where $\alpha_i^\pm, \lambda^\pm p_i^+ > 0$ with $\sum_{i=1}^{n^\pm} p_i^\pm = 1$. The corresponding Lévy exponent reads as

$$\Psi(u) = \mu u\mathrm{i} - \frac{\sigma^2}{2}u^2 + \lambda^+ \sum_i p_i^+ \left(\frac{\alpha_i^+}{\alpha_i^+ - u\mathrm{i}} - 1\right) + \lambda^- \sum_j p_j^- \left(\frac{\alpha_j^-}{\alpha_j^- + u\mathrm{i}} - 1\right). \tag{4.6}$$

The function Ψ in (4.6) can be analytically extended to the complex plane except the finite set

$$\{-\mathrm{i}\alpha_i^+, \mathrm{i}\alpha_i^-, i = 1, \ldots, n^\pm\},$$

and this extension will also be denoted by Ψ. Denoting by $\rho_i^+ = \rho_i^+(q)$, $i = 1, \ldots, m^+$ and $\rho_j^- = \rho_j^-(q)$, $j = 1, \ldots, m^-$ the roots of

$$\Psi(-\mathrm{i}s) = q$$

with positive and negative real parts respectively, the Wiener-Hopf factors Φ_q^+ and Φ_q^- are explicitly given as follows:

$$\Phi_q^+(u) = \frac{\prod_{i=1}^{n^+}\left(1-\frac{u\mathrm{i}}{\alpha_i^+}\right)}{\prod_{i=1}^{m^+}\left(1-\frac{u\mathrm{i}}{\rho_i^+(q)}\right)}, \qquad \Phi_q^-(u) = \frac{\prod_{j=1}^{n^-}\left(1+\frac{u\mathrm{i}}{\alpha_j^-}\right)}{\prod_{j=1}^{m^-}\left(1-\frac{u\mathrm{i}}{\rho_j^-(q)}\right)}.$$

Note that as a consequence of the intermediate value theorem and the fact that $s \mapsto \Psi(-\mathrm{i}s)$ is a rational function with real coefficients and single poles, it follows that the roots of the equation $\Psi(-\mathrm{i}s) = q$ are all real and distinct if $q \in \mathbb{R}_+$. Performing a partial fraction decomposition and termwise inverting the terms yields that the time-Laplace transforms of the distributions of $\overline{X}_t$ and $\underline{X}_t$ are given by[1]

$$\int_0^\infty \mathrm{e}^{-qt} P(\overline{X}_t \le z)\mathrm{d}t = \frac{1}{q}\left(1 - \sum_{i=1}^{m^+} A_i^+ \mathrm{e}^{-\rho_i^+(q)z}\right), \qquad z \ge 0, \tag{4.7}$$

$$\int_0^\infty \mathrm{e}^{-qt} P(-\underline{X}_t \le z)\mathrm{d}t = \frac{1}{q}\left(1 - \sum_{j=1}^{m^-} A_j^- \mathrm{e}^{\rho_j^-(q)z}\right), \qquad z \ge 0, \tag{4.8}$$

where the coefficients A_i^+ and A_j^- are given by

$$A_i^+ = \frac{\prod_{v=1}^{n^+}\left(1-\frac{\rho_i^+(q)}{\alpha_v^+}\right)}{\prod_{v=1,v\neq i}^{m^+}\left(1-\frac{\rho_i^+(q)}{\rho_v^+(q)}\right)}, \quad A_j^- = \frac{\prod_{v=1}^{n^-}\left(1+\frac{\rho_j^-(q)}{\alpha_v^-}\right)}{\prod_{v=1,v\neq j}^{m^-}\left(1-\frac{\rho_j^-(q)}{\rho_v^-(q)}\right)}.$$

4.3.2 Generalised hyper-exponential Lévy processes

For a generalised hyper-exponential Lévy process X the Wiener-Hopf factorisation is in general not known explicitly. However, due to its special form (4.1), its Lévy density can be approximated arbitrarily close by a hyper-exponential density (by approximating the measures $\mu_\pm$ by sums of point-masses), and for the resulting hyper-exponential Lévy process the Wiener-Hopf factorisation is explicitly given in the previous section. As hyper-exponential Lévy processes are

[1] In the case that there are multiple roots, which might be the case for some complex values of q, it is still possible to perform a partial fraction decomposition which results in similar but slightly different expressions – see Remark 4 in [7].

'dense' in the class GHE, the Wiener-Hopf factorisation of X can be approximated arbitrarily accurately using this idea.

More formally, a sequence of approximating processes $(X^{(n)})_n$ can be explicitly constructed as follows. Denote by k and σ^2 the Lévy density and the diffusion coefficient of X, respectively. Fix a sequence $(\varepsilon_n)_n$ of positive numbers converging to zero, and, for every n, let $(u_i)_i = (u_i^{(n)})_i$ and $(v_j)_j = (v_j^{(n)})_j$ be two finite partitions of $(0,\infty)$ with vanishing mesh[1] and let $(\Delta_i^+)_i = (\Delta_i^{+(n)})_i$, $(\Delta_j^-)_j = (\Delta_j^{-(n)})_j$ be two finite sets of positive weights, shortly to be determined. Set the approximating density equal to

$$k_n(y) = \mathbf{1}_{\{y>0\}} \sum_i \mathrm{e}^{-yu_i} \Delta_i^+ + \mathbf{1}_{\{y<0\}} \sum_j \mathrm{e}^{yv_j} \Delta_j^-. \tag{4.9}$$

For a given n, the partitions $(u_i)_i$ and $(v_j)_j$ and the weights $(\Delta_i^+)_i$, $(\Delta_j^-)_j$ are chosen such that the mass of k in the tails and the L^2 distance between the target density k and the approximating density k_n on a closed bounded set not containing zero is smaller than ε_n, that is,

$$\int_{\mathbb{R}\setminus A_n} k(y)\mathrm{d}y < \varepsilon_n, \qquad \int_{A_n\setminus B_n} (k(y)-k_n(y))^2 \mathrm{d}y < \varepsilon_n,$$

for some open bounded set A_n, B_n with $0 \in B_n \subset A_n \subset \mathbb{R}$. These requirements can be fulfilled since k has finite mass on the set $\{|y|>1\}$ and takes the special form (4.1). Set $X^{(n)}$ equal to the Lévy process with Lévy density k_n and Gaussian coefficient σ_n^2, where

$$\sigma_n^2 = \sigma^2 + \int_{-v_1^{(n)}}^{u_1^{(n)}} y^2 (k(y) - k_n(y))_+ \mathrm{d}y, \tag{4.10}$$

and with drift μ_n chosen such that $E[\mathrm{e}^{X^{(n)}(1)}] = \mathrm{e}^{r-d}$. The approximating processes $X^{(n)}$ constructed in this way can be shown to converge weakly to X. [2] Convergence of the barrier-option prices corresponding to log-stock-price $X^{(n)}$

[1] A partition $(t_i)_{i=1}^m$ of $(0,\infty)$ is an increasing set of times $0 < t_1 < t_2 \ldots$. The mesh of (t_i) is defined as $\max_{1\le i\le m} |t_i - t_{i-1}|$.

[2] This convergence takes place in the space $D(\mathbb{R}_+)$ endowed with the Skorokhod topology. A proof of this fact is given in Appendix 4.9.3, Lemma 4.9.1.

rests on the fact[1] that the weak convergence of $X^{(n)}$ to X carries over to convergence of the running supremum, infimum and the crossing times

$$T^{(n)}(x) = \inf\{t \geq 0 : X_t^{(n)} \leq x\} \qquad \text{and} \qquad T(x) = \inf\{t \geq 0 : X_t \leq x\},$$

as summarised in the following result.

Proposition 4.3.1 *Let X be generalised hyper-exponential and let $X^{(n)}$ be as defined. For $T > 0$, $(X_T^{(n)}, \overline{X}_T^{(n)})$ converges in distribution to $(X_T, \overline{X}_T)$ as $n \to \infty$. In particular, if X is not of type A,[2] it holds for $t > 0$ and $z > 0$ that*

$$P(\overline{X}_t^{(n)} \leq z) \to P(\overline{X}_t \leq z), \quad P(-\underline{X}_t^{(n)} \leq z) \to P(-\underline{X}_t \leq z), \tag{4.11}$$

$$P(T^{(n)}(-z) \leq t) \to P(T(-z) \leq t), \tag{4.12}$$

as $n \to \infty$.

4.4 Laplace transforms of barrier-option prices

In this section we employ the Wiener-Hopf factorisation results to derive the values of single barrier-options in a hyper-exponential Lévy model. We shall restrict ourselves to down-and-out and down-and-in digital and put options, but related options (such as up-and-in call options) can be derived similarly.

4.4.1 Digital options

A digital option is a derivative that pays €1 if the price of the underlying stock has up-crossed or down-crossed a level H before a maturity time T, with pay-off occurring either directly at the moment of crossing or at the maturity time T. We will derive the values of down-and-out and down-and-in digital options and denote by $EDOD$ and $EDID$ the respective prices corresponding to payment at maturity. We also consider the American version of the down-and-out digital option (denoted by $ADID$) that pays out at the moment of crossing the barrier.

[1] A proof is given in Appendix 4.9.3, Lemma 4.9.2.

[2] A Lévy process is called of type A (see Sato [78], p. 65) if its Lévy measure has finite mass and no Brownian motion is present. Type A Lévy processes are the compound Poisson processes added to a possibly zero deterministic drift.

The following result gives the Laplace transforms of the digital prices when $S_0 > H$. Denote by $\widehat{f}$ the Laplace transform of f:

$$\widehat{f}(q) = \int_0^\infty \mathrm{e}^{-qt} f(t)\mathrm{d}t.$$

Proposition 4.4.1 *If $q > 0$ and $H < S_0$ it holds that*

$$\begin{aligned}
\widehat{EDID}(q) &= \frac{1}{q+r}\sum_{j=1}^{k^-} A_j^- \left(\frac{S_0}{H}\right)^{\rho_j^-}, \\
\widehat{ADID}(q) &= \frac{q+r}{q}\widehat{EDID}(q), \qquad \widehat{EDOD}(q) = \frac{1}{q+r} - \widehat{EDID}(q).
\end{aligned}$$

where $\rho_j^- = \rho_j^-(q+r)$.

Proof of Proposition 4.4.1 Since the riskless rate of return is assumed to be constant and equal to r, it follows by standard no-arbitrage pricing arguments that the price of the down-and-in digital option is given by

$$EDID(T) = EDID(T; S_0, H) = \mathrm{e}^{-rT} P[\underline{X}_T \leq \log(H/S_0)], \tag{4.13}$$

where we have switched to log-scale. Also, if we denote the log-barrier $h = \log(H/S_0)$ then

$$ADID(T) = ADID(T; S_0, H) = E[\mathrm{e}^{-rT(h)} \mathbf{1}_{\{\underline{X}_T \leq h\}}].$$

Taking now the Laplace transforms of these expressions in T and combining with the first-passage distributions given in Section 5.3 we find if $h < 0$:

$$\begin{aligned}
\widehat{EDID}(q) &= \int_0^\infty \mathrm{e}^{-(q+r)T} P[\underline{X}_T \leq h]\mathrm{d}T = \int_0^\infty \mathrm{e}^{-(q+r)T} P[T(h) \leq T]\mathrm{d}T \\
&= \frac{1}{q+r}\int_{-h}^\infty \sum_{j=1}^{k^-} A_j^-(-\rho_j^-)\mathrm{e}^{\rho_j^- y}\mathrm{d}y = \frac{1}{q+r}\sum_{j=1}^{k^-} A_j^- \mathrm{e}^{-\rho_j^- h}, \\
\widehat{ADID}(q) &= \int_0^\infty \mathrm{e}^{-qT} E[\mathrm{e}^{-rT(h)} \mathbf{1}_{\{\underline{X}_T \leq H\}}]\mathrm{d}T = E\left[\int_0^\infty \mathrm{e}^{-qT - rT(h)} \mathbf{1}_{\{T(h) \leq T\}}\mathrm{d}t\right] \\
&= \frac{1}{q} E[\mathrm{e}^{-(q+r)T(h)}] = \frac{q+r}{q}\int_0^\infty \mathrm{e}^{-qT}\{\mathrm{e}^{-rT} P[T(h) \leq T]\}\mathrm{d}T.
\end{aligned}$$

The last identity follows by noting that $EDOD = \mathrm{e}^{-rT} - EDID$. □

4.4.2 Knock-out and knock-in put options

A down-and-out put pays out at maturity T the strike K less the value of the stock S_T (if this difference is positive) with the added feature that the put is worthless if the price of the stock has been below a level H by time T. In the next result we derive the Laplace transform in the maturity T of down-and-out put $DOP(T) = DOP(T; S_0, K, H)$. The value of the down-and-in put is presented in Appendix 4.9.1.

Proposition 4.4.2 *Let $q > 0$ and write the log-barrier $h = \log(H/S_0)$, the log-strike $\ell = \log(K/S_0)$. Then it holds that*

$$\widehat{DOP}(q) = \frac{1}{q+r} K C^{(0)}(\ell, h) - \frac{S_0}{q+r} C^{(1)}(\ell, h),$$

where, if $h < \ell < 0$,

$$\begin{aligned} C^{(b)}(\ell, h) &= \sum_{j=1}^{k^-} \sum_{i=1}^{k^+} \frac{\rho_i^+(-\rho_j^-)}{(\rho_j^- - \rho_i^+)(b - \rho_i^+)} A_i^+ A_j^- (\mathrm{e}^{(b-\rho_i^+)\ell + (\rho_i^+ - \rho_j^-)h} - \mathrm{e}^{(b-\rho_j^-)\ell}) \\ &+ \left(1 - \sum_{i=1}^{k^+} \frac{b}{b - \rho_i^+} A_i^+\right) \sum_{j=1}^{k^-} A_j^- \frac{(-\rho_j^-)}{\rho_j^- - b} (\mathrm{e}^{(b-\rho_j^-)h} - \mathrm{e}^{(b-\rho_j^-)\ell}) \end{aligned}$$

and, if $h < 0 < \ell$,

$$\begin{aligned} C^{(b)}(\ell, h) &= \sum_{j=1}^{k^-} \sum_{i=1}^{k^+} \frac{\rho_i^+(-\rho_j^-)}{(\rho_j^- - \rho_i^+)(b - \rho_i^+)} A_i^+ A_j^- \mathrm{e}^{(b-\rho_i^+)\ell} (\mathrm{e}^{(\rho_i^+ - \rho_j^-)h} - 1) \\ &+ \left(1 - \sum_{i=1}^{k^+} \frac{b}{b - \rho_i^+} A_i^+\right) \left(1 + \sum_{j=1}^{k^-} A_j^- \left(\frac{(-\rho_j^-)}{\rho_j^- - b} \mathrm{e}^{(b-\rho_j^-)h} - \frac{b}{\rho_j^- - b}\right)\right) \\ &+ \left(1 - \sum_{j=1}^{k^-} A_j^-\right) \sum_{i=1}^{k^+} \frac{\rho_i^+}{b - \rho_i^+} A_i^+ \mathrm{e}^{(b-\rho_i^+)\ell}, \end{aligned}$$

with $\rho_i^+ = \rho_i^+(q+r)$ and $\rho_j^- = \rho_j^-(q+r)$.

It is easy to check that in the case of exponential upward and downward jumps ($n^\pm = 1$) this result agrees with those obtained by Kou & Wang [59] and Sepp [81].

Proof of Proposition 4.4.2 By the theory of no-arbitrage-pricing it follows that an arbitrage-free price for the down-and-out barrier-option is given by

$$\begin{aligned} DOP(T;S_0,K,H) &= \mathrm{e}^{-rT}E[(K-S_T)^+\mathbf{1}_{\{\underline{S}_T>H\}}] \\ &= \mathrm{e}^{-rT}KP[\underline{X}_T>h, X_T<\ell] \\ &\quad -\mathrm{e}^{-rT}S_0E[\mathrm{e}^{X_T}\mathbf{1}_{\{\underline{X}_T>h, X_T<\ell\}}], \end{aligned} \tag{4.14}$$

where the log-barrier $h=\log(H/S_0)$ and the log-strike $\ell=\log(K/S_0)$. Denoting by $\tau=\tau(q+r)$ an independent random time with an exponential distribution with parameter $q+r$, the Laplace transform $\widehat{DOP}(q)$ of $DOP(T;S_0,K,H)$ can be compactly represented as

$$\begin{aligned} \widehat{DOP}(q) &= K\int_0^\infty \mathrm{e}^{-(q+r)T}P[\underline{X}_T>h, X_T<\ell]\mathrm{d}T \\ &\quad -S_0\int_0^\infty \mathrm{e}^{-(q+r)T}E[\mathrm{e}^{X_T}\mathbf{1}_{\{\underline{X}_T>h,\ X_T<\ell\}}]\mathrm{d}T \\ &= \frac{K}{q+r}P[\underline{X}_\tau>h,\ X_\tau<\ell]-\frac{S_0}{q+r}E[\mathrm{e}^{X_\tau}\mathbf{1}_{\{\underline{X}_\tau>h,\ X_\tau<\ell\}}]. \end{aligned} \tag{4.15}$$

To calculate the quantities

$$\begin{aligned} C^{(b)}(h,\ell) &:= E[\mathrm{e}^{bX_\tau}\mathbf{1}_{\{\underline{X}_\tau>h,\ X_\tau<\ell\}}] \\ g(y,b) &:= E[\mathrm{e}^{b\overline{X}_\tau}\mathbf{1}_{\{\overline{X}_\tau<y\}}] \end{aligned}$$

we shall appeal to the following two key properties:

(i) $\underline{X}_\tau$ and $X_\tau-\underline{X}_\tau$ are independent and

(ii) the pairs $(\overline{X}_\tau,\overline{X}_\tau-X_\tau)$ and $(X_\tau-\underline{X}_\tau,-\underline{X}_\tau)$ are identically distributed.

In view of (i) it follows that

$$\begin{aligned} C^{(b)}(h,\ell) &= E[\mathrm{e}^{b(X_\tau-\underline{X}_\tau)}\mathrm{e}^{b\underline{X}_\tau}\mathbf{1}_{\{-\min\{k,0\}<-\underline{X}_\tau<-h\}}\mathbf{1}_{\{X_\tau-\underline{X}_\tau+\underline{X}_\tau<k\}}] \\ &= \int_{-\min\{k,0\}}^{-h}\mathrm{e}^{-by}E[\mathrm{e}^{b(X_\tau-\underline{X}_\tau)}\mathbf{1}_{\{X_\tau-\underline{X}_\tau<k+y\}}]P(-\underline{X}_\tau\in\mathrm{d}y) \\ &= \int_{-\min\{\ell,0\}}^{-h}\mathrm{e}^{-by}g(\ell+y,b)f_{-\underline{X}_\tau}(y)\mathrm{d}y+g(\ell,b)P[\underline{X}_\tau=0], \end{aligned}$$

where we have used property (ii) in the last line. Inserting the explicit form of the distribution of $\overline{X}_\tau$, we find that for $y > 0$

$$\begin{aligned} g(y,b) &= \int_{0+}^{y} \mathrm{e}^{bz} f_{\overline{X}_\tau}(z)\mathrm{d}z + P[\overline{X}_\tau = 0] \\ &= \sum_{i=1}^{k^+} \frac{\rho_i^+}{b-\rho_i^+} A_i^+ (\mathrm{e}^{(b-\rho_i^+)y} - 1) + 1 - \sum_{i=1}^{k^+} A_i^+. \end{aligned}$$

The next step is to integrate $g(\ell + y, b)$ against $f_{-\underline{X}_\tau}$. If $\ell < 0$, this yields

$$\begin{aligned} C^{(b)}(h,\ell) &= \sum_{j=1}^{k^-}\sum_{i=1}^{k^+} \frac{\rho_i^+(-\rho_j^-)}{b-\rho_i^+} A_i^+ A_j^- \int_{-\ell}^{-h} (\mathrm{e}^{(b-\rho_i^+)(\ell+y)+(\rho_j^- - b)y} - \mathrm{e}^{(\rho_j^- - b)y})\mathrm{d}y \\ &+ \left(1 - \sum_{i=1}^{k^+} A_i^+\right) \sum_{j=1}^{k^-} A_j^-(-\rho_j^-) \int_{-\ell}^{-h} \mathrm{e}^{(\rho_j^- - b)y}\mathrm{d}y, \end{aligned}$$

and in the case that $\ell > 0$, it holds that

$$\begin{aligned} C^{(b)}(h,\ell) &= \sum_{j=1}^{k^-}\sum_{i=1}^{k^+} \frac{\rho_i^+(-\rho_j^-)}{b-\rho_i^+} A_i^+ A_j^- \int_{0}^{-h} (\mathrm{e}^{(b-\rho_i^+)(\ell+y)+(\rho_j^- - b)y} - \mathrm{e}^{(\rho_j^- - b)y})\mathrm{d}y \\ &+ \left(1 - \sum_{i=1}^{k^+} A_i^+\right) \sum_{j=1}^{k^-} A_j^-(-\rho_j^-) \int_{0}^{-h} \mathrm{e}^{(\rho_j^- - b)y}\mathrm{d}y \\ &+ \left(1 - \sum_{j=1}^{k^-} A_j^-\right) \left(\sum_{i=1}^{k^+} \frac{\rho_i^+}{b-\rho_i^+} A_i^+ (\mathrm{e}^{(b-\rho_i^+)\ell} - 1) + 1 - \sum_{i=1}^{k^+} A_i^+\right). \end{aligned}$$

It is then a straightforward matter of some calculus to arrive at the stated expressions. □

4.5 Calculating sensitivities

The analytical formulae for the barrier and digital prices in the previous section suggest the possibility of calculating the corresponding sensitivities by direct differentiation. In this section we make this idea precise by providing regularity results. The delta and gamma sensitivities of the option price with respect to the initial stock price S_0 will be denoted by

$$\Delta_V = \frac{\partial V}{\partial S_0}, \qquad \Gamma_V = \frac{\partial^2 V}{\partial S_0^2},$$

where $V = V(T, S_0)$ is the value function of the option under consideration (digital or down-and-out put). The sensitivity Θ_V with respect to the maturity T (the theta) is defined by a function that satisfies

$$V(T) - V(0) = \int_0^T \Theta_V(s)\mathrm{d}s,$$

for all $T > 0$. If V is continuously differentiable with respect to T then this definition is equivalent to $\Theta_V = \partial V/\partial T$. The first result in this direction concerns the theta of a digital option.

Lemma 4.5.1 *Let X be a general Lévy process not of type A. Then, for $q > 0$, $S_0 > H$ and $T > 0$,*

$$\begin{aligned} \widehat{\Theta}_{EDID}(q) &= q\widehat{EDID}(q), \\ \Theta_{ADID}(T) &= \Theta_{EDID}(T) + rEDID(T). \end{aligned}$$

Proof of Lemma 4.5.1 Since the map $F : [0,\infty) \to [0,\infty)$ given by $F(t) = P(T(x) \leq t)$ is an increasing function with $F(0) = 0$ it holds that

$$\int_0^\infty \mathrm{e}^{-qt}\mathrm{d}F(t) = q\int_0^\infty \mathrm{e}^{-qt}F(t)\mathrm{d}t. \tag{4.16}$$

Further, Lemma 49.3 in Sato [78] implies that $P(T(h) = t) = 0$ for $h < 0$, $t > 0$, for Lévy processes X not of type A, so that F is continuous. If we denote by f a density of F it follows that $\widehat{f}(q) = q\widehat{F}(q)$. In view of the form of the pay-off of the digital we deduce that

$$\widehat{\Theta}_{EDID}(q) = (q+r)\widehat{EDID}(q) - r\widehat{EDID},$$

and the assertion follows. The second equation follows from the relation between $EDID$ and $ADID$ given in Proposition 4.4.1. □

In the case of a Gaussian component $\sigma > 0$ general results are available in the literature regarding the smoothness and regularity of the solutions of partial integro-differential equations that imply, by the Feynman-Kac representation, that the value functions of the barrier-options are smooth (see Bensoussan & Lions [13] and Garroni & Menaldi [46]).

More specifically, for a hyper-exponential Lévy process with $\sigma > 0$ it holds that F with $F : (t,h) \mapsto P(\underline{X}_\tau \leq h)$ is an element of $C^{1,2}((0,\infty)\times(-\infty,0))$ and $G : (t,h,k) \mapsto P(\underline{X}_\tau > h, X_\tau < k)$ satisfies $G \in C^{1,2,2}((0,\infty)\times(-\infty,0)^2)$. In view of the probabilistic representations (4.13) and (4.14), this result directly implies that the delta and gamma of $EDID$ and DOP are well defined. The Laplace transforms of the delta and gamma of $EDID$ are given as follows:

Proposition 4.5.1 *Suppose X is a hyper-exponential Lévy process with $\sigma > 0$ and let $q > 0$ and $H < S_0$. Then we have*

$$\begin{aligned}\widehat{\Delta}_{EDID}(q) &= \frac{1}{q+r}\frac{1}{S_0}\sum_{j=1}^{k^-}\rho_j^- A_j^-(S_0/H)^{\rho_j^-},\\ \widehat{\Gamma}_{EDID}(q) &= \frac{1}{q+r}\frac{1}{S_0^2}\sum_{j=1}^{k^-}\rho_j^-(\rho_j^- - 1)A_j^-(S_0/H)^{\rho_j^-}.\end{aligned}$$

Proof of Proposition 4.5.1 Letting $H < c < S_0$, the fundamental theorem of calculus implies that

$$\begin{aligned}\frac{\partial}{\partial S_0}\widehat{EDID}(q) &= \frac{\partial}{\partial S_0}\int_0^\infty\int_c^{S_0}\Delta_{EDID}(t,y)\mathrm{d}y\mathrm{d}t\\ &= \frac{\partial}{\partial S_0}\int_c^{S_0}\int_0^\infty\Delta_{EDID}(t,y)\mathrm{d}t\mathrm{d}y = \widehat{\Delta}_{EDID}(q),\end{aligned}$$

where the change of the order of integration is justified (by Fubini's theorem) since $\Delta_{EDID} \geq 0$, and the last equality follows since

$$\widehat{EDID}(q) = \widehat{EDID}(q;S_0)$$

is continuously differentiable as a function of S_0. The form of the delta follows now from Proposition 4.4.1. The result for the gamma follows by similar reasoning as above, where the interchange of integration is justified since $\mathrm{e}^{-qt}|\Gamma_{EDID}(t,S_0)|$ is dominated by an integrable function (on $(0,\infty)\times(c,S_0)$).
To show the latter fact we note first that since $EDID$ is smooth enough it satisfies the partial integro-differential equation that reads in terms of the Greeks of $EDID$ as

$$\left[\Theta + \tfrac{\sigma^2}{2}S^2\Gamma + \mu S\Delta - (\lambda_+ + \lambda_- + r)EDID\right](t,S) + I(t,S) = 0,$$

for $t > 0, S > H > 0$, with boundary values $EDID(t,S) = 1$ for $S \leq H, t \in (0,T]$, and $EDID(0,S) = 1$ if $S \leq H$, and zero otherwise. Here I is the non-local part of the generator, given by

$$I(t,S) = \int_{-\infty}^{\infty} EDID(t, S\mathrm{e}^y)k(y)\mathrm{d}y.$$

Since $EDID \leq 1$ and the measure $k(y)\mathrm{d}y$ has finite mass, it thus follows that

$$|\Gamma_{EDID}(t,S)| \leq C(1 + |\Delta_{EDID}(t,S)| + |\Theta_{EDID}(t,S)|),$$

for some constant C. Further, as $\Delta_{EDID} \geq 0$, the integral

$$\int_0^{\infty} \int_c^x \mathrm{e}^{-qt}|\Delta_{EDID}(t,y)|\mathrm{d}y\mathrm{d}t$$

is for $H < c < x$ equal to

$$\int_c^x \widehat{\Delta}_{EDID}(t,y)\mathrm{d}y,$$

which is finite in view of the form of the delta. Similarly, it follows that

$$\int_0^{\infty} \int_c^x \mathrm{e}^{-qt}|\Theta(t,y)|\mathrm{d}y < \infty$$

and the proof is complete. □

Given the sensitivities of $EDID$, those of $ADID$ are calculated as follows:

Corollary 4.5.1 *Let $\sigma > 0$. For $q > 0$ and $H < S_0$ it holds that*

$$\begin{aligned} \Delta_{ADID}(T) &= \Delta_{EDID}(T) + r\int_0^T \Delta_{EDID}(s)\mathrm{d}s, \\ \Gamma_{ADID}(T) &= \Gamma_{EDID}(T) + r\int_0^T \Gamma_{EDID}(s)\mathrm{d}s. \end{aligned}$$

Proof of Corollary 4.5.1 The assertions follow the relation between $EDID$ and $ADID$ given in Proposition 4.4.1, and using that $\widehat{f}(q)/q$ is the Laplace transform of $\int_0^T f(s)\mathrm{d}s$. □

Following an analogous approach, similar formulae can be derived for the sensitivities of down-and-out put options; the results are reported in Appendix 4.9.2.

4.6 Numerical results

When the log-stock-price process is modelled by a generalised hyper-exponential Lévy process, we use the following algorithm to compute single barrier-option prices and corresponding sensitivities:

Algorithm

1. Approximate the target Lévy density by a hyper-exponential density.
2. Calculate the Laplace transforms of prices and sensitivities using the formulae in Sections 4.4 and 4.5.
3. Apply a Laplace inversion algorithm to the result of step 2.

Comments

Ad 1. Similarly as in Asmussen *et al.* [8] we specified the form of the density (4.5) by fixing the number of exponentials $n^{\pm}$ and the mean jump-sizes $(\alpha_i^+)^{-1}, (\alpha_j^-)^{-1}$ and then using a least-squares algorithm to determine the values of the remaining parameters p_i^+, p_j^- and λ_i^+, λ_j^- that minimise the squared distance between the density (4.5) and the target density. To improve the accuracy of the fit one could employ methods from the approximation theory of real-valued functions, or alternatively follow the approach developed by Feldmann & Whitt [41].

Ad 2. The roots of the characteristic exponent that appear in the formulae of the Laplace transforms were calculated using Laguerre's method (see e.g. Numerical Recipes [74]).

Ad 3. The quantity of interest V can be expressed in terms of the Laplace transform $\widehat{V}(q)$ by the Bromwich integral

$$V(T) = \frac{1}{2\pi \mathrm{i}} \int_{c-\mathrm{i}\infty}^{c+\mathrm{i}\infty} \mathrm{e}^{qT} \widehat{V}(q) dq. \tag{4.17}$$

To evaluate the integral (4.17) we employed the algorithm investigated by Abate & Whitt [2], which is based on approximation of the integral (4.17) by Euler summation with the trapezium rule that leads to the series

$$V(T) \approx \sum_{k=0}^{M} \binom{m}{k} 2^{-m} s_{N+k}(T),$$

where

$$s_n(T) = \frac{e^{A/2}}{2T}\mathrm{Re}\left[\widehat{V}\left(\frac{A}{2T}\right)\right] + \frac{e^{A/2}}{2T}\sum_{k=1}^{n}(-1)^k\mathrm{Re}\left[\widehat{V}\left(\frac{A+2k\pi\mathrm{i}}{2T}\right)\right].$$

Abate & Whitt [2] recommend the values: $M = 15$, $N = 11$, $A = 18.4$, where N should be increased if necessary.

We have implemented the above algorithm in the context of a variance gamma (VG) model and a normal inverse Gaussian (NIG) model to calculate the prices and the sensitivities of digital barrier-options and down-and-out put options. The parameters of the VG and NIG models were determined by calibrating the models to market quoted Stoxx50E call prices on 16 June 2006, using the fast Fourier transform (FFT) algorithm proposed by Carr & Madan [23]. This procedure yielded the following parameter values $C = 0.925$, $G = 4.667$, and $M = 11.876$ for the variance gamma model, and $\alpha = 8.858$, $\beta = -5.808$, $\delta = 0.174$ for the normal inverse Gaussian model. We employed these parameters in the subsequent calculations of barrier-option prices and sensitivities.

NIG	α_i^+	5	10	15	25	30	60	80	λ^+	5.1
	p_i^+	0.005	0.005	0.01	0.06	0.12	0.19	0.61	σ^2	0.042
	α_j^-	5	10	15	25	30	60	80	λ^-	6.4
	p_j^-	0.05	0.03	0.11	0.08	0.10	0.40	0.23	μ	0.15
VG	α_i^+	5	10	15	25	30	60	80	λ^+	2.2
	p_i^+	0.003	0.007	0.21	0.08	0.26	0.19	0.25	σ^2	0.011
	α_j^-	2	5	10	30	50	80	100	λ^-	3
	p_j^-	0.01	0.09	0.31	0.31	0.10	0.08	0.10	μ	0.13

Table 4.1: Parameter values for the approximation of the VG ($C = 0.925, G = 4.667, M = 11.876$) and NIG ($\alpha = 8.858, \beta = -5.808, \delta = 0.174$) Lévy densities.

As an initial step, the Lévy densities of the VG and NIG processes were approximated by hyper-exponential densities of the form (4.5) with fourteen different exponentials, seven upward phases ($n^+ = 7$), and seven downward phases ($n^- = 7$). Note that the parameters α_i^+ and α_j^- are equal to the reciprocals of the mean

sizes of upward and downward jumps of the (hyper-exponential) log-stock-price, respectively. The values of α_i^+ and α_j^- were fixed as in Table 4.1. The remaining parameters λ^+, λ^-, and the p_i^+, p_j^- were determined by using a least squares algorithm to minimise the sums of squares of the difference between the target density and the hyper-exponential density (4.5) over a time-grid inside the interval $[0.1, 5]$. The resulting parameter values of the hyper-exponential density are specified in Table 4.1.

	Normal inverse Gaussian Down-and-out put option									
Spot	Price			Delta			Gamma		Theta	
	LT	MC	RE	LT	MC	RE	LT	MC	LT	MC
			%	$\cdot 10$	$\cdot 10$	%	$\cdot 10^{-3}$	$\cdot 10^{-3}$		
64	486.8	(493, 507)	2.7	9.07	(9.20, 9.68)	4.1	-8.56	(-9.15, -8.98)	-360	(-365,-342)
66	532.7	(537, 551)	2.1	4.37	(4.14, 4.61)	0.3	-5.32	(-5.47, -5.31)	-373	(-377,-356)
68	551.8	(555, 568)	1.7	1.27	(1.07, 1.33)	5.1	-3.68	(-3.75, -3.60)	-369	(-373,-351)
70	552.6	(555, 567)	1.5	-0.92	(-1.10, -0.86)	6.9	-2.65	(-2.65, -2.51)	-354	(-358,-338)
72	540.4	(542, 553)	1.3	-2.51	(-2.70, -2.47)	3.1	-1.93	(-2.06, -1.92)	-333	(-338,-318)
74	518.6	(518, 530)	1.2	-3.66	(-3.85, -3.62)	2.2	-1.37	(-1.35, -1.22)	-309	(-316,-297)
76	490.0	(490, 501)	1.1	-4.45	(-4.62, -4.40)	1.4	-0.92	(-0.95, -0.91)	-281	(-286,-267)
78	456.9	(456, 467)	1.0	-4.96	(-5.13, -4.92)	1.4	-0.53	(-0.54, -0.50)	-250	(-255,-237)
80	421.2	(420, 430)	0.9	-5.21	(-5.37, -5.16)	1.2	-0.19	(-0.19, -0.14)	-217	(-224,-206)
82	384.6	(382, 393)	0.8	-5.24	(-5.40, -5.20)	1.3	0.10	(0.04, 0.12)	-181	(-187,-169)
84	348.4	(346, 356)	0.6	-5.08	(-5.25, -5.04)	1.3	0.33	(0.30, 0.38)	-145	(-147,-129)
86	313.8	(310, 321)	0.5	-4.79	(-4.97, -4.77)	1.7	0.49	(0.37, 0.49)	-110	(-112,-95)
88	281.5	(278, 287)	0.3	-4.41	(-4.59, -4.39)	2.0	0.58	(0.57, 0.69)	-77.5	(-80,-63)
90	252.1	(248, 257)	0.1	-3.99	(-4.15, -3.96)	1.8	0.61	(0.55, 0.67)	-49.2	(-54,-38)
92	225.7	(221, 230)	0.1	-3.56	(-3.73, -3.54)	2.3	0.60	(0.51, 0.63)	-25.6	(-30,-14)
94	202.2	(197, 206)	0.4	-3.15	(-3.32, -3.15)	2.6	0.56	(0.52, 0.64)	-6.7	(-12,3)
96	181.5	(176, 185)	0.7	-2.79	(-2.94, -2.77)	2.6	0.50	(0.44, 0.55)	8.0	(3,18)
98	163.1	(157, 166)	1.0	-2.46	(-2.59, -2.42)	2.1	0.43	(0.43, 0.54)	18.9	(15,30)
100	146.9	(141, 149)	1.3	-2.18	(-2.27, -2.11)	0.6	0.36	(0.36, 0.46)	26.9	(21,35)
102	132.5	(127, 135)	1.4	-1.93	(-2.00, -1.85)	0.1	0.35	(0.29, 0.39)	32.4	(25,39)
104	119.8	(114, 122)	1.5	-1.70	(-1.78, -1.63)	0.3	0.30	(0.25, 0.34)	36.2	(30,43)
106	108.7	(103, 111)	1.7	-1.50	(-1.57, -1.43)	0.3	0.27	(0.23, 0.32)	38.4	(33,45)
108	98.76	(93.5, 101)	1.8	-1.33	(-1.39, -1.25)	0.3	0.23	(0.19, 0.28)	39.7	(34,46)
110	90.00	(84.9, 91.7)	1.9	-1.18	(-1.24, -1.10)	0.5	0.20	(0.14, 0.23)	40.1	(34,45)
112	82.22	(77.3, 83.8)	2.0	-1.05	(-1.10, -0.97)	0.8	0.17	(0.15, 0.23)	39.9	(32,44)
114	75.29	(70.6, 76.4)	2.1	-0.93	(-0.98, -0.86)	1.1	0.15	(0.10, 0.17)	39.3	(31,42)
116	69.11	(64.6, 70.6)	2.2	-0.84	(-0.89, -0.77)	0.7	0.13	(0.10, 0.16)	38.4	(30,40)
118	63.57	(59.2, 65.1)	2.2	-0.75	(-0.80, -0.68)	0.7	0.12	(0.07, 0.12)	37.4	(29,38)
120	58.60	(54.4, 60.0)	2.4	-0.67	(-0.72, -0.61)	0.9	0.10	(0.07, 0.11)	36.1	(28,37)
122	54.13	(50.1, 55.5)	2.5	-0.61	(-0.65, -0.54)	0.6	0.09	(0.04, 0.10)	34.8	(27,36)

Table 4.2: The prices and sensitivities of a down-and-out put in an exponential NIG Lévy model with maturity $T = 1$ year, strike $K = 3500$ and barrier H set at 60% of K. The interest and dividend rates are taken to be $r = 0.03$ and $d = 0$. All columns except that of the price are expressed in percentage figures of K. The columns with LT contain the results obtained using the transform algorithm, whereas MC refers to Monte-Carlo results, which are reported in the form of a 95% confidence interval. The columns with RE contain the relative errors, which are computed as $|MC^{\pm} - LT|/LT$ respectively, where $MC^{\pm}$ is the mid-point of the confidence interval.

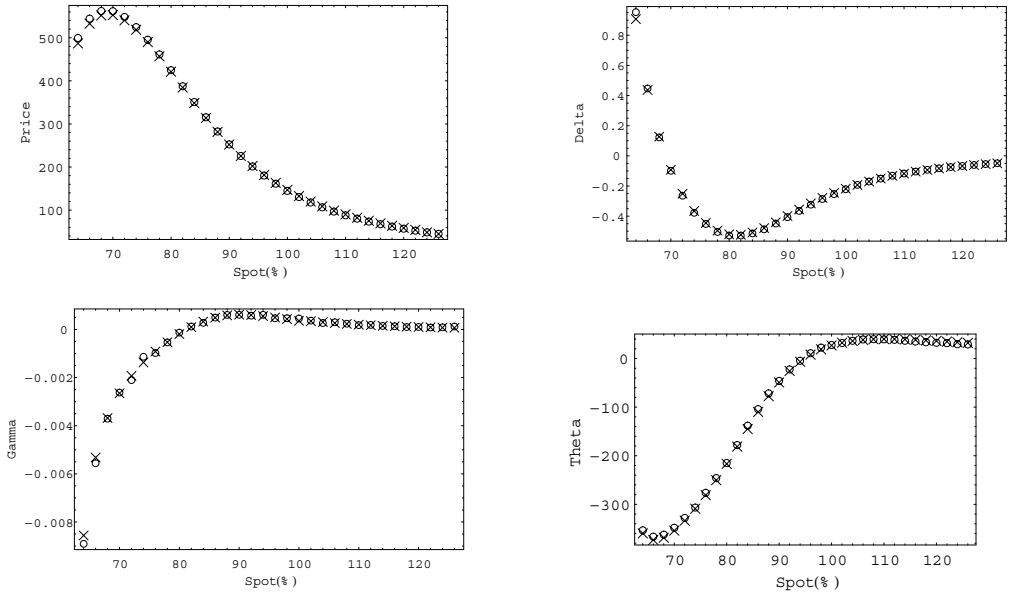

Figure 4.1: Prices and sensitivities of a down-and-out put option with strike $K = 3500$ and barrier H set at 60% of K in an exponential NIG model. Price (upper left) - Delta (upper right), Gamma (lower left) and Theta (lower right). Results from the transform algorithm are indicated with a $\times$ and Monte-Carlo results with a $\circ$.

We simulated paths of variance gamma and normal inverse Gaussian processes by employing the representations of these processes as random time-changes of a Brownian motion by an independent gamma and an independent inverse Gaussian subordinator, respectively. The sensitivities were calculated by approximating the derivative by a finite difference and subsequently evaluating this using Monte-Carlo simulations.

Tables 4.2 and 4.3 and Figures 4.1 and 4.2 report prices and Greeks for down-and-in digital and down-and-out put options calculated by using Algorithm 1 and Monte-Carlo simulations. The options are priced at different spot levels that are expressed as a percentage of the spot price ($S_0 = 3500$) on 16 June 2006. The value of a sensitivity is expressed as a fraction of S_0. Down-and-in digital options are priced under the VG model with barrier level H set at 60%, and down-and-out puts under the NIG model with barrier H and strike K set respectively at 60% and 100%.

The results show a general agreement between the Monte-Carlo simulation results and those from the semi-analytical approximation. The relative errors for the prices are less than 0.6% for VG and about 2% for NIG, and for the delta about 2% - 2.5% for both, if, for NIG, we stay some distance away from the barrier. We observe that, close to the barrier, the result for the gamma falls outside the confidence interval. In the case of the NIG Lévy model, the larger errors close to the barrier may be explained by the fact that the option price is not smooth under this model whereas it is for the approximating hyper-exponential model (see [21] for an analysis of the smoothness of option prices under an NIG or, more generally, a regular Lévy process).

The convergence of Monte-Carlo estimators of quantities involving first-passage is known to be very slow, requiring a small mesh of the time-grid. Since this effect is magnified when one is calculating the numerical derivatives, a large number of paths and time-steps was needed to obtain convergence. For the Monte-Carlo calculations we used one million paths and twenty thousand time-steps per year, which made the calculation of the Greeks using Monte-Carlo simulations computationally demanding and time-consuming.

In C++ on a 3189 Mhz computer the valuation of all option prices and sensitivities took 40 seconds for digital options and 55 seconds for down-and-out put options, compared to a couple of hours when using Monte-Carlo simulations. Here we should remark that we did not employ any special methods that could have considerably improved the speed of convergence of the Monte-Carlo simulation, such as Malliavin weights, likelihood ratio methods, or sampling techniques such as the bridge (see, e.g., Glasserman [48]). We noted that if the spot price was close to the barrier the Monte-Carlo estimators of the Greeks tended to be unstable.

	Variance Gamma Down-and-in digital option - payment at first-passage									
Spot	Price			Delta			Gamma		Theta	
	LT	MC	RE	LT	MC	RE	LT	MC	LT	MC
	$\cdot 10^{-2}$	$\cdot 10^{-2}$	$\cdot 10^{-3}$	$\cdot 10^{-5}$	$\cdot 10^{-5}$	%	$\cdot 10^{-7}$	$\cdot 10^{-7}$	$\cdot 10^{-2}$	$\cdot 10^{-2}$
64	39.89	(39.6, 40.1)	0.5	-104	(-108, -106)	2.9	43.2	(44.4, 45.4)	19.0	(16.3,19.4)
66	33.50	(33.2, 33.7)	1.0	-80.3	(-82.7, -81.0)	1.9	27.4	(27.4, 28.3)	18.5	(16.3,19.3)
68	28.47	(28.2, 28.6)	2.1	-64.2	(-65.7, -64.3)	1.3	19.4	(19.5, 20.9)	17.6	(16.2,19.1)
70	24.41	(24.1, 24.6)	2.2	-52.5	(-53.4, -52.1)	0.7	14.6	(14.1, 15.2)	16.6	(14.8,17.6)
72	21.06	(20.8, 21.2)	2.4	-43.5	(-44.2, -43.0)	0.3	11.4	(10.9, 12.2)	15.4	(13.2,15.8)
74	18.27	(18.1, 18.4)	2.1	-36.4	(-36.9, -35.8)	0.0	9.06	(8.55, 9.57)	14.2	(12.5,15.0)
76	15.93	(15.8, 16.1)	1.5	-30.7	(-31.0, -30.1)	0.4	7.34	(7.07, 7.99)	13.1	(11.6,14.0)
78	14.96	(13.8, 14.1)	0.3	-26.0	(-26.3, -25.4)	0.4	6.02	(5.35, 6.17)	12.1	(11.2,13.5)
80	12.27	(12.2, 12.4)	0.2	-22.2	(-22.3, -21.6)	0.8	4.97	(4.85, 5.89)	11.1	(10.1,12.2)
82	10.84	(10.8, 11.0)	2.6	-19.0	(-19.1, -18.4)	0.9	4.13	(3.22, 4.15)	10.2	(9.4,11.4)
84	9.60	(9.53, 9.72)	3.3	-16.4	(-16.6, -16.0)	0.2	3.46	(3.05, 3.89)	9.34	(8.2,10.2)
86	8.54	(8.48, 8.65)	4.2	-14.1	(-14.4, -13.8)	0.1	2.90	(2.36, 3.11)	8.57	(7.6,9.4)
88	7.61	(7.56, 7.72)	4.0	-12.3	(-12.5, -12.0)	0.5	2.45	(2.14, 2.82)	7.87	(6.7,8.4)
90	6.81	(6.76, 6.90)	4.0	-10.7	(-10.8, -10.4)	0.4	2.08	(2.06, 2.64)	7.22	(6.6,8.2)
92	6.11	(6.08, 6.21)	5.9	-9.3	(-9.4, -9.1)	0.6	1.77	(1.26, 1.81)	6.64	(6.2,7.8)
94	5.50	(5.47, 5.58)	6.0	-8.2	(-8.4, -8.0)	0.1	1.52	(1.28, 1.79)	6.11	(5.9,7.4)
96	4.96	(4.94, 5.04)	6.3	-7.2	(-7.4, -7.1)	0.7	1.30	(1.08, 1.38)	5.63	(5.4,6.8)
98	4.49	(4.46, 4.55)	4.9	-6.4	(-6.5, -6.2)	0.6	1.12	(0.92, 1.29)	5.19	(4.9,6.3)
100	4.07	(4.04, 4.13)	5.2	-5.6	(-5.8, -5.5)	0.6	0.97	(0.64, 0.99)	4.79	(4.3,5.2)
102	3.70	(3.66, 3.74)	3.4	-5.0	(-5.1, -4.9)	1.0	0.84	(0.54, 0.89)	4.42	(4.1,5.3)
104	3.37	(3.25, 3.53)	2.8	-4.5	(-4.6, -4.4)	0.3	0.73	(0.47, 0.84)	4.09	(3.6,4.8)
106	3.07	(3.04, 3.11)	1.8	-4.0	(-4.1, -3.9)	0.1	0.64	(0.40, 0.78)	3.78	(3.5,4.6)
108	2.81	(2.78, 2.84)	1.2	-3.6	(-3.7, -3.5)	1.4	0.56	(0.31, 0.72)	3.51	(3.2,4.3)
110	2.57	(2.55, 2.60)	2.6	-3.2	(-3.3, -3.1)	1.4	0.49	(0.28, 0.63)	3.25	(3.0,4.0)
112	2.36	(2.33, 2.38)	1.5	-2.9	(-3.0, -2.8)	0.3	0.43	(0.25, 0.51)	3.02	(2.7,3.7)
114	2.17	(2.14, 2.19)	0.9	-2.6	(-2.7, -2.5)	0.2	0.38	(0.23, 0.48)	2.81	(2.5,3.4)
116	2.00	(1.98, 2.02)	1.8	-2.3	(-2.4, -2.2)	1.8	0.34	(0.22, 0.41)	2.62	(2.3,3.2)
118	1.84	(1.83, 1.86)	0.8	-2.1	(-2.2, -2.1)	0.2	0.30	(0.21, 0.37)	2.44	(2.2,3.1)
120	1.70	(1.68, 1.71)	1.3	-1.9	(-2.0, -1.9)	0.5	0.27	(0.17, 0.33)	2.27	(2.0,2.9)
122	1.58	(1.57, 1.59)	4.0	-1.7	(-1.7, -1.7)	0.6	0.24	(0.16, 0.30)	2.12	(1.8,2.6)
124	1.46	(1.45, 1.47)	4.9	-1.6	(-1.6, -1.6)	2.3	0.21	(0.15, 0.26)	1.98	(1.7,2.5)
126	1.35	(1.34, 1.36)	5.8	-1.4	(-1.5, -1.4)	2.2	0.19	(0.14, 0.23)	1.86	(1.6,2.4)

Table 4.3: The prices and sensitivities of an American down-and-in digital option with maturity $T = 1$ year barrier and H set at 60% of the spot level 3500 in an exponential VG Lévy model. The interest and dividend rates are taken to be $r = 0.03$ and $d = 0$. All columns except that of the prices are expressed in percentage figures of 3500. The columns with LT contain the results obtained using the transform algorithm, whereas MC refers to Monte-Carlo results, which are reported in the form of a 95% confidence interval. The columns RE contain the relative error, which is computed as $|MC^{\pm} - LT|/LT$ respectively, where $MC^{\pm}$ is the mid-point of the confidence interval.

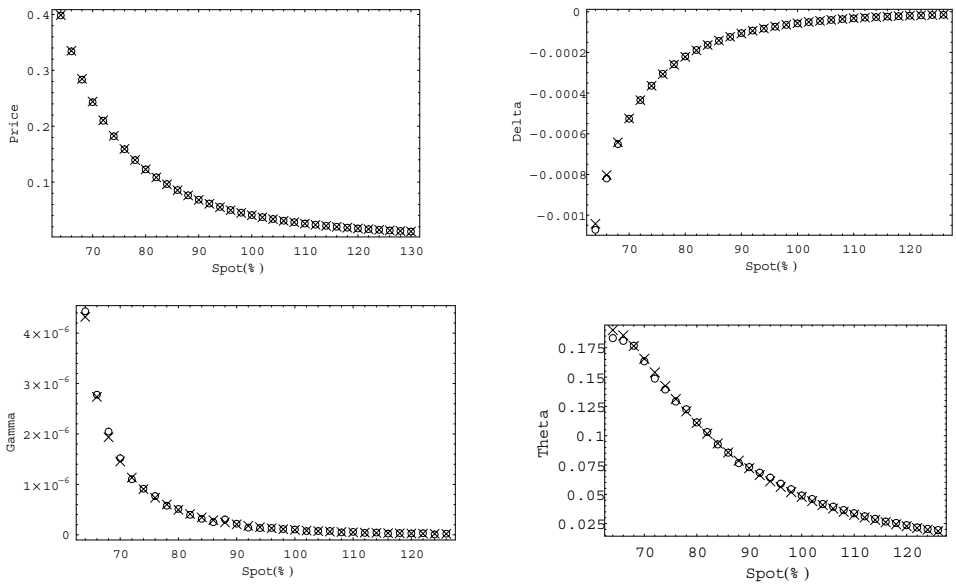

Figure 4.2: Prices and sensitivities of an American down-and-in digital option with a barrier H set at 60% of the spot level 3500 in an exponential VG model. Price (upper left) - Delta (upper right), Gamma (lower left) and Theta (lower right). Results from the transform algorithm are indicated with a $\times$ and Monte-Carlo results with a $\circ$.

4.7 Convergence of prices and sensitivities

A generalised hyper-exponential Lévy process can, as we showed in Section 4.3.2, be approximated arbitrarily closely by a hyper-exponential jump-diffusion, by specifying appropriate values for the parameters of the latter process. Under such a model analytical expressions were derived in Sections 4.4 and 4.5 for the values $EDID$, $EDOD$, $ADID$, DOP of digital and down-and-out put options, and the corresponding sensitivities. The results in Section 4.6 provided numerical evidence to show that a good approximation of prices and sensitivities in a GHE Lévy model can be obtained by carrying out the computations in a suitably chosen approximating hyper-exponential jump-diffusion model. In this section we provide further justification for the algorithm by proving a convergence result: for a given GHE Lévy process X and a sequence of $HEJD$ processes $X^{(n)}$ weakly converging to X (as constructed in Section 4.3.2), we shall show that the corresponding prices $EDID^{(n)}$, $EDOD^{(n)}$, $ADID^{(n)}$, $DOP^{(n)}$ of digital and down-and-out put options converge pointwise to those in the limiting model X,

as $n \to \infty$:

Proposition 4.7.1 *Suppose that X is GHE and is not of type A, and let V be any of $EDID, ADID, EDOD, DOP$ with $V^{(n)}$ the corresponding approximation. Then for $S_0 > H$ and $T > 0$, it holds that*

$$V^{(n)}(T, S_0) \to V(T, S_0) \quad \text{as } n \to \infty. \tag{4.18}$$

Proof of Proposition 4.7.1 The convergence of $EDID^{(n)}(T, S_0)$ to $EDID(T, S_0)$ is a direct consequence of the convergence of $P(T^{(n)}(h) < t)$ (Proposition 4.3.1). Further, by interchanging the order of integration it follows that the value function $ADID$ can be written as

$$ADID(T) = \int_0^\infty r\mathrm{e}^{-rt} P(T(h) < T \wedge t)\mathrm{d}t.$$

Thus, in view of the dominated convergence theorem and again Proposition 4.3.1 it follows that

$$ADID^{(n)}(T, S_0) \to ADID(T, S_0).$$

Also, since $(K - \mathrm{e}^x)^+$ is a continuous bounded function, Lemma 4.9.2 implies that

$$E[(K - \mathrm{e}^{X^{(n)}(T)})^+ \mathbf{1}_{\{T^{(n)}(h) < T\}}] = DOP^{(n)}(T, S_0)$$

converges to $DOP(T, S_0)$ as $n \to \infty$. □

Note that Proposition 4.7.1 implies that the finite difference approximations of the sensitivities of the digital and down-and-out put options also converge pointwise as $n \to \infty$ for any spot price S_0 away from the barrier H and any maturity $T > 0$. To prove pointwise convergence of the sensitivities, uniform estimates would be needed of the errors in (4.18). It is worth noting that, while for Lévy processes with positive Gaussian component first-passage probabilities and value-functions of barrier-options are smooth up to the barrier, such is not necessarily the case for a Lévy process without Gaussian component, especially at the barrier where the spatial derivatives may be infinite. However, when suitably *smoothed*, the sensitivities do converge pointwise:

Corollary 4.7.1 *For some $\epsilon > 0$ let $V^\epsilon(s) = \int V(T,y)\phi_\epsilon(s-y)\mathrm{d}y$, where ϕ_ϵ is a C^2 probability density with support in $(-\epsilon,\epsilon)$. Then it holds that*

$$\Delta_{V_\epsilon^{(n)}}(S_0,T) \to \Delta_{V_\epsilon}(S_0,T), \quad \Gamma_{V_\epsilon^{(n)}}(S_0,T) \to \Gamma_{V_\epsilon}(S_0,T),$$

for $S_0 > H+\epsilon, T > 0$, as $n \to \infty$.

A similar statement holds for the theta, replacing smoothing in space by smoothing in time. Note that, if $s \mapsto V(T,s)$ is C^1 on (H,∞), then $\Delta_{V_\epsilon}(S_0,T) - \Delta_V(S_0,T)$, $S_0 > H$, can be made arbitrarily small by choosing ϵ small enough (similar remarks apply to the other Greeks).

Proof of Corollary 4.7.1 In view of the definition of $V_\epsilon^{(n)}$ and integration by parts it follows that

$$\Delta_{V_\epsilon^{(n)}}(S_0,T) = \frac{\partial}{\partial S_0} V_\epsilon^{(n)}(S_0,T) = \int V^{(n)}(y)\phi_\epsilon'(S_0-y)\mathrm{d}y. \tag{4.19}$$

By the dominated convergence theorem and Proposition 4.7.1 it thus follows that the rhs of (4.19) converges to

$$\int V(y)\phi_\epsilon'(S_0-y)\mathrm{d}y = \Delta_{V_\epsilon}(S_0,T) \quad \text{as } n \to \infty.$$

The convergence of the gamma follows by a similar reasoning. □

4.8 Concluding remarks

In this chapter we have developed an efficient algorithm for computing prices and sensitivities of barrier-options driven by an exponential Lévy model of generalised hyper-exponential type. We showed that the latter class contains many of the Lévy models that are employed in financial modelling. We first approximated the target Lévy measure by a hyper-exponential one. Subsequently, for log-stock-price processes in this class, jump-diffusions with hyper-exponential jumps, we derived analytical expressions for the prices and sensitivities (Greeks) of digital, knock-in and knock-out option prices, up to a single Laplace transform. Inversion of this Laplace transform yielded fast and accurate results for the option prices and sensitivities. We proved convergence of this algorithm.

To provide a numerical illustration we implemented the algorithm for the VG and NIG Lévy models, approximating the NIG and VG Lévy densities by hyper-exponential ones with seven upward and seven downward phases. Compared with Monte-Carlo simulation results we found relative errors of about 0.5-2.5% for prices and deltas some distance away from the barrier. What the rate of convergence of this algorithm is when increasing the number of terms in the approximation, and how this rate depends on the quality of the approximation of the target density, the parameters and the distance to the barrier, are open questions that are left for future research.

4.9 Appendix Chapter 4

4.9.1 Additional pricing formulae

Upward digital options

The arbitrage free prices of the corresponding up-and-in digitals (contracts that pay out €1 if an upper barrier is crossed, either at T or at the moment $T^+(h)$ of up-crossing) are given by

$$EUID(T;S_0,H) = \mathrm{e}^{-rT}P[\overline{S}_T > H], \quad AUID(T;S_0,H) = E[\mathrm{e}^{-rT^+h}\mathbf{1}_{\{\overline{S}_T>H\}}],$$

where $\overline{S}_T = \sup_{0\le s\le T} S_s$ denotes the running supremum of S up to T. Their respective Laplace transforms in T follow by applying the formulae of the down-and-in digital options to the process $-X$:

$$\widehat{EUID}(q) = \frac{1}{q+r}\sum_{i=1}^{k^+} A_i^+ \mathrm{e}^{-\rho_i^+ h}, \quad \widehat{AUID}(q) = \frac{q+r}{q}\widehat{EUID}(q), \quad h \ge 0.$$

Down-and-in put

The Laplace transform $\widehat{DIP}(q)$ of the arbitrage-free price of the down-and-in put option $DIP(T;S_0,K,H)$ with strike K and barrier H can be decomposed as

$$\begin{aligned}\widehat{DIP}(q) &= \frac{K}{q+r}P[\underline{X}_\tau < h, X_\tau < k] - \frac{S_0}{q+r}E[\mathrm{e}^{X_\tau}\mathbf{1}_{\{\underline{X}_\tau<h, X_\tau<k\}}] \\ &= \frac{K}{q+r}D^{(0)}(h,k) - \frac{S_0}{q+r}D^{(1)}(h,k),\end{aligned}$$

where $h = \log(H/S_0)$, $k = \log(K/S_0)$ and $D^{(b)}(h,k)$ is defined as

$$D^{(b)}(h,k) := E[\mathrm{e}^{bX_\tau}\mathbf{1}_{\{\underline{X}_\tau<h, X_\tau<k\}}].$$

Reasoning as in Proposition 4.4.2, we find that

$$D^{(b)}(h,k) = \int_{-h}^{\infty} \mathrm{e}^{-by} E[\mathrm{e}^{b(X_\tau - \underline{X}_\tau)}\mathbf{1}_{\{X_\tau - \underline{X}_\tau < k+y\}}] P(-\underline{X}_\tau \in \mathrm{d}y).$$

After some calculations we arrive at

$$\begin{aligned}D^{(b)}(h,k) &= \sum_{j=1}^{k^-}\sum_{i=1}^{k^+} \frac{\rho_i^+\rho_j^-}{(\rho_j^- - \rho_i^+)(b-\rho_i^+)} A_i^+ A_j^- \mathrm{e}^{(b-\rho_i^+)k + (\rho_i^+ - \rho_j^-)h} \\ &+ \left(1 - \sum_{i=1}^{k^+}\frac{b}{b-\rho_i^+}A_i^+\right)\sum_{j=1}^{k^-} A_j^- \frac{\rho_j^-}{\rho_j^- - b}\mathrm{e}^{(b-\rho_j^-)h}.\end{aligned}$$

4.9.2 Sensitivities for down-and-out-puts

Proposition 4.9.1 *Suppose X is a hyper-exponential Lévy process with $\sigma > 0$ and let $q > 0$ and $H < \min\{K, S_0\}$.*

(i) *It holds that $\widehat{\Theta}_{DOP}(q) = \widehat{qDOP}(q) - (K - S_0)^+$.*

(ii) *If $S_0 < K$, it holds that*

$$\begin{aligned}
\widehat{\Delta}_{DOP}(q) &= \sum_{j=1}^{k^-} A_j^-(\rho_j^-)^2 S_0^{\rho_j^- - 1}[KB_j^{(0)} - B_j^{(1)}], \\
\widehat{\Gamma}_{DOP}(q) &= \sum_{j=1}^{k^-} A_j^-(\rho_j^-)^2(\rho_j^- - 1) S_0^{\rho_j^- - 2}[KB_j^{(0)} - B_j^{(1)}],
\end{aligned}$$

where

$$\begin{aligned}
B_j^{(b)} &= \sum_{i=1}^{k^+} A_i^+ \left[\frac{(-\rho_i^+)H^{\rho_i^+ - \rho_j^-} K^{b-\rho_i^+}}{(\rho_j^- - \rho_i^+)(b - \rho_i^+)} + \frac{bH^{b-\rho_i^+}}{(b-\rho_j^-)(b-\rho_i^+)} - \frac{(-\rho_i^+)K^{b-\rho_j^-}}{(\rho_j^- - \rho_i^+)(b-\rho_j^-)} \right] \\
&+ \frac{1}{b - \rho_j^-}[H^{b-\rho_j^-} - K^{b-\rho_j^-}].
\end{aligned}$$

(iii) *If $K < S_0$, it holds that*

$$\begin{aligned}
\widehat{\Delta}_{DOP}(q) &= \sum_{j=1}^{k^-} A_j^-(\rho_j^-)^2 S_0^{\rho_j^- - 1}[KF_j^{(0)} - F_j^{(1)}] \\
&\quad + \sum_{i=1}^{k^+} A_i^+(\rho_i^+)^2 S_0^{\rho_i^+ - 1}[KG_i^{(0)} - G_i^{(1)}] + \delta_+\delta_-, \\
\widehat{\Gamma}_{DOP}(q) &= \sum_{j=1}^{k^-} A_j^-(\rho_j^-)^2(\rho_j^- - 1) S_0^{\rho_j^- - 2}[KF_j^{(0)} - F_j^{(1)}] \\
&\quad + \sum_{i=1}^{k^+} A_i^+(\rho_i^+)^2(\rho_i^+ - 1) S_0^{\rho_i^+ - 2}[KG_j^{(0)} - G_j^{(1)}],
\end{aligned}$$

where $\delta_+ = 1 - \sum_{i=1}^{k^+} A_i^+ \frac{1}{1-\rho_i^+}$ and $\delta_- = 1 - \sum_{j=1}^{k^-} A_j^- \frac{1}{1-\rho_j^-}$ and

$$\begin{aligned}
F_j^{(b)} &= \frac{H^{b-\rho_j^-}\rho_j^-}{b - \rho_j^-} + \sum_{i=1}^{k^+} A_i^+ \left[\frac{(-\rho_i^+)K^{b-\rho_i^+}H^{\rho_i^+ - \rho_j^-}}{(\rho_j^- - \rho_i^+)(b-\rho_i^+)} - \frac{H^{b-\rho_j^-}b}{(b-\rho_j^-)(b-\rho_i^+)} \right], \\
G_i^{(b)} &= \frac{K^{b-\rho_i^+}}{b - \rho_i^+} \left[\sum_{j=1}^{k^-} A_j^- \frac{\rho_i^+}{\rho_j^- - \rho_i^+} + 1 \right].
\end{aligned}$$

Proof of Proposition 4.9.1 The formula of the Laplace transform of theta is a consequence of integration by parts and the fact that $G(\cdot, h, k)$ is continuously differentiable on $(0, \infty)$. Those of the Laplace transforms of the delta and the gamma follow by differentiating the expressions in Proposition 4.4.2, following a reasoning analogous to the one in Proposition 4.5.1. □

4.9.3 Proofs of the weak convergence

Let X be a generalised hyper-exponential Lévy process and define $X^{(n)}$ as in Section 5.3. We refer to Jacod & Shiryaev [51, Chapter VI] for details of the Skorokhod topology and weak convergence of stochastic processes. Let $D(\mathbb{R}_+)$ denote the space of real-valued right-continuous functions with left-limits on $\mathbb{R}_+$.

Lemma 4.9.1 *$X^{(n)}$ converge weakly to X in the Skorokhod topology on $D(\mathbb{R}_+)$, as $n \to \infty$.*

Proof of Lemma 4.9.1 With regard to Corollary VII.3.6 in Jacod & Shiryaev [51, Chapter VI] it follows that it is equivalent to show that $X^{(n)}(1)$ converges in distribution to X_1, and that the latter assertion follows if

$$\mu_n \to \mu, \quad \int g(u)k_n(u)\mathrm{d}u \to \int g(u)k(u)\mathrm{d}u,$$
$$\sigma_n^2 + \int_{-1}^{1} x^2 k_n(x)\mathrm{d}x \to \sigma^2 + \int_{-1}^{1} x^2 k(x)\mathrm{d}x,$$

for any continuous bounded function g that is zero around zero, as $n \to \infty$. As a consequence of the definitions of k_n and σ_n^2 given in (4.9) and (4.10) it is not difficult to verify that these three conditions are indeed satisfied. □

Lemma 4.9.2 *$(X_T^{(n)}, \overline{X}_T^{(n)})$ converges in distribution to $(X_T, \overline{X}_T)$.*

Proof of Lemma 4.9.2 It follows from Proposition VI.2.4 and remark VI.2.3 in Jacod & Shiryaev [51] that for each fixed T such that $\Delta\omega(T) = 0$, the function $f : D(\mathbb{R}_+) \to \mathbb{R}$ given by

$$f : \omega \mapsto (\omega(T), \sup\{\max\{\omega(s), 0\}, s \leq T)$$

is continuous (in the Skorokhod topology). In particular, if $\omega^{(n)} \to \omega$ in the Skorokhod topology, then $f(\omega^{(n)}) \to f(\omega)$, as $n \to \infty$. In view of the fact that Lévy processes are continuous at each fixed time almost surely, it holds that

$$P(\Delta X_T \neq 0) = 0,$$

and the asserted convergence follows in view of Lemma 4.9.1. □

Proof of Proposition 4.3.1 The convergence of $(X^{(n)}(T), \overline{X}^{(n)}(T))$ is proved in Lemma 4.9.2. If X is not of type A, it is shown in Lemma 49.3 in Sato[78] that $\overline{X}_T$ and $-\underline{X}_T$ are continuous random variables on $(0, \infty)$ (with possibly an atom in zero if X is of bounded variation). The statement (4.11) thus follows in view of the continuity theorem. Since

$$P(T(x) \leq T) = P(\underline{X}_T \leq x),$$

equation (4.12) follows also. □

Chapter 5

Pricing and hedging barrier options in a hyper-exponential additive model

5.1 Introduction

barrier-options are contracts whose pay-offs are activated or de-activated when the stock price process crosses a specified barrier level. To value barrier-options, a model needs to be sufficiently flexible to be able to calibrate call option prices at different strikes and maturities. However, it is desirable to maintain a degree of analytical tractability to facilitate the calculations, especially for the sensitivities (Greeks). These sensitivities describe the change in the model price with respect to a change in the underlying parameter, and are important for an appreciation of the robustness of the model's results. It is well known that the accurate evaluation of the Greeks is a challenging numerical problem, since standard PDE or Monte-Carlo methods generally tend to be slow and unstable.

It is well established that the geometric Brownian motion model lacks the flexibility to capture features in financial stock price return data such as the skewness and the excess kurtosis. It cannot calibrate simultaneously to a set of call option prices. To address these limitations, one of the approaches consists of introducing jumps in the price process by replacing the Brownian motion by a Lévy process.

Lévy models, such as the VG, CGMY, NIG, KoBoL, generalised hyperbolic, and Kou's double exponential model, have been successfully applied to the valuation of European-type options. We refer the reader to Cont & Tankov [30], Boyarchenko & Levendorskiĭ[21], and Schoutens [80] for general background and references on the application of Lévy models in option pricing.

As has been observed by many authors, such as Eberlein & Kluge [38], and Carr & Wu [25], Lévy models are generally not capable of calibrating option prices simultaneously across strikes and maturities. Empirical studies of S&P-500 index data by Carr & Wu [25] and Pan [71] show that the implied jump intensities and the implied jump-size distributions vary greatly over time. The prices of short-dated options exhibit a significantly larger risk-premium than that of long-dated options. This is reflected in the thicker tails of the implied marginal risk-neutral distributions, especially at short maturities. For example, in the equity markets, short-dated out-of-the money put options are relatively expensive since the risk of a large negative jump in the stock is priced. Because of the stationarity and independence of the Lévy process increments, the moments exhibit a rigid term structure that is different from what is observed in market data. This lack of flexibility can be overcome by considering models driven by additive processes, which have independent and time-inhomogeneous increments.

Additive models have been used for equity option pricing by Carr *et al.* [24] and Galloway & Nolder [45], and for interest rate option pricing by Eberlein & Kluge [38]. Motivated by modelling considerations, Carr *et al.* [24] proposed a self-similar additive model for the log-stock-price, and reported good calibration results across time. Galloway & Nolder [45] carried out a calibration study for various related models. Eberlein & Kluge [38] constructed an HJM model driven by an additive process with continuous characteristics, and they obtained a good fit for swaptions by using piecewise constant parameters.

In this chapter we follow a similar approach: we model the stock price by an additive process with hyper-exponential jumps. Hyper-exponential distributions are finite mean-mixtures of exponential distributions which can approximate monotone distributions arbitrarily closely. As first observed by Asmussen *et al.* [8],

most of the popular Lévy models used in mathematical finance possess completely monotone Lévy densities and can therefore be approximated well by hyper-exponential Lévy models. A hyper-exponential additive model is sufficiently flexible to allow for an accurate calibration to European option prices across strikes and multiple maturities. In addition, if the parameters are piecewise constant, the model admits semi-analytical expressions for prices and Greeks of barrier-options.

There currently is a body of literature devoted to various aspects of pricing barrier-options. In the setting of Lévy models, a transform-based approach to price barrier options has been developed in a number of papers, including Geman & Yor [47], Kou & Wang [60], Davydov & Linetsky [33], Boyarchenko & Levendorskiĭ[18]. In particular, Kou & Wang [60], Kou *et al.* [58], Sepp [81], Lipton [64], and Jeannin & Pistorius [53] considered the cases of Lévy processes with double-exponential and hyper-exponential jumps.

The transform algorithm that we develop is based on a so-called matrix Wiener-Hopf factorisation. Such matrix factorisations were first studied by London *et al.* [65] and Rogers [75] for (noisy) fluid models. Jiang & Pistorius [54] developed matrix-Wiener factorisation results for regime-switching models with jumps. We show that by suitably randomising the parameters of the distributions of the infimum and supremum of the randomised hyper-exponential additive process can be explicitly expressed in terms of a matrix Wiener-Hopf factorisation. We use these results to derive semi-analytical expressions for the first-passage time probabilities, for the prices, and for the Greeks of barrier-options, up to a multi-dimensional transform. The actual prices are then obtained by inverting this transform.

As a numerical illustration, we calibrate the hyper-exponential additive model to Stoxx50E prices quoted on 27 February 2007 at four different maturities. We calculate in this setting down-and-in digital and down-and-in call option prices and Greeks (delta and gamma). To invert the transform, we use a contour deformation algorithm and a fractional fast Fourier transform algorithm, developed by Talbot [84], Bailey & Swarztrauber [11], and Chourdakis [29]. We also compare it to Monte-Carlo Euler scheme simulations. We find that the algorithm

is accurate and stable, and much faster than Monte-Carlo simulations especially for the Greeks. This method is suitable for applications in which the number of periods is not too large up to four. When a larger number of periods is required, the direct inversion method used here is no longer feasible. The subject needs to be further investigated and is left for future research.

In Section 5.2 we define the hyper-exponential additive model and present its application to European call option pricing. In Sections 5.3 and 5.4 we derive semi-analytical expressions for the first-passage probabilities of a hyper-exponential additive process in terms of a matrix Wiener-Hopf factorisation, and for the prices and Greeks of barrier-options. In Section 5.5 we present numerical results.

5.2 Log-additive models

5.2.1 Additive processes

We consider a stock price process S modelled for $t \geq 0$ as the exponential $S_t = S_0 \exp(X_t)$ of an additive process X. Informally, an additive process can be described as a Lévy process with time-dependent characteristics or, equivalently, as a process with independent but non-stationary increments. We briefly review below some key properties of additive processes. For further background on additive processes and their applications in finance, we refer the reader to Sato [78] and to Cont & Tankov [30].

An additive process can be defined more formally as follows.

Definition 5.2.1 *For a given $T > 0$, $X = \{X_t, t \in [0, T]\}$ is an additive process on $\mathbb{R}$ if the following conditions are satisfied:*

(i) $X_0 = 0$,

(ii) *For any finite partition $0 \leq t_0 < t_1 \cdots < t_k \leq T$, the random variables $X_{t_k} - X_{t_{k-1}}, \cdots, X_{t_0}$ are independent,*

(iii) *The sample paths $t \mapsto X_t$ have càdlàg modifications almost surely.*

If X is an additive process, then, for every $t \in [0,T]$, X_t has an infinitely divisible distribution with Lévy triplet $(M_t, \Sigma_t^2, \Lambda_t)$; that is, the characteristic function of X_t is given by $\Phi_t(u) = \exp[\Psi_t(u)\,]$.

According to the Lévy-Khintchine formula, Ψ_t is the characteristic exponent given by

$$\Psi_t(u) = \mathrm{i}uM_t - \frac{\Sigma_t^2}{2}u^2 + \int_{-1}^{1} \left\{ \mathrm{e}^{\mathrm{i}ux} - 1 - \mathrm{i}ux1_{\{|x|<1\}} \right\} \Lambda_t(\mathrm{d}x),$$

with M_t, $\Sigma_t \in \mathbb{R}$, and where Λ_t the Lévy measure satisfies the integrability constraint

$$\int (1 \wedge x^2)\Lambda_t(dx) < \infty.$$

The law of the additive process $\{X_t, t \in [0,T]\}$ is determined by the family of Lévy triplets $\{(M_t, \Sigma_t^2, \Lambda_t)$ for $t \in [0,T]\}$. If the Lévy triplets are time-independent, X is a Lévy process. If the additive process has absolutely continuous characteristics, the Lévy triplets take the explicit form

$$\begin{aligned} M_t &= \int_0^t \mu(s)\mathrm{d}s, \qquad \Sigma_t^2 = \int_0^t \sigma^2(s)\mathrm{d}s, \\ \Lambda_t(B) &= \int_0^t \int_B g(s,x)\mathrm{d}x\mathrm{d}s \qquad \text{for Borel sets } B, \end{aligned}$$

where $\mu, \sigma^2 : [0,T] \to \mathbb{R}$ and $g : [0,T] \times \mathbb{R} \to \mathbb{R}$ are integrable functions, with g and σ^2 non-negative. We call the functions (μ, σ^2, g) the local triplet of X.

We assume that we have been given deterministic integrable functions $r(t)$ and $d(t)$ representing the short rate and the dividend yield, and that the characteristic exponent of X_t satisfies

$$\Psi_t(-\mathrm{i}) = \int_0^t [r(s) - d(s)]\mathrm{d}s, \tag{5.1}$$

or equivalently

$$\mu(t) + \frac{\sigma^2(t)}{2} + \int_{-\infty}^{\infty} [\mathrm{e}^x - 1 - 1_{\{|x|<1\}}x]g(t,x)\mathrm{d}x = r(t) - d(t). \tag{5.2}$$

It follows that the discounted process is a martingale if and only if (5.1) (or, equivalently, (5.2)) holds.

5.2.2 Hyper-exponential additive processes

In what follows we restrict the discussion to a hyper-exponential additive process X which is specified by its local triplet (μ, σ^2, g) where g is given by

$$g(t,x) = \sum_{k=1}^{n^+} \pi_k^+(t)\alpha_k^+(t)\mathrm{e}^{-\alpha_k^+(t)x}1_{\{x>0\}} + \sum_{j=1}^{n^-} \pi_j^-(t)\alpha_j^-(t)\mathrm{e}^{-\alpha_j^-(t)|x|}1_{\{x<0\}},$$

where $\pi_k^\pm(t)$ and $\alpha_k^\pm(t)$ are non-negative. The continuous part of X consists of a diffusion with time-dependent drift $\mu(t)$ and volatility $\sigma(t)$. The jump part of X is of finite activity and forms an inhomogeneous compound Poisson process where positive and negative jumps occur at the rates

$$\lambda^+(t) := \sum_{k=1}^{n^+} \pi_k^+(t) \qquad \text{and} \qquad \lambda^-(t) := \sum_{j=1}^{n^-} \pi_j^-(t),$$

and the jump-sizes are distributed according to a hyper-exponential distribution. Small random price movements are intuitively modelled by the diffusion part, whereas sudden changes of the price are captured by the jump-part of X. If we take $n^\pm = 1$, the jump-sizes are exponentially-distributed, and this model reduces to an extension of the Kou model with time-dependent parameters.

5.2.3 Piecewise constant parameters

To reduce the dimension of the available parameter set, we take the functions $\mu(t), \sigma(t)$ and $g(t,\cdot)$ to be piecewise constant. Given that we have a finite set of European call options with different maturities $T_1, \ldots, T_N$, we take the local parameters to be constant between the different maturities T_i. Then for all $t \in (T_{i-1}, T_i]$, (with $T_0 = 0$) we set

$$\mu(t) = \mu^{(i)}, \quad \sigma^2(t) = \sigma^{2(i)}, \quad g(t,x) = g^{(i)}(x), \quad i = 1, \ldots, N. \tag{5.3}$$

For $t \in (T_{i-1}, T_i]$ the characteristic exponent of $X_t - X_{T_{i-1}}$ is given by

$$\Psi_{T_{i-1},t}(u) =: \Psi^{(i)}(u),$$

where

$$\Psi^{(i)}(u) = \mu^{(i)}u\mathrm{i} - \frac{\sigma^{2(i)}}{2}u^2 + \sum_{k=1}^{n^+} \pi_k^{+(i)} \left(\frac{u\mathrm{i}}{\alpha_k^{+(i)} - u\mathrm{i}} \right) - \sum_{j=1}^{n^-} \pi_j^{-(i)} \left(\frac{u\mathbf{i}}{\alpha_j^{-(i)} + u\mathrm{i}} \right). \tag{5.4}$$

5.3 First-passage probabilities

The value of a digital barrier-option can be expressed in terms of the distribution

$$F^{(+)}(x;T) = P(\overline{X}_T \leq x)$$

of the running supremum

$$\overline{X}_T = \sup_{s \leq T} X_s$$

of X, or equivalently, the distribution of the first-passage time

$$T^+(x) = \inf\{t \geq 0 : X_t > x\}$$

which is related to $F^{(+)}$ by

$$P(T^+(x) \leq T) = 1 - F^{(+)}(x;T).$$

Whereas for a Lévy process the distributions of the infimum and supremum are linked to the characteristic exponent by the so-called Wiener-Hopf factorisation, such a result does not exist for general additive processes, because of the time-dependence of the parameters. However, in the case of piecewise constant parameters, the triplet changes only at deterministic times, so that as a consequence the distribution function

$$F^{(+)}(x) = F^{(+)}(x; T^{(1)}, \ldots, T^{(N)}),$$

only depends on the inter-jump times $T^{(i)} = T_i - T_{i-1}$ (with $T_0 = 0$). In this case, as we show below, the N-dimensional Laplace transform $G^{(+)}(x, \mathbf{q})$ of $F^{(+)}$, given by

$$G^{(+)}(x, \mathbf{q}) = \int \mathrm{e}^{-(q_1 u_1 + \cdots + q_N u_N)} F^{(+)}(x; u_1, \ldots, u_N) \mathrm{d}u_1 \cdots \mathrm{d}u_N,$$

where $\mathbf{q} = (q_1, \ldots, q_N)$, is expressed explicitly in terms of a matrix Wiener-Hopf factorisation. To state this result we need to introduce some further notation.

For any vector $\mathbf{v} = (v_1, \ldots, v_n)$, we denote by $\Delta_{\boldsymbol{v}}$ the diagonal matrix $\Delta_{\boldsymbol{v}} = (v_i, i = 1, \ldots, n)_{\text{diag}}$. Let Q be the $N(1+n^+ +n^-) \times N(1+n^+ +n^-)$ matrix given in block notation by

$$Q = \begin{pmatrix} H^+ & D^- \\ C^- & T^- \end{pmatrix}, \tag{5.5}$$

where

$$H^+ = \begin{pmatrix} G - \Delta_{\boldsymbol{\lambda}} & b^+ \\ t^+ & T^+ \end{pmatrix}. \tag{5.6}$$

Here $\boldsymbol{\lambda} = (\lambda_i^+ + \lambda_i^-, i = 1, \ldots, N)$, and G and b^+ are the $N \times N$ and $N \times Nn^+$ matrices in block notation given by

$$G = \begin{pmatrix} -q_1 & q_1 & & & \\ & -q_2 & q_2 & & \\ & & \ddots & & \\ & & & -q_{N-1} & q_{N-1} \\ & & & & -q_N \end{pmatrix}, \; b^+ = \begin{pmatrix} \pi^{+(1)} & & & \\ & \pi^{+(2)} & & \\ & & \ddots & \\ & & & \pi^{+(N)} \end{pmatrix}. \tag{5.7}$$

Here $\pi^{+(i)}$ is the row-vector $\boldsymbol{\pi}^{+(i)} = (\pi_l^{+(i)}, l = 1, \ldots, n)$, and where t^+, T^+ are given by

$$T^+ = \begin{pmatrix} -\Delta_{\boldsymbol{\alpha}^+} & & & \\ & -\Delta_{\boldsymbol{\alpha}^+} & & \\ & & \ddots & \\ & & & -\Delta_{\boldsymbol{\alpha}^+} \end{pmatrix}, \quad t^+ = \begin{pmatrix} \alpha^+ & & & \\ & \alpha^+ & & \\ & & \ddots & \\ & & & \alpha^+ \end{pmatrix}, \tag{5.8}$$

where α^+ is the column-vector $\alpha^+ = (\alpha_i^+, i = 1, \ldots, n^+)'$, and

$$C^- = \begin{pmatrix} t^- & O^- \end{pmatrix}, \qquad D^- = \begin{pmatrix} b^- \\ O^+ \end{pmatrix}, \tag{5.9}$$

where $O^\pm$ are $n^\pm N \times n^\pm N$ zero matrices, and b^-, T^-, and t^- are given by (5.7) and (5.8) with $\boldsymbol{\pi}^{+(i)}$ and $\boldsymbol{\alpha}^+$ replaced by $\boldsymbol{\pi}^{-(i)}$ and $\boldsymbol{\alpha}^-$. The matrix Q is a generator matrix, that is, a square matrix with non-negative off-diagonal elements and non-positive row sums, and defines a Markov chain. This Markov chain is associated to a randomisation and embedding of the additive process X which will be illustrated with a concrete example below. We recall that a sub-probability matrix is a matrix with non-negative elements and row sums not larger than one. By applying the matrix Wiener-Hopf factorisation results of Jiang & Pistorius [54] to the current setting we arrive at the following conclusion.

Theorem 5.3.1 *It holds that*

$$G^{(+)}(x, \boldsymbol{q}) = \frac{1}{q_1 \ldots q_N} \times \left[1 - e_1' \mathrm{e}^{Q_+ x} \mathbf{1}\right], \tag{5.10}$$

where

$$\mathbf{e}_1' = (1, 0, \ldots, 0) \qquad \textit{and} \qquad \mathbf{1} = (1, \ldots, 1)'.$$

Q_+ is an $N(1+n^+) \times N(1+n^+)$ generator matrix that together with η^+ an $Nn^- \times N(1+n^+)$ sub-probability matrix, solves the system of matrix equations

$$\frac{1}{2}S^2 Q_+^2 - V^+ Q_+ + H^+ + D^- \eta^+ = O, \tag{5.11}$$

$$-\eta^+ Q_+ + C^- + T^- \eta^+ = O. \tag{5.12}$$

Here the O's are zero matrices of appropriate sizes, and in block notation we have

$$S^2 = \begin{pmatrix} \Delta_{\boldsymbol{\sigma}^2} & \\ & O^+ \end{pmatrix}, \qquad V^+ = \begin{pmatrix} +\Delta_{\boldsymbol{\mu}} & \\ & I^+ \end{pmatrix}, \tag{5.13}$$

with

$$\boldsymbol{\sigma}^2 = (\sigma_i^2, i = 1, \ldots, N), \qquad \boldsymbol{\mu} = (\mu_i, i = 1, \ldots, N).$$

O^+ and I^+ represent $n^+N \times n^+N$ zero and identity matrices, respectively.

By applying Theorem 5.3.1 to $-X$, we find the corresponding pair of matrices (Q_-, η_-). The quadruple $(Q_+, \eta_+, Q_-, \eta_-)$ is called a matrix Wiener-Hopf factorisation of Q.

Example 5.3.1 *To illustrate this approach, we consider a hyper-exponential additive process X on $[0, T_2]$ whose parameters are constant during the periods $[0, T_1]$ and $[T_1, T_2]$. In the first period X evolves as a jump-diffusion with positive and negative exponential jumps with means and jump rates $1/\alpha^+, \lambda^+$ and $1/\alpha^-, \lambda^-$. In the second period X is a Brownian motion with drift. The idea is to randomise the times between maturities by replacing $T^{(1)} = T_1$ and $T^{(2)} = T_2 - T_1$ with independent exponential random variables having means q_1^{-1} and q_2^{-1}. This results in a regime-switching jump-diffusion with the regime only jumping from state 1 to state 2, according to the generator matrix*

$$G = \begin{pmatrix} -q_1 & q_1 \\ 0 & -q_2 \end{pmatrix}.$$

We associate to the regime-switching process a continuous Markov additive process, which can be informally obtained by replacing positive and negative jumps with stretched slopes of $+1$ *and* -1 *(see Asmussen* [5] *for background on this embedding). As described in* [54]*, in this case the generator of the modulating Markov process is given by*

$$Q = \begin{pmatrix} H^+ & D^- \\ C^- & T^- \end{pmatrix} = \left(\begin{array}{ccc|c} -q_1 - \lambda^+ - \lambda^- & q_1 & \lambda^+ & \lambda^- \\ 0 & -q_2 & 0 & 0 \\ \alpha^+ & 0 & -\alpha^+ & 0 \\ \hline \alpha^- & 0 & 0 & -\alpha^- \end{array}\right),$$

with the matrices S^2 *and* V^+ *in Theorem 5.3.1 given by*

$$S^2 = \begin{pmatrix} \sigma_1^2 & & \\ & \sigma_2^2 & \\ & & 0 \end{pmatrix}, \qquad V^+ = \begin{pmatrix} \mu_1 & & \\ & \mu_2 & \\ & & 1 \end{pmatrix}.$$

5.3.1 Solution of the matrix equation

To solve the system (5.11), which is a Ricatti-type matrix equation, we follow a spectral approach and determine the spectral decomposition of Q^+. Denoting by $h(\rho)$ a (column) eigenvector of Q^+ corresponding to the eigenvalue ρ, one finds that it is a matter of algebra to verify that the system (5.11) can be equivalently rewritten as

$$\frac{1}{2}\tilde{S}^2 \begin{pmatrix} I \\ \eta^+ \end{pmatrix} Q_+^2 - \tilde{V} \begin{pmatrix} I \\ \eta^+ \end{pmatrix} Q_+ + Q \begin{pmatrix} I \\ \eta^+ \end{pmatrix} = O.$$

Here O is a $N(1+n^+ +n^-)$ square zero matrix, I is an $N(1+n^+)$ identity matrix, and

$$\tilde{S}^2 = \begin{pmatrix} \Delta_{\boldsymbol{\sigma}^2} & & \\ & O^+ & \\ & & O^- \end{pmatrix}, \qquad \tilde{V} = \begin{pmatrix} \Delta_{\boldsymbol{\mu}} & & \\ & I^+ & \\ & & -I^- \end{pmatrix}.$$

Defining the matrix $K(s)$ by

$$K(s) = \frac{s^2}{2}\tilde{S}^2 + s\tilde{V} + Q, \tag{5.14}$$

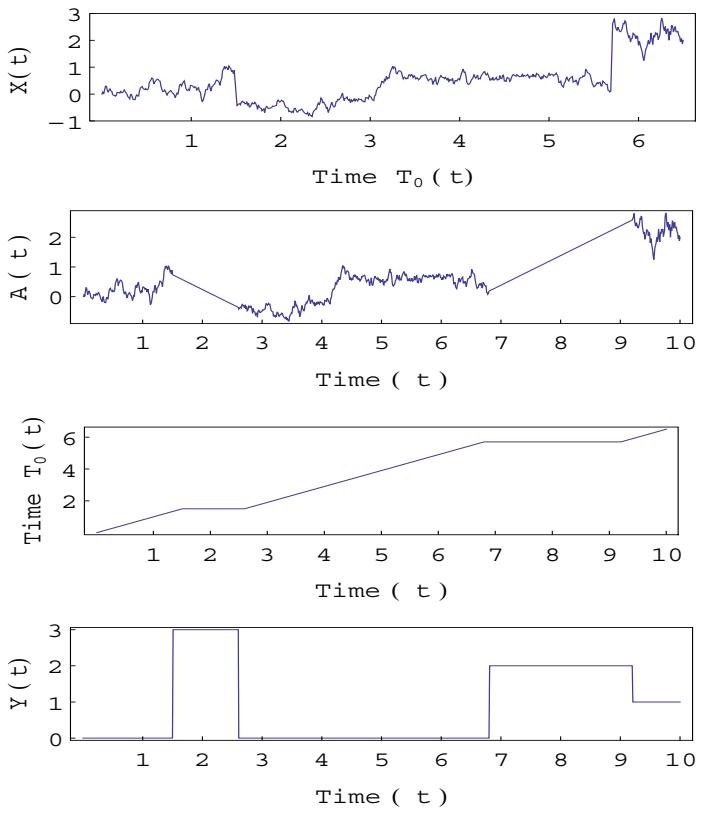

Figure 5.1: X is a hyper-exponential additive process on the period $[0, T_2]$ whose parameters are constant during the periods $[0, T_1]$ and $[T_1, T_2]$. During the first period $[0, T_1]$, the process X evolves as a jump-diffusion with volatility σ_1, drift $\mu_1 = 0$, and exponentially-distributed jumps. During the second period $[T_1, T_2]$, X evolves as a linear Brownian motion with parameters σ_2 and $\mu_2 = 0$. Associated to X is a continuous Markov additive process A, which can be obtained from X by replacing the positive and negative jumps with linear stretches of path of slopes $+1$ and -1, and replacing the fixed times T_1, $T_2 - T_1$ by independent exponential random times $\mathbf{e}_1$ and $\mathbf{e}_2$ with parameters q_1, q_2. The process Y that records the current state or regime of A is a Markov process with generating matrix Q. When Y takes values 1 and 2, A evolves as a linear Brownian motion with zero drift and volatility σ_1 or σ_2; and when Y is 3 and 4, A is a positive or negative unit drift. These linear stretches of paths of A originate from the jumps of X. A jump of Y from one state to another is induced either by a jump of X or by a switch of the set of parameters that determine the dynamics of X. By time-changing A by the time $T_0(t)$ up to time t that Y was equal to 1 and 2, we recover a regime-switching jump-diffusion; that is, the process $\{A(T_0(t)), t \geq 0\}$ is in law a regime-switching jump-diffusion. Finally, replacement of the times at which a regime switch occurs by T_1 and T_2 results in a process with the same distribution as X.

we find that $h(\rho)$ solves the linear system

$$K[-\rho]\begin{pmatrix} I \\ \eta^+ \end{pmatrix} h(\rho) = \mathbf{0},$$

which implies that ρ is a root of the equation $\det K(s) = 0$. The following result characterises the eigenvalues of Q^+ (see Appendix 5.6.1):

Lemma 5.3.1

(i) *It holds that*

$$|\det(K(s))| = \prod_{i=1}^{N}\left\{|\Psi^{(i)}(-\mathrm{i}s) - q_i|\prod_{k=1}^{n^+}|s-\alpha_k^+|\prod_{l=1}^{n^-}|s+\alpha_l^-|\right\}, \qquad (5.15)$$

where $\Psi^{(i)}$ is given in (5.4).

(ii) *The equation*

$$\det K(s) = 0 \qquad (5.16)$$

has $N(1+n^+)$ positive roots and $N(1+n^-)$ negative roots.

Since $-Q^+$ is the negative of a generator matrix, it is non-negative definite, so its eigenvalues are non-negative and are given by the positive roots of (5.16). In particular, if the positive roots

$$\boldsymbol{\rho}_+ = \left(\rho_i^+ : i = 1,\ldots,N(n^+ + 1)\right)$$

of equation (5.16) are distinct, it follows from Lemma 5.3.1 and Theorem 5.3.1 that

$$G^{(+)}(x,\mathbf{q}) = (q_1\cdots q_N)^{-1} \times [1 - \mathbf{e}_i' U_+ \mathrm{e}^{-\Delta\boldsymbol{\rho}_+ x} U_+^{-1}\mathbf{1}],$$

where $U_+ = (h(\rho_i^+), i = 1,\ldots,N(n^+ + 1))$.

5.3.2 The final position and the first exit time

The valuation of barrier-options involves the joint distribution of the final position at maturity T and the first-exit time. We will extend the results in the previous section by considering the following:

$$\begin{aligned}\overline{F}^{(+)}(x,s) &:= E[\mathrm{e}^{sX_T}\mathbf{1}_{\{\overline{X}_T > x\}}] \\ &= E[\mathrm{e}^{sX_T}\mathbf{1}_{\{T^+(x)<T\}}].\end{aligned}$$

$\overline{F}^{(+)}(x,s)$ depends on time only through the inter-maturity times $(T^{(1)},\dots,T^{(N)})$. The Laplace transform $\overline{G}^{(+)}(x,s;q)$ of $\overline{F}^{(+)}(x,s)$ in $(T^{(1)},\dots,T^{(N)})$, can be expressed in terms of Q^+ and $K(s)$ as follows:

Proposition 5.3.1 *It holds that*

$$\overline{G}^{(+)}(x,s,\mathbf{q}) = \frac{\mathrm{e}^{sx}}{q_1\cdots q_N} \times \mathbf{e}_1' \mathrm{e}^{Q^+ x} K(s)^{-1} K(0)\mathbf{1} \tag{5.17}$$

for all $s \in \mathbb{C}$ *with* $\mathrm{Re}(s) \in (-\min_{j=1,\dots,n^-} \alpha_j^-, \min_{k=1,\dots,n^+} \alpha_k^+)$.

A proof is given in Appendix 5.6.1.

5.3.3 First-passage to a lower level

The form of the analogous distributions concerning the infimum

$$F^{(-)}(x) = P(-\underline{X}_T \le x), \qquad \overline{F}^{(-)}(x,s) = E[\mathrm{e}^{sX_T}\mathbf{1}_{\{-\underline{X}_T > x\}}], \quad x>0,$$

can be found by applying the results in the previous section to the process $-X$. More specifically, it is straightforward to check that the N-dimensional Laplace transforms $G^{(-)}(x,q)$ and $\overline{G}^{(-)}(x,s,q)$ are given by (5.10) and (5.17) replacing Q^+ by Q^-. (Q^-,η^-) satisfies the system of matrix equations (5.11) with V^+,H^+,D^-,C^-,T^- replaced by V^-,H^-,D^+,C^+,T^+, where the latter set is defined by interchanging $+$ and $-$ in equations (5.13), (5.9), (5.8) and (5.6). It is straightforward to verify that *(i)* an eigenvector $h(\rho)$ of Q^- corresponding to eigenvalue ρ satisfies

$$K[\rho]\begin{pmatrix}\eta^-\\ I\end{pmatrix} h(\rho) = 0,$$

where I is an $N(1+n^-)$ identity matrix, and *(ii)* that, in view of Lemma 5.3.1, the eigenvalues of Q^- are given by the negative roots

$$\boldsymbol{\rho}^- = \big(\rho_j^-, j=1,\dots,N(n^-+1)\big)$$

of $\det K(\rho)=0$.

5.4 Prices and Greeks of digital and barrier options

By use of the first-passage results from the previous section we derive semi-analytical expressions for the prices and sensitivities of down-and-in digital and knock-in call options. A down-and-in digital option at level $H < S_0$ is a contract that pays out one unit at maturity T if the price S has down-crossed the level H before T. Similarly, a down-and-in call option at level $H < S_0$ and with strike K is a call option whose pay-off is activated once S down-crosses H.

Taking the risk-free rate r and the dividend rate d to be constant, the arbitrage-free prices of a down-and-in digital ($EDID$) and a call option (DIC) are given respectively by

$$EDID(T) = EDID(T; S_0, H) = \mathrm{e}^{-(r-d)T} E\left[\mathbf{1}_{\{\inf_{s\le T} S_s < H\}}\right] = \mathrm{e}^{-(r-d)T} P(\underline{X}_T < h),$$

where $h = \log(H/S_0)$ is the log-barrier, and

$$DIC(T) = DIC(T; S_0, K, H) = \mathrm{e}^{-(r-d)T} S_0 E\left[(\mathrm{e}^{X_T} - \mathrm{e}^{l})^+ \mathbf{1}_{\{\underline{X}_T < h\}}\right],$$

where $l = \log(K/S_0)$ denotes the log-strike. Let $\widehat{EDID}(\mathbf{q})$ denote the joint Laplace transform of $EDID$ in the inter-maturity times $(T^{(1)}, \ldots, T^{(N)})$ (with $T^{(N)} = T$), and denote by $\widehat{DIC}^*(\mathbf{q}, s)$ the Laplace-Fourier transform in $(T^{(1)}, \ldots, T^{(N)})$ and in the log-strike l. Then we have the following result:

Proposition 5.4.1 *For $h = \log(H/S_0) < 0$ it holds that*

$$\widehat{EDID}(\mathbf{q}) = \frac{1}{c(q)} \times \mathbf{e}_1' \mathrm{e}^{Q^- h} \mathbf{1}, \tag{5.18}$$

$$\widehat{DIC}^*(\mathbf{q}, s) = \frac{S_0 \mathrm{e}^{bl}}{c(\mathbf{q}) b(b-1)} \times \mathbf{e}_1' \mathrm{e}^{Q^- h} K(s)^{-1} K(0) \mathbf{1}, \tag{5.19}$$

where

$$l = \log(K/S_0), \quad \mathbf{q} = (q_1, \ldots, q_N), \quad b = \alpha + \mathrm{i}s + 1, \quad c(\mathbf{q}) = (q_1 + r) \cdots (q_N + r).$$

Before we give the proof we observe that from the explicit expressions (5.18) and (5.19) semi-analytical formulae can be obtained for the delta and gamma

of the down-and-in digital and call options (i.e. the first and second derivatives of the option value with respect to the spot S_0). Indeed, the derivatives of the expressions (5.18) and (5.19) with respect to S_0 are equal to the Laplace-Fourier transforms of the derivatives of the option, as integration and differentiation are interchangeable in this case.

In the case of a down-and-in digital option we find that the Laplace transforms $\widehat{\Delta}_{EDID}$ and $\widehat{\Gamma}_{EDID}$ of the delta Δ_{EDID} and gamma Γ_{EDID} are given by

$$\widehat{\Delta}_{EDID}(\mathbf{q}) = -\frac{1}{c(q)S_0} \times e_1' Q^- \mathrm{e}^{Q^- h}\mathbf{1}, \tag{5.20}$$

$$\widehat{\Gamma}_{EDID}(\mathbf{q}) = \frac{1}{c(q)S_0^2} \times e_1' [(Q^-)^2 + Q^-] \mathrm{e}^{Q^- h}\mathbf{1}. \tag{5.21}$$

Proof of Proposition 5.4.1 The expression (5.18) is a direct consequence of Theorem 5.3.1 (see also Section 5.3.3). To verify (5.19) we start by taking the Fourier transform in l and find as in (5.24) that the Fourier transform DIC^* is

$$DIC^*(\alpha + \mathrm{i}s) = \frac{\overline{F}^{(-)}(-h, b)}{b(b-1)}, \tag{5.22}$$

where $b = \alpha + \mathrm{i}s + 1$ and

$$\overline{F}^{(-)}(x, b) = E[\mathrm{e}^{bX_T}\mathbf{1}_{\{-\underline{X}_T \geq x\}}].$$

From Proposition 5.3.1 we deduce that the form the joint Laplace transform $\overline{G}(x, b, \mathbf{q})$ of $\overline{F}^{(-)}(x, b)$ in $(T^{(1)}, \ldots, T^{(N)})$ is given by

$$\overline{G}(x, b, \mathbf{q}) = \frac{\mathrm{e}^{bx}}{c(\mathbf{q})} \times \mathbf{e}_1' \mathrm{e}^{Q^- h} K(s)^{-1} K(0)\mathbf{1}. \tag{5.23}$$

Combining (5.22) and (5.23) completes the proof. □

5.5 Numerical results

5.5.1 Calibration of the additive hyper-exponential model

We calibrate the hyper-exponential additive model to Stoxx50E call options at four different maturities, observed in the market on 20 February 2007. The spot

level is 4150, the risk-free rate is assumed to be fixed at $r = 0.03$, and the dividend rate is taken to be zero. As we find that inclusion of positive jumps does not substantially improve the calibration results, we only consider negative jumps, and we specify the jump-size parameters to be $(\alpha_1^-, \alpha_2^-) = (3, 10)$. The jump arrival rates $\boldsymbol{\pi}^-$ and the volatility are piecewise constant in time, and are estimated by minimising the root-mean-square error between model and observed market call prices. Using the well-known Fourier transform method (briefly recalled in Appendix 5.6.2) the calibration is carried out maturity by maturity under constraints through a bootstrapping method with well-defined local triplets.

In Figure 5.2 the calibration results are presented with plots of the market and model implied volatility surfaces corresponding to the four maturities 6m, 1Y, 3Y and 5Y. The root-mean-square error (RMSE) and the average relative percentage error (ARPE) are equal to 5.30 and 1.1%. We compare it to a price process that follows a Lévy process with hyper-exponential jumps (i.e. with constant parameters over time), and find that the calibration of the four maturities in that case give a RMSE of 9.82 and an ARPE of 2.9%. In Table 5.1 the resulting parameter sets are displayed under the hyper-exponential additive and Lévy models. In the case of the hyper-exponential model we observe a high jump intensity of small jumps for short maturities that decrease substantially over time. This is consistent with the findings of Carr & Wu [25] and Pan [71].

5.5.2 Results for barrier-option prices and Greeks

Using the parameter set found in the calibration of the Stoxx50E call options, we value barrier and digital options on the Stoxx50E index, modelling its price process as the exponential of a hyper-exponential additive process. We use the semi-analytical results in Proposition 5.4.1. To invert the multi-dimensional Laplace transforms we choose Talbot's method [84] (see also [28]) for down-and-in digital options. We combine it with the fractional fast Fourier transform (FrFFT) algorithm of Bailey & Swarztrauber [11] and Chourdakis [29] for down-and-in call options. See Appendix 5.6.3 for a detailed description of the implementation of these transform algorithms. We compare it to the same quantities calculated by Monte-Carlo simulations, using a standard Euler scheme.

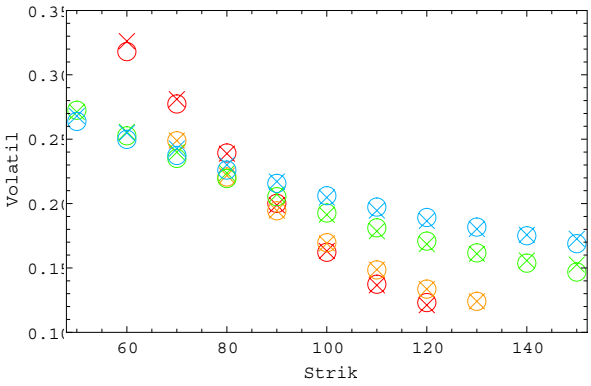

Figure 5.2: Calibration of Stoxx50E call option prices on 20 February 2007 for an additive hyper-exponential model with piecewise constant parameters. Crosses represent market implied volatilities and circles model implied volatilities for four maturities: 6 months (red), 1 year (orange), 3 years (green), 5 years (blue).

Additive hyper-exponential model				
T_{Start}	T_{End}	σ	π_1^-	π_2^-
0	0.5	0.0995	0.0371	11.1819
0.5	1	0.0759	0.2091	9.9540
1	3	0.0786	0.4738	7.0322
3	5	0.0858	0.8084	0.2361
Lévy hyper-exponential model				
T_{Start}	T_{End}	σ	π_1^-	π_2^-
0	5	0.1171	0.5693	0.0165

Table 5.1: Calibration of Stoxx50E call option prices quoted on 20 February 2007 for an additive hyper-exponential model with piecewise constant parameters and for a Lévy hyper-exponential model with jump parameters $\alpha_1^- = 3$ and $\alpha_2^- = 10$. The interest rate and dividend rate are $r = 0.03$ and $d = 0$. The maturities are given in years.

Down-and-in digital options

We price down-and-in digital options with a maturity of five years for different spot levels. We evaluate the required four-dimensional Laplace transform over two time increments of six months, and two time increments of two years; that is, $T^{(1)} = 0.5$, $T^{(2)} = 0.5$, $T^{(3)} = 2$, $T^{(4)} = 2$. We use Talbot's algorithm with $M = 6$ (see Appendix 5.6.3 for an explanation of this parameter). Using Mathematica to run the algorithm, the computation time was five minutes on a 3189 Mhz computer to calculate prices and Greeks for fourteen different spot levels. The calculation of first-passage probabilities using Monte-Carlo simulations requires a large number of time-steps and paths. We use one million paths with $\delta t = 5 \times 10^{-5}$ and it takes several hours to obtain stable Greeks in C++. Error bounds cannot be obtained analytically, but we observe in Table 5.2 that the results of the transform method agree with Monte-Carlo simulation results. Figures 5.3 and 5.4 report prices and Greeks for down-and-in digital options. The options are expressed as a percentage of the spot price. The values of the sensitivities are expressed as fractions of the spot price S_0.

This transform algorithm is particularly efficient at a book level, since once the generating matrices Q^- of the infimum have been calculated for different values of the vector $\mathbf{q}$ the calculation of prices and Greeks of any digital barrier product is just a matter of summation.

Down-and-in call options

We value down-and-in call options with a maturity of one year for different strike levels. In this case, a two-dimensional Laplace inversion is required over time increments $T^{(1)} = 0.5$ and $T^{(2)} = 0.5$. For the inversions of the Laplace transform and the Fourier transform, we set $M = 7$ and $N = 1024$ (refer to Appendix 5.6.3 for an explanation of these parameters). For Monte-Carlo simulations, we use one million paths with time-step $\delta t = 2.5 \times 10^{-5}$. The option prices and Greeks obtained by the two methods are reported in Table 5.3 and Figures 5.5 and 5.6. We observe that the results of the transform method agree with the Monte-Carlo simulation results.

By the use of Mathematica again to run the algorithm, the computation time is ten minutes to calculate the option prices, delta and gamma for eleven different levels of the strike. Since the option prices and Greeks of a down-and-in call option are obtained via a Fourier-Laplace transform, it takes more time than in the case of a digital option (approximately twice as long), which is still much faster than a Monte-Carlo Euler scheme. We note that the transform algorithm is particularly efficient for the pricing of options with different strikes, as we obtain by FrFFT inversion the prices and Greeks of any down-and-in call options on a log-strike grid.

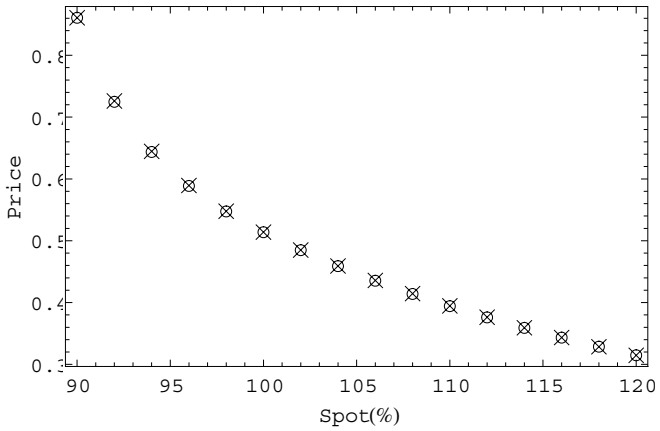

Figure 5.3: Prices of down-and-in digital options with a barrier H set at 90% of the spot level 4150 and maturity $T = 5$ years. Semi-analytical results are indicated with the symbol $\times$ and Monte-Carlo results with the symbol $\circ$.

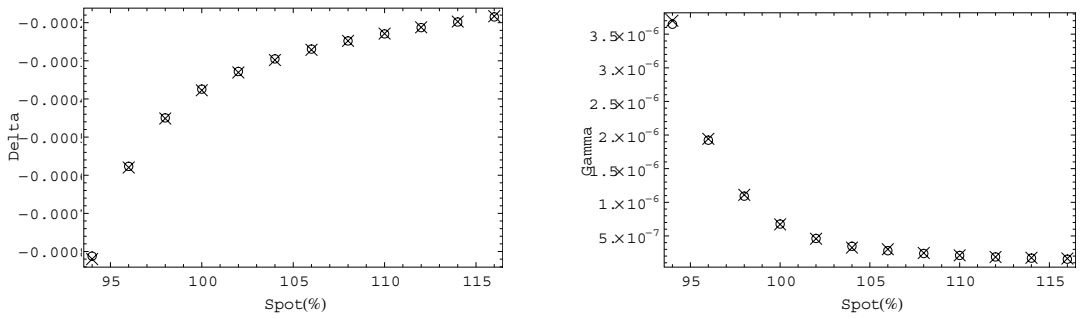

Figure 5.4: Greeks of down-and-in digital options with a barrier H set at 90% of the spot level 4150 and maturity $T = 5$ years. Semi-analytical results are indicated with the symbol $\times$ and Monte-Carlo results with the symbol $\circ$.

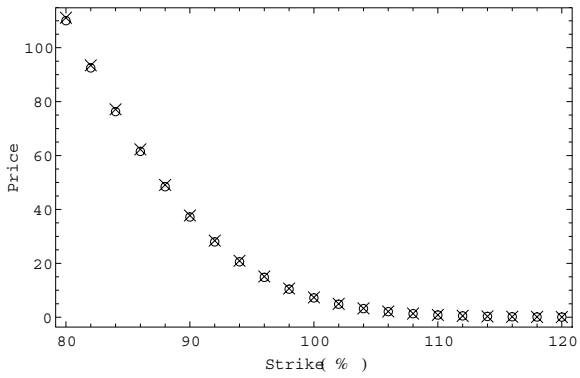

Figure 5.5: Prices of down-and-in call options with a barrier H set at 90%, a spot level at 4150 and maturity $T = 1$ year. Semi-analytical results are indicated with the symbol $\times$ and Monte-Carlo results with the symbol $\circ$.

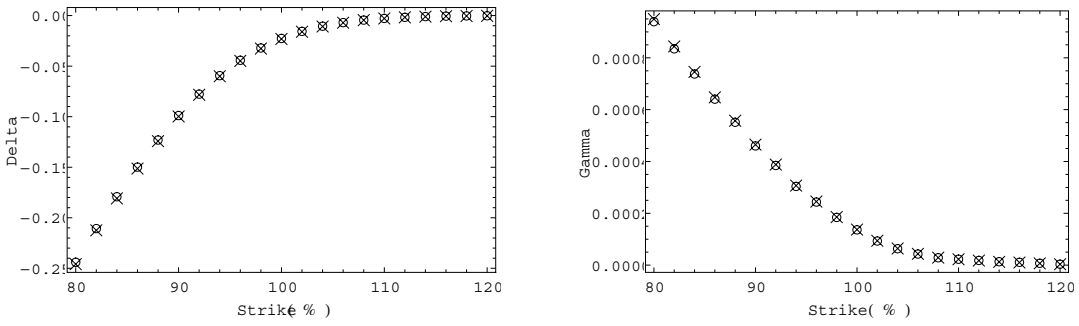

Figure 5.6: Greeks of down-and-in call options with a barrier H set at 90%, a spot level at 4150 and maturity $T = 1$ year. Semi-analytical results are indicated with the symbol $\times$ and Monte-Carlo results with the symbol $\circ$.

	Down-and-in digital options					
	Price		Delta ($\times 10^{-3}$)		Gamma ($\times 10^{-7}$)	
%	TA	(MC−, MC+)	TA	MC	TA	MC
92	0.7261	(0.7000, 0.7499)	-1.226	-1.232	7.34	7.54
94	0.6446	(0.6137, 0.6735)	-0.812	-0.819	3.64	3.70
96	0.5893	(0.5566, 0.6207)	-0.577	-0.579	1.92	1.94
98	0.5478	(0.5143, 0.5805)	-0.450	-0.451	1.09	1.11
100	0.5140	(0.4800, 0.5475)	-0.374	-0.377	0.67	0.67
102	0.4850	(0.4506, 0.5189)	-0.328	-0.330	0.46	0.45
104	0.4592	(0.4245, 0.4932)	-0.294	-0.297	0.34	0.33
106	0.4358	(0.4008, 0.4697)	-0.269	-0.271	0.28	0.30
108	0.4144	(0.3795, 0.4483)	-0.247	-0.247	0.24	0.24
110	0.3946	(0.3599, 0.4285)	-0.229	-0.228	0.21	0.21
112	0.3762	(0.3518, 0.4010)	-0.212	-0.212	0.19	0.19
114	0.3592	(0.3250, 0.3917)	-0.198	-0.197	0.17	0.17
116	0.3433	(0.3095, 0.3771)	-0.184	-0.182	0.15	0.16
118	0.3285	(0.3012, 0.3632)	-0.172	-0.170	0.14	0.14

Table 5.2: Down-and-in digital options with barrier H set at 90% of the spot level 4150. The first column contains the spot price as a percentage figure of the spot level 4150. The columns with TA contain the results obtained using the transform algorithm, whereas MC refers to Monte-Carlo results. In the case of the price the Monte-Carlo results are reported in the form of a 95% confidence interval, and in the other cases as a point estimate.

	Down-and-in call options					
	Price		Delta ($\times 10^{-1}$)		Gamma ($\times 10^{-4}$)	
%	TA	(MC− , MC+)	TA	MC	TA	MC
80	111.13	(108.85, 111.20)	-2.458	-2.440	9.49	9.39
82	93.48	(91.46, 93.55)	-2.124	-2.107	8.43	8.34
84	77.14	(75.35, 77.19)	-1.808	-1.792	7.45	7.37
86	62.28	(60.71, 62.33)	-1.514	-1.499	6.47	6.40
88	49.08	(47.71, 49.13)	-1.242	-1.231	5.57	5.51
90	37.63	(36.7, 37.80)	-0.991	-0.988	4.65	4.59
92	28.11	(27.43, 28.46)	-0.783	-0.776	3.88	3.84
94	20.94	(20.13, 21.01)	-0.599	-0.593	3.07	3.03
96	15.11	(14.45, 15.16)	-0.448	-0.443	2.45	2.43
98	10.66	(10.12, 10.72)	-0.326	-0.320	1.85	1.84
100	7.36	(6.92, 7.41)	-0.231	-0.226	1.37	1.36
102	4.97	(4.63, 5.02)	-0.159	-0.156	0.94	0.93
104	3.28	(3.03, 3.34)	-0.107	-0.104	0.64	0.63
106	2.12	(1.94, 2.18)	-0.070	-0.069	0.43	0.42
108	1.35	(1.22, 1.41)	-0.045	-0.044	0.28	0.28
110	0.84	(0.74, 0.89)	-0.028	-0.027	0.23	0.22
112	0.51	(0.47, 0.54)	-0.017	-0.017	0.18	0.18
114	0.30	(0.25, 0.34)	-0.010	-0.009	0.13	0.13
116	0.18	(0.16, 0.19)	-0.006	-0.006	0.10	0.10
118	0.10	(0.08, 0.11)	-0.003	-0.003	0.07	0.07
120	0.06	(0.03, 0.06)	-0.002	-0.002	0.03	0.03

Table 5.3: Down-and-in call options with a barrier H set at 90%, a spot level at 4150 and maturity $T = 1$ year for a range of strikes. The first column contains the strike level as a percentage figure of the spot level 4150. The columns with TA contain the results obtained using the transform algorithm, whereas MC refers to Monte-Carlo results. In the case of the price the Monte-Carlo results are reported in the form of a 95% confidence interval, and in the other cases as a point estimate.

5.6 Appendix Chapter 5

5.6.1 Proofs

Proof of Lemma 5.3.1

(i) It is straightforward to verify that $K^{\#}(s)$ can be obtained from $K(s)$ by interchanging some columns and rows, where $K^{\#}(s)$ is given by

$$K^{\#}(s) = \begin{pmatrix} K_1(s) & D_1 & & & \\ & K_2(s) & D_2 & & \\ & & . & . & \\ & & & K_{N-1}(s) & D_{N-1} \\ & & & & K_N(s) \end{pmatrix},$$

where $K_w(s)$ and D_w are square matrices of dimension $n^+ + n^- + 1$. These are defined respectively by

$$K_w(s) = \begin{pmatrix} \frac{\sigma_w^2 s^2}{2} + \mu_w s - q_w - \lambda_w^+ - \lambda_w^- & \pi_1^-(w) & . & \pi_m^-(w) & \pi_1^+(w) & . & \pi_n^+(w) \\ \alpha_1^- & -s - \alpha_1^- & 0 & 0 & 0 & 0 & 0 \\ . & 0 & . & 0 & 0 & 0 & 0 \\ \alpha_m^- & 0 & 0 & -s - \alpha_m^- & 0 & 0 & 0 \\ \alpha_1^+ & 0 & 0 & 0 & s - \alpha_1^+ & 0 & 0 \\ . & 0 & 0 & 0 & 0 & . & 0 \\ \alpha_n^+ & 0 & 0 & 0 & 0 & 0 & s - \alpha_n^+ \end{pmatrix},$$

where $\lambda_w^{\pm} = \sum_i \pi_i^{\pm}(w)$, and

$$(D_w)_{ij} = \begin{cases} q_w & \text{if } i = j = 1 \\ 0 & \text{otherwise} \end{cases}.$$

Therefore $|\det(K(s))|$ is equal to $|\det(K^{\#}(s)|$. To proceed we recall an identity from matrix algebra. Let M be a matrix of the form

$$M = \begin{pmatrix} M_{11} & M_{12} \\ M_{21} & M_{22} \end{pmatrix}$$

in block notation, where M_{22} is invertible. Then

$$\det(M) = \det(M_{22}) \det(M_{11} + M_{12} M_{22}^{-1} M_{21}).$$

Using this identity, it is a matter of algebra to verify by induction that

$$\det(K^{\#}(s)) = \det(K_1(s)) \cdots det(K_N(s)).$$

As a consequence we find, by applying this matrix identity, that

$$\det(K_w(s)) = \left(\frac{\sigma_w^2}{2} s^2 + \mu_w s + \sum_{i=1}^{n^+} \pi_i^+(w) \frac{\alpha_i^+}{s - \alpha_i^+} + \sum_{j=1}^{n^-} \pi_j^-(w) \frac{\alpha_j^-}{-s - \alpha_j^-} - \lambda_w^+ - \lambda_w^- - q_w \right) \times \\ \times \prod_{i=1}^{n^+} (s - \alpha_i^+) \prod_{j=1}^{n^-} (-s - \alpha_j^-),$$

and the assertion follows in view of (5.4).

(ii) Using the intermediate value theorem and the specific form of Ψ, it is straightforward to check that the equation $\Psi(-ui) = q$, $q > 0$ has $n+1$ positive roots ρ_i^+ and $m+1$ negative roots ρ_j^-, satisfying

$$\rho_{m+1}^- < -\alpha_m^- < \rho_m^- < \ldots < -\alpha_1^- < \rho_1^- < 0 < \rho_i^+ < \alpha_1^+ < \ldots < \rho_n^+ < \alpha_n^+ < \rho_{n+1}^+.$$

Since $\det(K_w(s))$ is a polynomial of degree $n+m+2$, it follows that all the roots of $\det(K_w(s)) = 0$ are given by $(\rho_i^+, i = 1, \ldots, n+1)$ and $(\rho_j^-, j = 1, \ldots, m+1)$. In view of the form of $\det(K(s))$ derived in (i) the assertion follows.

□

Proof of Proposition 5.3.1 Consider the following randomisation of X obtained by randomising the inter-maturity times $T^{(i)}$ by replacing them by independent exponential random times with means q_i^{-1}, and call this process $\widetilde{X}$. The process $\widetilde{X}$ is a regime-switching jump-diffusion, where the only regime switches that can occur are from i to $i+1$ at rate q_i $(i = 1, \ldots, N-1)$, and from the final state N to an absorbing 'graveyard state' ∂. As shown in [54], the process $\widetilde{X}$ is equal to a time-changed continuous process A, say. Denoting by ζ the epoch at which A is sent to ∂, by Y the modulating Markov chain, and by $\tau = \inf\{t \geq 0 : A_\tau = x\}$,

we have

$$\begin{aligned} q_1 \cdots q_N \overline{G}(x,s,q) &= E[\mathrm{e}^{sA_{\zeta-}} \mathbf{1}_{\{\overline{A}_{\zeta-} > x\}}] \\ &= E[\mathrm{e}^{sA_{\zeta-}} \mathbf{1}_{\{\tau < \zeta\}}] \\ &= E[\mathrm{e}^{sA_{\tau}} \mathbf{1}_{\{\tau < \zeta\}} f(Y_\tau)] \\ &= \mathrm{e}^{sx} E[\mathbf{1}_{\{\tau < \zeta\}} f(Y_\tau)], \end{aligned}$$

with

$$f(y) = E[\mathrm{e}^{sA_{\zeta-}} | A_0 = 0, Y_0 = y],$$

where the last two lines follow by the Markov property of (A, Y) and the fact that A is continuous. To guarantee that all the expressions are well defined in this calculation s has to be such that $E[\mathrm{e}^{sX_1}] < \infty$, which corresponds to the restriction that

$$Re(s) \in (-\min_j \alpha_j^-, \min_i \alpha_i^+).$$

In [54] it was shown that the vector $\mathbf{f} = (f(y), y \in N)$, where N denotes the state space of Y, is given by

$$\mathbf{f} = K(s)^{-1} Q \mathbf{1},$$

where the matrix $K(s)$ is given in (5.14). Combining these results with Theorem 5.3.1 we find that

$$q_1 \cdots q_N \overline{G}(x,s,q) = e_1' \mathrm{e}^{Q^+ x} K(s)^{-1} Q \mathbf{1},$$

and the proof is complete. □

5.6.2 European call options

Under the hyper-exponential additive model with piecewise constant parameters (5.3), the characteristic function at time T is explicitly given by

$$\Phi^{(i)}(u) = \exp\left(\sum_{j=1}^{i} \Psi^{(j)}(u) \right),$$

with $\Psi^{(j)}$ as given in (5.4). The price of a European call with maturity T_i can thus be efficiently calculated using a well-established Fourier transform method,

which we briefly recall. The Fourier transform $C^*_{T_i}$ over l of $C_{T_i}(l)$, the price of a call option with log-strike $l = \log(K/S_0)$ and maturity T_i, can be explicitly expressed in terms of the characteristic function $\Phi^{(i)}(u)$ as follows:

$$\begin{aligned} C^*_{T_i}(v - \mathrm{i}\alpha) &= S_0 \mathrm{e}^{-rT_i} \int_{-\infty}^{\infty} \mathrm{e}^{\mathrm{i}vl} E[\mathrm{e}^{\alpha l}(\mathrm{e}^{X_{T_i}} - \mathrm{e}^{l})^+]\mathrm{d}l \\ &= S_0 \mathrm{e}^{-rT_i} \frac{\Phi^{(i)}(v - (\alpha+1)\mathbf{i})}{(\alpha + \mathrm{i}v)(\alpha + 1 + \mathrm{i}v)}. \end{aligned} \tag{5.24}$$

Since the call pay-off function itself is not square-integrable in the log-strike, the axis of integration is here shifted over $\mathrm{i}\alpha$ which corresponds to dampen exponentially the pay-off function at a rate α, which is usually taken to be $\alpha = 0.75$ (see Carr & Madan [23]). The call option prices are then determined by inverting the Fourier transform:

$$C_{T_i}(l) = \frac{S_0 \mathrm{e}^{-\alpha l} \mathrm{e}^{-rT_i}}{\pi} \int_0^{\infty} \mathrm{e}^{-\mathrm{i}lv} \frac{\Phi^{(i)}(v - (\alpha+1)\mathbf{i})}{(\alpha + \mathrm{i}v)(\alpha + 1 + \mathrm{i}v)} \mathrm{d}v. \tag{5.25}$$

5.6.3 Transform inversion algorithms

Multi-dimensional Laplace inversion

To evaluate down-and-in digital option prices (EDID), we invert the multi-dimensional Laplace transform (5.18) to obtain

$$EDID(T) = \frac{1}{(2\pi\mathbf{i})^N} \int_{C_N} \cdots \int_{C_1} \mathrm{e}^{q_1 T_1 + \ldots + q_N T_N} \widehat{EDID}(\mathbf{q}) \mathrm{d}\mathbf{q}. \tag{5.26}$$

where C_n are vertical lines in the complex plane defined by $q_n = r_n + \mathrm{i}y_n$ for $n = 1, \ldots N$ with $-\infty < y_n < \infty$ and fixed values of r_n, chosen such that all the singularities of the transform $\widehat{EDID}(\mathbf{q})$ are coordinate-wise on the left of the lines C_n. Many algorithms approximate the integrals in (5.26) by a finite linear combination of the transform at some specific nodes with certain weights. Three approaches have been studied by Abate *et al.* [3], based on Fourier series expansion, combinations of Gaver functionals, and deformation of the integral contour. Here we concentrate on the last method developed by Talbot [84], since reports in the literature (e.g. [3]) suggest that this approach offers high performance for a short time of execution, which our numerical results confirm. We write

$$EDID(T) = \frac{1}{(2\pi\mathbf{i})^N} \int_{-\pi}^{\pi} \cdots \int_{-\pi}^{\pi} \beta_1(\theta) \cdots \beta_N(\theta) \widehat{EDID}(S_0, h, \mathbf{q}(\theta)) \mathrm{d}\boldsymbol{\theta}, \tag{5.27}$$

with $n = 1, \ldots N$, $\beta_n(\theta) = w_n \mathrm{e}^{\mathrm{i}r_n w_n T_n}$, $q_n(\theta) = \mathrm{i}r_n w_n$, and

$$w_n = -1 + \mathrm{i}\theta + \mathrm{i}(\theta \cot\theta - 1)\cot\theta.$$

Since $EDID$ is a real-valued function, $EDID$ is also equal to the real part of the integral on the right-hand side of (5.27), which can be used to reduce the calculation by a factor of two. To illustrate the evaluation of the integrals (5.27), we present concrete expressions for the approximating sums when $N = 4$ (which is the setting that will be implemented later on). Defining

$$\theta_n^k = k\pi/M \quad \text{and} \quad r_n = \frac{2M}{5T_n},$$

we obtain

$$\begin{aligned}
EDID(T) \approx \frac{2}{5^4 T_1 T_2 T_3 T_4} \sum_{k_1=0}^{M-1}\sum_{k_2=0}^{M-1}\sum_{k_3=0}^{M-1}\sum_{k_4=0}^{M-1} & \\
\beta_{k_1}\beta_{k_2}\beta_{k_3}\beta_{k_4} f(q_{k_1}/T_1, q_{k_2}/T_2, q_{k_3}/T_3, q_{k_4}/T_4) + \overline{\beta}_{k_1}\beta_{k_2}\beta_{k_3}\beta_{k_4} f(\overline{q}_{k_1}/T_1, q_{k_2}/T_2, q_{k_3}/T_3, q_{k_4}/T_4) & \\
+ \quad \beta_{k_1}\overline{\beta}_{k_2}\beta_{k_3}\beta_{k_4} f(q_{k_1}/T_1, \overline{q}_{k_2}/T_2, q_{k_3}/T_3, q_{k_4}/T_4) + \beta_{k_1}\beta_{k_2}\overline{\beta}_{k_3}\beta_{k_4} f(q_{k_1}/T_1, q_{k_2}/T_2, \overline{q}_{k_3}/T_3, q_{k_4}/T_4) & \\
+ \quad \beta_{k_1}\beta_{k_2}\beta_{k_3}\overline{\beta}_{k_4} f(q_{k_1}/T_1, q_{k_2}/T_2, q_{k_3}/T_3, \overline{q}_{k_4}/T_4) + \overline{\beta}_{k_1}\overline{\beta}_{k_2}\beta_{k_3}\beta_{k_4} f(\overline{q}_{k_1}/T_1, \overline{q}_{k_2}/T_2, q_{k_3}/T_3, q_{k_4}/T_4) & \\
+ \quad \beta_{k_1}\overline{\beta}_{k_2}\beta_{k_3}\overline{\beta}_{k_4} f(q_{k_1}/T_1, \overline{q}_{k_2}/T_2, q_{k_3}/T_3, \overline{q}_{k_4}/T_4) + \overline{\beta}_{k_1}\overline{\beta}_{k_2}\overline{\beta}_{k_3}\beta_{k_4} f(\overline{q}_{k_1}/T_1, \overline{q}_{k_2}/T_2, \overline{q}_{k_3}/T_3, q_{k_4}/T_4), &
\end{aligned}$$

where f is equal to $\widehat{EDID}$. The weights and the nodes are given by

$$\begin{aligned}
q_0 &= \frac{2M}{5}, \quad q_k = \frac{2k\pi}{5}(\cot(k\pi/M) + \mathrm{i}), \qquad 0 < k < M, \\
\beta_0 &= 0.5e^{q_0}, \quad \beta_k = (1 + \mathrm{i}(k\pi/M)(1 + [\cot(k\pi/M)]^2) - \mathrm{i}\cot(k\pi/M))e^{q_k}.
\end{aligned}$$

Since the weights and nodes are independent of the transform, the calculation time of the algorithm can be reduced by pre computing and storing weights and nodes. The speed of convergence and the accuracy of the Talbot algorithm will depend on the regularity of the Laplace transform f. Although universal error bounds are not known, Abate *et al.* [1] showed numerically that the single parameter M can be used to control the error and can be seen as a measure for the precision. They found after extensive numerical experiments that for a large class of Laplace transforms the relative error is approximately $10^{-0.6M}$. For high-dimensional inversion, extra accuracy in the inner sums may be needed to obtain a sufficient degree of precision for the outer sums, which can be achieved by increasing M.

Fractional Fourier Transform

To evaluate down-and-in call option prices (DIC), we invert the Fourier-Laplace transform (5.19) over log-strike and time periods. For the inversion of the Laplace transform we again apply the Talbot algorithm. In the case of two time periods, with

$$f_s(q_1, q_2) = \widehat{DIC}^*(\mathbf{q}, s),$$

we find that the Fourier transform DIC^* can be approximated by the following sums:

$$\begin{aligned} &DIC^*(s) \\ &\approx \frac{1}{5^2 T_1 T_2} \sum_{k_1=0}^{M-1} \sum_{k_2=0}^{M-1} \left\{ \beta_{k_1} \beta_{k_2} f_s(q_{k_1}/T_1, q_{k_2}/T_2) + \overline{\beta}_{k_1} \overline{\beta}_{k_2} f_s(\overline{q}_{k_1}/T_1, \overline{q}_{k_2}/T_2) \right. \\ &\qquad \left. + \overline{\beta}_{k_1} \beta_{k_2} f_s(\overline{q}_{k_1}/T_1, q_{k_2}/T_2) + \beta_{k_1} \overline{\beta}_{k_2} f_s(q_{k_1}/T_1, \overline{q}_{k_2}/T_2) \right\}. \end{aligned}$$

Unlike the case of the inversion of $\widehat{EDID}$, we cannot reduce the calculation time by two by using complex conjugates, since the function DIC^* is not real valued. Down-and-in call prices are then obtained by inverting the Fourier transform over strike:

$$DIC(T) = \frac{\mathrm{e}^{-\alpha l}}{\pi} \int_0^\infty \mathrm{e}^{-\mathbf{i} v l} DIC^*(s) \mathrm{d}s,$$

where α is the rate of exponential dampening. This integral is approximated for a set of log-strikes between $(-x_0, x_0)$ as a summation:

$$DIC(T) \approx \frac{S \mathrm{e}^{-\alpha l} \mathrm{e}^{-rT}}{\pi} \sum_{j=0}^{N-1} w_j \mathrm{e}^{-\mathrm{i}\delta j(-x_0 + l\lambda)} DIC^*(\delta j)\delta, \qquad l = 1 \cdots N-1, \quad (5.28)$$

where $(w_j)_{j=0}^{N-1}$ are the integration weights defined by the trapezoidal rule with $w_0 = w_{N-1} = 0.5$ and 1 otherwise, $\lambda = 2x_0/N$ is the log-strike grid step-size and δ is the v-grid step-size. Carr & Madan [23] and Chourdakis [29] set $\delta = 0.25$.

To have accurate prices for any strike, the log-strike grid spacing λ needs to be sufficiently small. A common approach is to apply directly the fast Fourier transform (FFT) and to compute the summation (5.28) on a fixed log-strike range $(-x_0, x_0)$ with $x_0 = \pi/\delta$ using many points N. Bailey & Swarztrauber [10, 11] propose an alternative approach, and define the fractional fast Fourier transform

(FrFFT), which uses an arbitrary range. Chourdakis [29] showed that the FrFFT can be used to calculate option prices with less points without losing accuracy. He reported that the FrFFT is 45 times faster than the FFT for the calculation of European option prices. Since in our case the Fourier transform DIC^* is obtained numerically, we chose to employ the FrFFT. We now briefly specify the form of this algorithm in our setting, and refer for further details to [10, 11], [29]. The resulting sum is then given by

$$DIC(T) \approx \frac{S_0 \mathrm{e}^{-(\alpha l + \mathrm{i}\pi l^2 \nu)} \mathrm{e}^{-rT}}{\pi} \sum_{j=0}^{N-1} \widetilde{w}_j \mathrm{e}^{-\pi \mathbf{i} j^2 \nu} \mathrm{e}^{-\pi \mathrm{i}(l-j)^2 \nu} DIC^*(\delta j)\delta,$$

where $l = 1 \cdots N-1$, $\widetilde{w}_j = w_j e^{\mathrm{i}x_0 \delta j}$ and $\nu = \delta x_0 / N\pi$. Extending this summation into a circular convolution over $2N$ yields

$$DIC(T) \approx \frac{S_0 \mathrm{e}^{-(\alpha l + \mathrm{i}\pi l^2 \nu)} \mathrm{e}^{-rT}}{\pi} \sum_{j=0}^{2N-1} y_j z_{l-j}, \qquad l = 1 \cdots N-1,$$

where

$$y_j = \widetilde{w}_j \mathrm{e}^{-\pi \mathrm{i} j^2 \nu} DIC^*(\delta j)\delta, \quad z_j = \mathrm{e}^{-\pi \mathrm{i} j^2 \nu}, \quad j < N,$$

and

$$y_j = 0, \quad z_j = \mathrm{e}^{-\pi \mathrm{i}(j-2N)^2 \nu}, \quad j \geq N.$$

This equation can be rewritten in terms of three discrete Fourier transforms:

$$DIC(l) \approx \frac{S_0 \mathrm{e}^{-(\alpha l + \mathrm{i}\pi l^2 \nu)} \mathrm{e}^{-rT}}{\pi} F_l^{-1}(F_l(y) F_l(z)), \qquad l = 1 \cdots N-1,$$

with

$$F(x) = \sum_{j=0}^{N-1} x_j \mathrm{e}^{-2\pi \mathrm{i} j l / N}, \qquad F^{-1}(x) = \sum_{j=0}^{N-1} x_j \mathrm{e}^{2\pi \mathrm{i} j l / N}.$$

Although the latter sum is computed by invoking two Fourier transforms and one inverse Fourier transform, this approach has the advantage of computing the option prices on a specific log-strike window $(-x_0, x_0)$ with independent grids δ and λ and requires fewer points.

Bibliography

[1] J. Abate & P. P. Valko. Multi-precision Laplace transform. *International Journal for Numerical Methods in Engineering*, 60:979–993, 2004. 97

[2] J. Abate & W. Whitt. Numerical inversion of Laplace transforms of probability distributions. *ORSA Journal on Computing*, 7:36–43, 1995. 39, 57, 58

[3] J. Abate & W. Whitt. A unified framework for numerically inverting Laplace transforms. *Informs Cournal on Computing*, 18:408–421, 2006. 96

[4] M. Abramowitz & I. A. Stegun. *Handbook of Mathematical Functions with Formulas, Graphs, and Mathematical Tables*. Dover, New York, 1964. 44

[5] S. Asmussen. *Ruin Probabilities*. World Scientific, Singapore, 2000. 80

[6] S. Asmussen. *Applied probability and queues*. Springer-Verlag, New York, second edition, 2003. 46

[7] S. Asmussen, F. Avram, & M. Pistorius. Russian and american put options under exponential phase-type Lévy models. *Stochastic Processes and their Applications*, 109:79–111, 2004. 43, 46, 47

[8] S. Asmussen, D. B. Madan, & M. R. Pistorius. Pricing equity default swaps under the CGMY Lévy model. *Journal of Computational Finance*, 11:79–93, 2008. 39, 57, 72

[9] M. Avellaneda & M. Lipkin. A market induced mechanism for stock pinning. *Quantitative Finance*, 5:417–425, 2003. 13, 21, 22, 23, 25

[10] D. H. Bailey & P. N. Swarztrauber. The fractional Fourier transform and applications. *SIAM Review*, 33:389–404, 1991. 98, 99

[11] D. H. Bailey & P. N. Swarztrauber. A fast method for the numerical evaluation of continuous Fourier and Laplace transforms. *SIAM Journal on Scientific Computing*, 55:205–238, 1994. 73, 86, 98, 99

[12] O. E. Barndorff-Nielsen. Processes of normal inverse gaussian type. *Finance and Stochastics*, 2:41–68, 1998. 38, 44

[13] A. Bensoussan & J. L. Lions. *Impulse control and quasi variational inequalities*. Gauthier-Villars, Paris, 1984. 54

[14] J. Bertoin. *Lévy processes*. Cambridge university press, Cambridge, 1996. 15, 41

[15] N. H. Bingham. Fluctuation theory in continuous time. *Journal of Advances in Applied Probability*, 7:705–766, 1975. 41

[16] A. A. Borovkov. *Stochastic processes in queueing theory*. Springer-Verlag, Berlin, 1976. 46

[17] J. P. Bouchaud, M. Mezard, & M. Potters. Statistical properties of stock order books: empirical results and models. *Quantitative Finance*, 2:251–256, 2002. 32

[18] M. Boyarchenko & S. Z. Levendorskiĭ. Prices and sensitivities of barrier and first-touch digital options in Lévy driven models. *Preprint downloadable at* `SSRN.com/abstract=1155149`, 2009. 73

[19] S. I. Boyarchenko & S. Z. Levendorskiĭ. Option pricing for truncated Lévy processes. *International Journal of Theoretical and Applied Finance*, 3:549–552, 2000. 38, 44

[20] S. I. Boyarchenko & S. Z. Levendorskiĭ. Barrier options and touch and out options under regular Lévy processes of exponential type. *The Annals of Applied Probability*, 12:1261–1298, 2002. 39

[21] S. I. Boyarchenko & S. Z. Levendorskiĭ. *Non-gaussian Merton Black Scholes theory*. World scientific, Singapore, 2002. 15, 61, 72

[22] P. Carr & H. Geman. The fine structure of asset returns: An emperical investigation. *Journal of Business*, 75:305–332, 2002. 44

[23] P. Carr & D. Madan. Option valuation using the fast Fourier transform. *Journal of Computational Finance*, 2:61–73, 1998. 58, 96, 98

[24] P. Carr, D. Madan, H. Geman, & M. Yor. Self decomposability and option pricing. *Mathematical Finance*, 17:31–57, 2007. 72

[25] P. Carr & L. Wu. What type of processes underlies options? a simple robust test. *Journal of Finance*, 58:2581–2610, 2003. 72, 86

[26] D. Challet & R. Stinchcombe. Analyzing and modelling 1+1d markets. *Physica A: Statistical Mechanics and its Applications*, 300:285–299, 2001. 32

[27] C. Chiarella & G. Iori. A simulation analysis of the microstructure model of double auction markets. *Quantitative Finance*, 2:346–353, 2002. 32

[28] G. L. Choudhury, W. Whitt, & G. L. Lucantoni. Multidimensional transform inversion with applications to the transient m/g/1 queue. *Annals of Applied Probability*, 4:719–740, 1994. 86

[29] K. Chourdakis. Option pricing using the fractional fft. *Journal of Computational Finance*, 8:1–18, 2004. 73, 86, 98, 99

[30] R. Cont & P. Tankov. *Financial modelling with jump processes*. Chapman & Hall/CRC, 2004. 15, 39, 41, 72, 74

[31] R. Cont & E. Voltchkova. A finite difference scheme for option pricing in jump-diffusion and exponential Lévy models. *SIAM Journal on Numerical Analysis*, 43:1596–1626, 2005. 39

[32] M. G. Daniels, J. D. Farmer, L . Gillemot, G. Iori, & E. Smith. Quantitative model of price diffusion and market friction based on trading as a mechanistic random process. *Physical Review Letters*, 90, 2003. 22, 32, 33

[33] D. Davydov & V. Linetsky. The valuation and hedging of barrier and lookback options under the CEV process. *Management Science*, 47:949–965, 2001. 73

[34] E. Derman & I. Kani. Riding on a smile. *Risk Magazine*, 7:32–39, 1994. 14

[35] B. Dumas, J. Fleming, & R. E. Whaley. Implied volatility functions: Emperical tests. *Journal of Finance*, 53:2059–2106, 1998. 15

[36] B. Dupire. Pricing with a smile. *Risk Magazine*, 7:18–20, 1994. 14

[37] E. Eberlein, U. Keller, & K. Prause. New insights into smile, mispricing and value at risk: the hyperbolic model. *Journal of Business*, 71:371–405, 1998. 38, 44

[38] E. Eberlein & W. Kluge. Exact pricing formulae for caps and swaptions in a Lévy term structure model. *Journal of Computational Finance*, 9:99–125, 2006. 72

[39] A. Esser & B. Mönch. Modelling feedback effects with stochastic liquidity in strategic trading in illiquid markets. *Lecture Notes in Economics and Mathematical Systems*, 553, 2006. 31

[40] R. N. Mantegna F. Lillo, J. D. Farmer. Single curve collapse of the price impact function for the New York stock exchange. *Nature*, 421:129–130, 2003. 31

[41] A. Feldmann & W. Whitt. Fitting mixtures of exponentials to long-tail distributions to analyze network performance models. *Performance Evaluation Journal*, 31:963–976, 1998. 57

[42] W. Feller. *An Introduction to probability and its applications*. John Wiley and Sons, 1971. 46

[43] R. Frey & A. Stremme. Perfect option replication for a large trader. *Finance and Stochastics*, 2:115–142, 1998. 10, 13, 21, 22, 24, 34

[44] R. Frey & A. Stremme. Market illiquidity as a source of model risk in dynamic hedging. *Risk Magazine*, pages 125–136, 2000. 10, 13, 21, 24, 34

[45] M. L. Galloway & C. A. Nolder. Subordination, self similarity, and option pricing. *Journal of Applied Mathematics and Decision Sciences*, pages 30–60, 2008. 72

[46] M. G. Garroni & J. L. Menaldi. *Green functions for second order parabolic integro-differential problems*. Longman scientific & technical, Harlow, 1992. 54

[47] H. Geman & M. Yor. Pricing and hedging double barrier options: a probabilistic approach. *Mathematical Finance*, 6:365–378, 1996. 39, 73

[48] P. Glasserman. *Monte-Carlo methods in financial engineering*. Applications of Mathematics. Springer-Verlag, New York, 2004. 61

[49] G. Iori & M. Jeannin. Modelling stock pinning. *Quantitative Finance*, 8:823–831, 2008. 9

[50] K. Itô. On stochastic processes. *Japanese Journal of Mathematics*, 18:261–301, 1942. 16

[51] J. Jacod & A. N. Shiryaev. *Limit theorems for stochastic processes*. Springer-Verlag, Berlin, second edition, 2003. 69

[52] M. Jeannin & M. R. Pistorius. Pricing and hedging barrier options in a hyper-exponential additive model. *International Journal of Theoretical and Applied Finance*, 13(5):1–25, 2010. 9

[53] M. Jeannin & M. R. Pistorius. A transform approach to compute prices and greeks of barrier options driven by a class of Lévy processes. *Quantitative Finance*, 10:629–644, 2010. 9, 73

[54] Z. Jiang & M. R. Pistorius. On perpetual american put valuation and first-passage in a regime-switching model with jumps. *Finance and Stochastics*, 12:31–355, 2008. 73, 78, 80, 94, 95

[55] A. Khintchine. A new derivation of a formula of Paul Lévy. *Bull. Moscow State University*, 1:1–5, 1937. 15

[56] A. Kolmogoroff. Sulla forma generale di un processo stocastico omogeneo (un problema di Bruno de Finetti). *Mathematiche e Naturali*, 15:208–220, 1932. 15, 16

[57] S. G. Kou. A jump-diffusion model for option pricing. *Management Science*, 48:1086–1101, 2002. 43

[58] S. G. Kou, G. Petrella, & H. Wang. Pricing path-dependent options with jump risk via Laplace transforms. *Kyoto Economic Review*, 74:1–23, 2005. 73

[59] S. G. Kou & H. Wang. First passage times of a jump-diffusion process. *Advances in Applied Probablity*, 35:504–531, 2003. 39, 51

[60] S. G. Kou & H. Wang. Option pricing under a double exponential jump-diffusion model. *Management Science*, 50:1179–1192, 2004. 73

[61] O. E. Kudryatsev & S. Z. Levendorskiĭ. Pricing of first touch digitals under normal inverse gaussian processes. *International Journal of Theoretical and Applied Finance*, 9:915–949, 2006. 40

[62] P. Lévy. Sur les integrales dont les elements sont des variables aleatoires independantes. *Annale Scuola Normal Superior Pisa*, 3:337–366, 1934. 15, 16

[63] P. Lévy. *Theorie de l'addition des variables aléatoires*. Gauthier-Villars, Paris, second edition, 1954. 16

[64] A. Lipton. Assets with jumps. *Risk Magazine*, pages 149–153, 2002. 39, 46, 73

[65] R. R. London, M. Kean, L. C. G Rogers, & D. Williams. A martingale approach to some Wiener Hopf problems i,ii. *Seminar on Probability*, pages 41–67, 68–90, 1982. 73

[66] D. B. Madan & F. Milne. Option pricing with v.g martingale components. *Mathematical Finance*, 1:39–55, 1991. 38

[67] P. Malliavin & A. Thalmaier. *Stochastic Calculus of Variations in Mathematical Finance*. Springer, first edition, 2005. 20

[68] F. Mercurio & T. Vorst. Option pricing with hedging at fixed trading dates. *Applied Mathematical Science*, 3:135–158, 1996. 13

[69] E. Mordecki. Optimal stopping and perpetual options for Lévy processes. *Finance and Stochastics*, 6:473–493, 2002. 46

[70] S. X. Ni, N. D. Pearson, & A. M. Poteshmana. Stock price clustering on option expiration dates. *Journal of Financial Economics*, 78:49–87, 2005. 21

[71] J. Pan. The jump-risk premia implicit in options: evidence from integrated time-series study. *Journal of Financial Economics*, 63:3–50, 2002. 72, 86

[72] N. D. Pearson, A. M. Poteshman, & J. S. White. Does option trading have a pervasive impact on stock prices? *Working Paper*, 2007. 29

[73] E. Platen & M. Schweizer. On feedback effects from hedging derivatives. *Mathematical Finance*, 8:67–68, 1998. 13, 22

[74] W. Press, S. Teukolsky, W. Vetterling, & B. Flannery. *Numerical Recipes in C*. Cambridge University Press, Cambridge, 1992. 57

[75] L. C. G. Rogers. Fluid models in queueing theory and Wiener-Hopf factorization of markov chain. *The Annals of Applied Probability*, 4(2):390–413, 1994. 73

[76] L. C. G. Rogers. Evaluating first passage probabilities for spectrally one-sided Lévy processes. *Journal of Applied Probability*, 37:1173–1180, 2000. 39

[77] B. A. Rogozin. On the distribution of functionals related to boundary problems for processes with independent increments. *Theory of Probability And its Applications*, 11:580–591, 1966. 45

[78] K. Sato. *Lévy processes and infinitely divisible distributions*. Cambridge University Press, Cambridge, 1999. 15, 42, 49, 54, 70, 74

[79] P. Schönbucher & P. Willmott. The feedback effect of hedging in illiquid markets. *SIAM Journal of Applied Mathematics*, 6:232–272, 2000. 13

[80] W. Schoutens. *Lévy processes in finance*. John Wiley and Sons, 2003. 15, 44, 72

[81] A. Sepp. Analytical pricing of double barrier options under a double-exponential jump-diffusion process: Applications of Laplace transform. *International Journal of Theoretical and Applied Finance*, 7:151–175, 2004. 39, 51, 73

[82] A. V. Skorohod. *Random processes with independent increments*. Kluwer Academic Publishers, first edition, 1991. 19

[83] E. Smith, J. D. Farmer, L. Gillemot, & S. Krishnamurthy. Statistical theory of the continuous double auction. *Quantitative Finance*, 6:481–514, 2006. 22

[84] A. Talbot. The accurate numerical inversion of Laplace transforms. *Journal of the Institute of Mathematics and its Applications*, 23(1):97–120, 1979. 73, 86, 96

[85] A. Whalley & P. Willmott. Counting the costs. *Risk Magazine*, 6:59–66, 1993. 13